IAEA TECDOC SERIES

IAEA-TECDOC-1955

Production of Emerging Radionuclides towards Theranostic Applications: Copper-61, Scandium-43 and -44, and Yttrium-86

IAEA
International Atomic Energy Agency

PRODUCTION OF EMERGING RADIONUCLIDES TOWARDS THERANOSTIC APPLICATIONS: COPPER-61, SCANDIUM-43 AND -44, AND YTTRIUM-86

The following States are Members of the International Atomic Energy Agency:

AFGHANISTAN
ALBANIA
ALGERIA
ANGOLA
ANTIGUA AND BARBUDA
ARGENTINA
ARMENIA
AUSTRALIA
AUSTRIA
AZERBAIJAN
BAHAMAS
BAHRAIN
BANGLADESH
BARBADOS
BELARUS
BELGIUM
BELIZE
BENIN
BOLIVIA, PLURINATIONAL STATE OF
BOSNIA AND HERZEGOVINA
BOTSWANA
BRAZIL
BRUNEI DARUSSALAM
BULGARIA
BURKINA FASO
BURUNDI
CAMBODIA
CAMEROON
CANADA
CENTRAL AFRICAN REPUBLIC
CHAD
CHILE
CHINA
COLOMBIA
COMOROS
CONGO
COSTA RICA
CÔTE D'IVOIRE
CROATIA
CUBA
CYPRUS
CZECH REPUBLIC
DEMOCRATIC REPUBLIC OF THE CONGO
DENMARK
DJIBOUTI
DOMINICA
DOMINICAN REPUBLIC
ECUADOR
EGYPT
EL SALVADOR
ERITREA
ESTONIA
ESWATINI
ETHIOPIA
FIJI
FINLAND
FRANCE
GABON
GEORGIA
GERMANY
GHANA
GREECE
GRENADA
GUATEMALA
GUYANA
HAITI
HOLY SEE
HONDURAS
HUNGARY
ICELAND
INDIA
INDONESIA
IRAN, ISLAMIC REPUBLIC OF
IRAQ
IRELAND
ISRAEL
ITALY
JAMAICA
JAPAN
JORDAN
KAZAKHSTAN
KENYA
KOREA, REPUBLIC OF
KUWAIT
KYRGYZSTAN
LAO PEOPLE'S DEMOCRATIC REPUBLIC
LATVIA
LEBANON
LESOTHO
LIBERIA
LIBYA
LIECHTENSTEIN
LITHUANIA
LUXEMBOURG
MADAGASCAR
MALAWI
MALAYSIA
MALI
MALTA
MARSHALL ISLANDS
MAURITANIA
MAURITIUS
MEXICO
MONACO
MONGOLIA
MONTENEGRO
MOROCCO
MOZAMBIQUE
MYANMAR
NAMIBIA
NEPAL
NETHERLANDS
NEW ZEALAND
NICARAGUA
NIGER
NIGERIA
NORTH MACEDONIA
NORWAY
OMAN
PAKISTAN
PALAU
PANAMA
PAPUA NEW GUINEA
PARAGUAY
PERU
PHILIPPINES
POLAND
PORTUGAL
QATAR
REPUBLIC OF MOLDOVA
ROMANIA
RUSSIAN FEDERATION
RWANDA
SAINT LUCIA
SAINT VINCENT AND THE GRENADINES
SAN MARINO
SAUDI ARABIA
SENEGAL
SERBIA
SEYCHELLES
SIERRA LEONE
SINGAPORE
SLOVAKIA
SLOVENIA
SOUTH AFRICA
SPAIN
SRI LANKA
SUDAN
SWEDEN
SWITZERLAND
SYRIAN ARAB REPUBLIC
TAJIKISTAN
THAILAND
TOGO
TRINIDAD AND TOBAGO
TUNISIA
TURKEY
TURKMENISTAN
UGANDA
UKRAINE
UNITED ARAB EMIRATES
UNITED KINGDOM OF GREAT BRITAIN AND NORTHERN IRELAND
UNITED REPUBLIC OF TANZANIA
UNITED STATES OF AMERICA
URUGUAY
UZBEKISTAN
VANUATU
VENEZUELA, BOLIVARIAN REPUBLIC OF
VIET NAM
YEMEN
ZAMBIA
ZIMBABWE

The Agency's Statute was approved on 23 October 1956 by the Conference on the Statute of the IAEA held at United Nations Headquarters, New York; it entered into force on 29 July 1957. The Headquarters of the Agency are situated in Vienna. Its principal objective is "to accelerate and enlarge the contribution of atomic energy to peace, health and prosperity throughout the world''.

IAEA-TECDOC-1955

PRODUCTION OF EMERGING RADIONUCLIDES TOWARDS THERANOSTIC APPLICATIONS: COPPER-61, SCANDIUM-43 AND -44, AND YTTRIUM-86

INTERNATIONAL ATOMIC ENERGY AGENCY
VIENNA, 2021

COPYRIGHT NOTICE

For further information on this publication, please contact:

Radioisotope Products and Radiation Technology Section
International Atomic Energy Agency
Vienna International Centre
PO Box 100
1400 Vienna, Austria
Email: Official.Mail@iaea.org

Printed by the IAEA in Austria
April 2021

IAEA Library Cataloguing in Publication Data

Names: International Atomic Energy Agency.
Title: Production of emerging radionuclides towards theranostic applications : copper-61, scandium-43 and -44, and yttrium-86 / International Atomic Energy Agency.
Description: Vienna : International Atomic Energy Agency, 2021. | Series: IAEA TECDOC series, ISSN 1011–4289 ; no. 1955 | Includes bibliographical references.
Identifiers: IAEAL 21-01404 | ISBN 978-92-0-107321-1 (paperback : alk. paper) |
ISBN 978-92-0-107221-4 (pdf)
Subjects: LCSH: Radioisotopes in medical diagnosis. | Radioisotopes — Therapeutic use. | Scandium — Isotopes. | Copper — Isotopes. | Yttrium — Isotopes.

FOREWORD

Treatment of cancer using radionuclides is gaining importance worldwide. Radionuclides that can be paired for therapeutic and diagnostic applications, that have the potential for widespread production and that have established methods for separation and radiolabelling — for example, $^{43/44}$Sc as a theranostic pair with ^{47}Sc, ^{61}Cu as a pair with ^{67}Cu, and ^{86}Y as a pair with ^{90}Y — are of particular interest. Demand for these radioisotopes is expected to grow in in the coming years. As part of the its ongoing support in the area of cyclotron based radioisotopes and radiopharmaceutical production and their applications, in November 2019 the IAEA brought together a team of experts from academia and industry to develop an IAEA publication focusing on therapeutic radiopharmaceuticals labelled with $^{43/44}$Sc, ^{61}Cu and ^{86}Y.

The present publication describes the direct and indirect cyclotron based aspects of production of $^{43/44}$Sc, ^{61}Cu and ^{86}Y, including target preparation, irradiation considerations, target processing and recovery, radioisotope purification and radiolabelling examples. The publication is expected to be a useful tool for interested medical cyclotron centres and nearby application sites.

The IAEA wishes to thank the participating experts for their valuable work and scientific contributions. Special thanks are due to C. Hoehr (Canada) for her efforts to finalize the manuscript, and to J. Vera Araujo (Bolivarian Republic of Venezuela) for her editorial support. The IAEA officer responsible for this publication was A. Jalilian of the Division of Physical and Chemical Sciences.

EDITORIAL NOTE

This publication has been prepared from the original material as submitted by the contributors and has not been edited by the editorial staff of the IAEA. The views expressed remain the responsibility of the contributors and do not necessarily represent the views of the IAEA or its Member States.

Neither the IAEA nor its Member States assume any responsibility for consequences which may arise from the use of this publication. This publication does not address questions of responsibility, legal or otherwise, for acts or omissions on the part of any person.

The use of particular designations of countries or territories does not imply any judgement by the publisher, the IAEA, as to the legal status of such countries or territories, of their authorities and institutions or of the delimitation of their boundaries.

The mention of names of specific companies or products (whether or not indicated as registered) does not imply any intention to infringe proprietary rights, nor should it be construed as an endorsement or recommendation on the part of the IAEA.

The authors are responsible for having obtained the necessary permission for the IAEA to reproduce, translate or use material from sources already protected by copyrights.

The IAEA has no responsibility for the persistence or accuracy of URLs for external or third party Internet web sites referred to in this publication and does not guarantee that any content on such web sites is, or will remain, accurate or appropriate.

CONTENTS

1. INTRODUCTION

1.1. BACKGROUND

The production and purification of positron emitting radiometal nuclides such as $^{43/44}$Sc, ^{61}Cu, and ^{86}Y for radiolabelling applications is far from new [1–6]. These radionuclides can be used as surrogates to their therapeutic partners to provide a theranostic approach. The diagnostic set ($^{43/44}$Sc, ^{61}Cu, and ^{86}Y) can be used to detect and follow up the disease as integrated into a targeting molecule, while the therapeutic set (^{47}Sc, ^{67}Cu and ^{90}Y) can be used in the treatment of the disease. However, access to these and other radiometals for positron emission tomography (PET) applications has been previously restricted almost exclusively to laboratories with significant targetry and radiochemistry experience. Without such expertise, sites wanting to work with a radiometal were previously often limited to commercial supply of long-lived single photon emitters for planar imaging or single photon emission computed tomography (SPECT).

Positron emission tomography allows for improved spatial and temporal resolution and quantification of tracer uptake. The past decade, fortunately, has been met with significant change in the PET radiometal landscape. The trivalent metallic positron emitter ^{68}Ga has significantly contributed to the molecular imaging of various diseases in oncology. The first commercial ^{68}Ge/^{68}Ga generators providing cationic ^{68}Ga(III) were introduced in the early 2000s, with the first pharmaceutical grade ^{68}Ge/^{68}Ga generators made available in 2014. The access to such generators enabled ^{68}Ga to become the first widely accessible PET radiometal for radiolabelling applications on a global scale, with two ^{68}Ga neuroendocrine tumour tracers and a ^{68}Ga based PSMA targeting tracer, having obtained US Food and Drug Administration market authorization since 2016. The increasing demand of ^{68}Ga has also motivated the direct cyclotron based production of ^{68}Ga in solid [7] and liquid targets [8, 9] – a method which has been implemented at many sites across the globe [10–13] – both to address supply shortages of generators, and to allow for larger scale production quantities and greater radiometal variety. A strong community interest in the cyclotron based approach of ^{68}Ga is evidenced by the recent publication of IAEA-TECDOC-1863 [14], European Pharmacopoeia monograph [15], and a growing number of clinical trials, see Fig. 1.

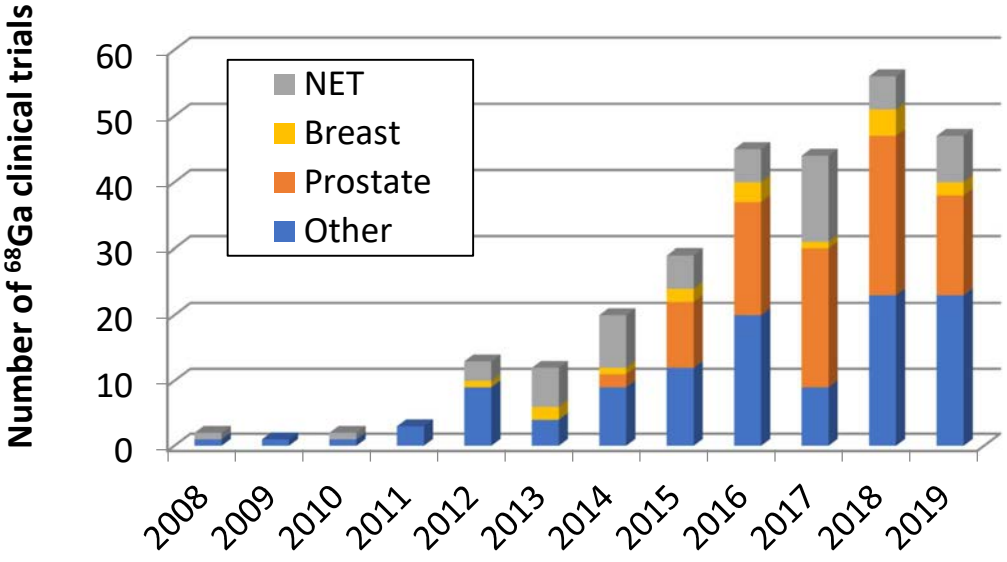

FIG. 1. The number of clinical trials starting per year (courtesy of K. Gagnon, GE Healthcare, Sweden, data compiled from several reports accessed at https://clinicaltrials.gov/).

In parallel to its immediate use for PET imaging, ^{68}Ga has an enormous impact on treatment decisions in general, and for nuclear medicine therapies using analogue targeting vectors labelled with trivalent particle emitters such as ^{90}Y ($t_{½}$ = 2.67 days), ^{177}Lu ($t_{½}$ = 6.7 days) and ^{225}Ac ($t_{½}$ = 10 days), with the first ^{64}Cu tracer obtaining FDA market authorization in 2020. The combination of both ^{68}Ga or another imaging radionuclide, and the therapeutic radionuclides in the same tumour targeting vector is referred to as theranostics, which increases the quality of patient care (see Fig. 2). In addition to its role of identifying the right tracer for the right patient at the right time, the estimation and planning of a patient's individual therapeutic radiation dose is an essential aspect in radiotheranostics. Quantification of radiation doses is enhanced by measurement of not only standardized uptake value for both tumour and healthy organs at certain time points, but a more detailed understanding of the kinetics of tracer uptake.

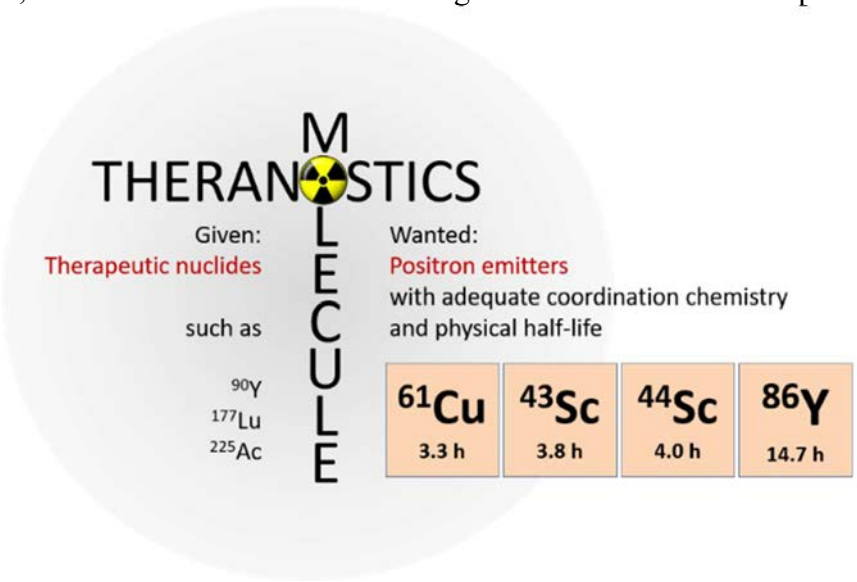

FIG. 2. Common therapeutic isotopes and possible positron emitters for theranostics (courtesy of F. Rösch, Johannes Gutenberg-Universität Mainz, Germany).

However, the rather short lived ^{68}Ga ($t_{½}$ = 67.71 min) is not able to cover the relevant integral of the pharmacokinetics of most of the current therapeutic tracers, as illustrated in Fig. 3. This would ideally require a positron emitter with a longer physical half-life. To this end, longer lived PET radiometals such as ^{43}Sc ($t_{½}$ = 3.9 h), ^{44}Sc ($t_{½}$ = 4.0 h), ^{61}Cu ($t_{½}$ = 3.3 h), ^{64}Cu ($t_{½}$ = 12.7h), and ^{86}Y ($t_{½}$ = 14.7 h) have recently started to gain attention. These nuclides offer not only simplified logistics due to their longer half-lives versus ^{68}Ga, but moreover, are unique in that there is a corresponding therapeutic radioisotope for each of these, ^{47}Sc ($t_{½}$ = 3.3 d), ^{67}Cu ($t_{½}$ = 62 h), and ^{90}Y ($t_{½}$ = 64 h), respectively, which can allow for a 'true match' pairing in the context of theranostics. Strategies for production and purification of $^{43/44}$Sc, ^{61}Cu, and ^{86}Y are therefore the focus of this publication. While also a matched pair candidate, ^{64}Cu is not discussed herein, as it has recently been published in an IAEA report named 'Cyclotron produced radionuclides: emerging positron emitters for medical application ^{64}Cu and ^{124}I' [16].

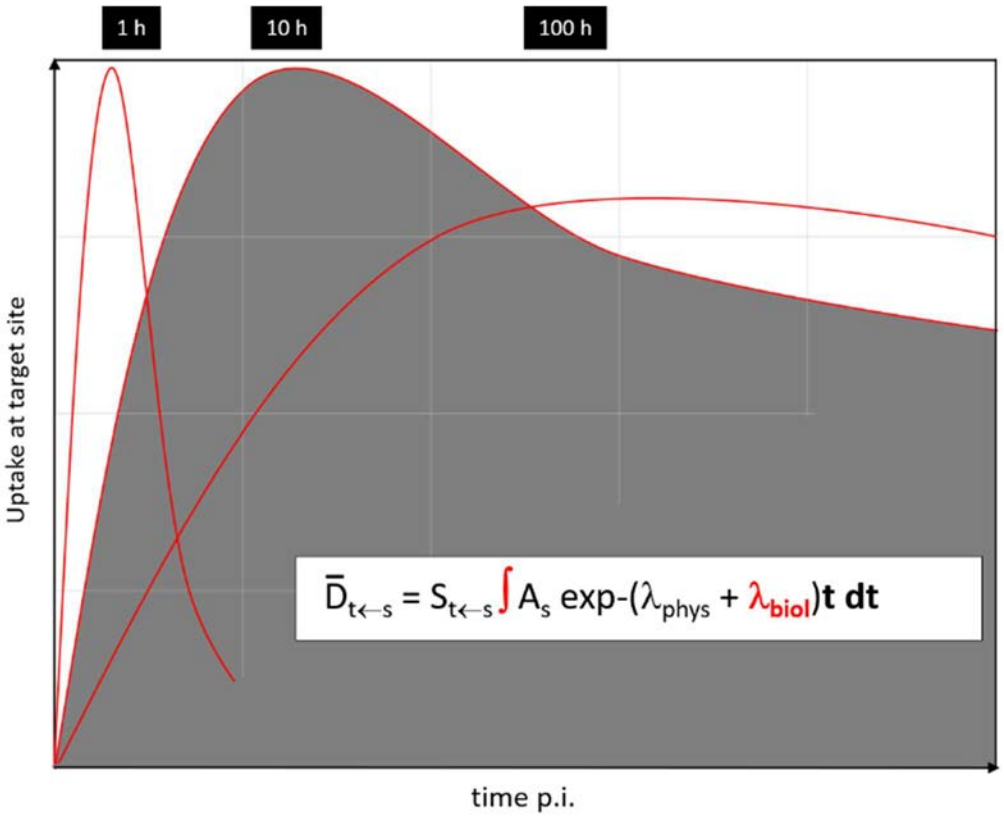

FIG. 3. Uptake of tracers with different physical half-lives as a function of time post injection. The red line represents the pharmacokinetics of a typical blood flow tracer. The left line is typical for radiolabelled peptides, while the right line has the time behaviour of antibodies (courtesy of F. Rösch, Johannes Gutenberg-Universität Mainz, Germany).

In considering $^{43/44}$Sc, ^{61}Cu, and ^{86}Y, Table 1 summarizes basic nuclear data and candidate production routes anticipated to be the most accessible to the community. While the listed production routes are not meant to be exhaustive, the list includes both (p,n) and (p,α) reactions suitable for use by sites with low energy proton capability (e.g. <20 MeV) and (d,n) and (d,α) reactions suitable for use by sites with low energy deuteron capability (e.g. <10 MeV). In addition, although α particle irradiation was generally omitted from the table, the ^{40}Ca(α,p)^{43}Sc route was included given the high natural isotopic abundance of ^{40}Ca and the generally high cost of the other isotopically enriched calcium isotopes. Finally, two (p,2n) reactions are listed which may have advantages when higher energy protons are available: in the case of ^{43}Sc production via the ^{44}Ca(p,2n)^{43}Sc, this could reduce the cost of the target material given the particularly low natural abundance of ^{43}Ca; and, in the case of ^{45}Sc(p,2n)^{44}Ti → ^{44}Sc, although production rates of ^{44}Ti are low, such a route enables a ^{44}Ti/^{44}Sc generator approach given the 60 year half-life of ^{44}Ti. These reactions, their trade-offs due to natural isotopic abundance and cost of the target material, insight into which reaction may be best suited for a particular accelerator, ease of target preparation and processing, among others, are discussed in the respective section for each nuclide.

TABLE 1. EMERGING NUCLIDES FOR THERNANOSTIC APPLICATIONS

(courtesy of K. Gagnon, GE Healthcare, Sweden)

	Half - life (h)	β^+ (%)	β^+_{mean} (keV)	Candidate routes	Nat. abundance (%)	Threshold energy (MeV)
^{43}Sc	3.891	88.1	476	^{43}Ca(p,n)^{43}Sc ^{44}Ca(p,2n)^{43}Sc ^{42}Ca(d,n)^{43}Sc ^{40}Ca(α,p)^{43}Sc ^{46}Ti(p,α)^{43}Sc	0.135 2.09 0.647 96.94 8.25	3.0735 14.4582 0 3.8751 3.1431
^{44g}Sc	3.97	94.27	632.0	^{44}Ca(p,n)^{44}Sc ^{47}Ti(p,α)^{44}Sc ^{46}Ti(d,α)^{44}Sc ^{45}Sc(p,2n)^{44}Ti→^{44}Sc	2.09 7.44 8.25 100	4.5367 2.3058 0 12.6544
^{61}Cu	3.336	61	500	^{61}Ni(p,n)^{61}Cu ^{60}Ni(d,n)^{61}Cu ^{64}Zn(p,α)^{61}Cu	1.1399 26.223 49.17	3.0701 0 0
^{86}Y	14.74	31.92	660	^{86}Sr(p,n)^{86}Y	9.86	6.0930

As noted above, the barrier to use and to expand the variety of radionuclides has been lowered in recent years thanks to technology advances which include, but are not limited to, commercial solid target systems as well as development and commercial availability of unique resins which simplify purification processes. Furthermore, yields may be reduced by more than an order of magnitude versus solid targets due to significant interaction of the particle beam with water, see Fig. 4. For sites which do not have solid target infrastructure, or perhaps require only low quantities of radioactivity, solution targets can be irradiated by dissolving an appropriate salt.

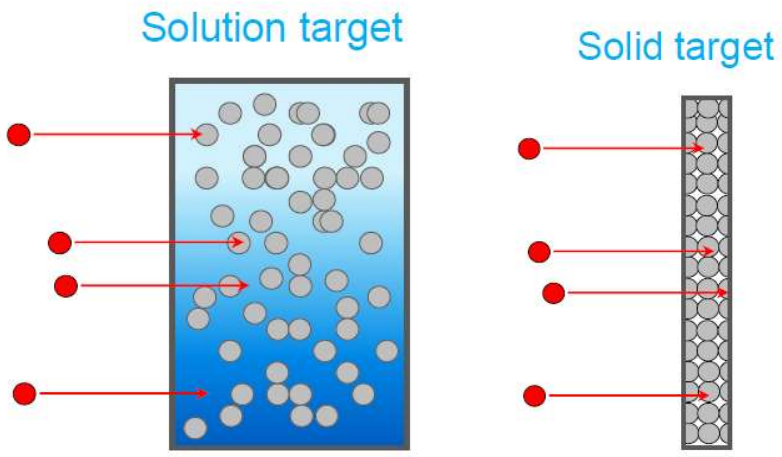

FIG. 4. Depiction of a solution vs. a solid target to illustrate reduced yields for solution targets as particles will also interact with the water (courtesy of C. Hoehr, TRIUMF, Canada).

1.2. OBJECTIVES

The objectives of this publication are to collect and summarize relevant experiences and data for the production of $^{43/44}$Sc, ^{61}Cu and ^{86}Y as theranostic pairs to the therapeutic nuclides ^{47}Sc, ^{67}Cu and ^{90}Y for the reader interested in producing these nuclides. The guidance provided here represents expert opinion but does not intend to exclude other valuable input should it happen to be omitted. This publication is meant to give the reader hands on information to select the

appropriate radioisotope to be used. It discusses the different production routes and shows advantages and disadvantages of direct production vs. generator production in some cases. It lists different purification techniques including recovery of the starting material where necessary, and quality control (QC) from the different options.

1.3. SCOPE

The present publication focused on a specific set of some newcomers, namely ^{43}Sc, ^{44}Sc, ^{61}Cu, and ^{86}Y. The reason is not only the primary quality of precision oncology provided by potent tumour targeting vectors labelled with the mentioned isotopes, but also the enormous potential impact those PET radiometals may offer on treatment decisions for nuclear medicine therapies in the sense of theranostics. It is the matching of a positron emitter with its β^- or α-emitting companion, exemplified in the ideal version of ^{86}Y and ^{90}Y [17]. Yet, the two scandium positron emitters follow the same principle, when used to mirror the pharmacology of analogue targeting vectors labelled with trivalent particle emitters such as ^{90}Y ($t_{½}$ = 2.67 days), ^{177}Lu ($t_{½}$ = 6.7 days) and ^{225}Ac ($t_{½}$ = 10 days) [18]. Finally, ^{61}Cu may work in the same direction for ^{67}Cu.

This publication is meant to give the reader hands on information to select the appropriate nuclide to be used in the imaging application of a theranostic pair. It discusses the different production routes and outlines advantages and disadvantages of direct production vs. generator production in some cases. It lists different purification techniques including recovery of the starting material where necessary, and QC from the different options. The overall aim is to enable the reader to investigate and start their own production of these isotopes in their facilities for their respective theranostic programmes.

1.4. STRUCTURE

The publication is divided into three sections according to the three isotope groups discussed. Section 2 discusses the scandium isotopes ^{43}Sc and ^{44}Sc. Production via different routes, purification and radiolabelling examples are described. Section 3 then covers the production, purification and radiolabelling examples of ^{61}Cu. And finally, section 4 summarizes production, purification and radiolabelling of ^{86}Y, and section 5 summarizes the publication in a conclusion. All reported nuclear data is from the NNDC National Nuclear Data Center of Brookhaven National Laboratory [19].

2. PRODUCTION OF $^{43/44}$Sc

The theranostics concept in nuclear medicine depends on the use of nuclides of preferably the same element to enable the application of identical radiopharmaceuticals with the same chemistry for both diagnosis and therapy. The combination of suitable radionuclides is known as ‘matched pair’ and can be formed by different isotopes of scandium, ^{43}Sc or ^{44}Sc with the therapeutic isotope ^{47}Sc [20].

The suitable decay properties of ^{43}Sc ($t_{½}$ = 3.891 h, $E_{\beta+av}$ = 476 keV, E_{γ}= 372.9 keV, I= 22.5%) and ^{44}Sc ($t_{½}$ = 3.97 h, $E_{\beta+av}$ = 632.0 keV, E_{γ}= 1157.020 keV, I= 99.9%) for cancer diagnosis using PET suggests their promising application for nuclear medicine. They could be used as an alternative to the currently clinically utilized ^{68}Ga ($t_{½}$ = 67.71 min), with their longer half-life, lower average positron energy, and higher positron intensities, all of which would improve image quality, particularly when ‘tumour to background’ ratios are enhanced at later time

stages. With chemistry similar to therapeutic ^{90}Y and ^{177}Lu, $^{43/44}$Sc can additionally be used for diagnosis, planning, staging and radionuclide therapy monitoring of ^{90}Y and ^{177}Lu. The ^{44}Sc production and application has been comprehensively investigated, however in the case of ^{43}Sc, further development is required. The physical half-lives of the scandium radioisotopes in question also make them attractive to produce from a commercial perspective, as it is easier to distribute them compared to ^{68}Ga, be it as the radionuclide or as a radiopharmaceutical.

Patient studies were performed at Zentralklinik Bad Berka, Germany, using both generator and cyclotron produced ^{44}Sc. Whole body PET/ computed tomography (CT) scans were performed followed by the injection of [^{44}Sc]Sc-DOTA-TOC. Patient scans showed excellent uptake in liver metastases of a neuroendocrine tumour, high resolution and excellent contrast, especially at later time points [20, 21].

2.1. $^{43/44}$Sc PRODUCTION ROUTES

In the context of ^{44}Sc, there exists both ^{44g}Sc ($t_{½}$= 4.0 h) and ^{44m}Sc ($t_{½}$= 58.6 h); however, for brevity, unless required for clarification, this report uses ^{44}Sc to denote the ground state.

2.1.1. ^{44}Sc production from generator

Compared to direct nuclear reactions to produce ^{44}Sc using a cyclotron, the ^{44}Ti/^{44}Sc radionuclide generator system is convenient due to its cyclotron independent availability comparable with a ^{68}Ge/^{68}Ga generator, see Fig. 5 [18]. The long lived ^{44}Ti ($t_{½}$ ~ 60 a) generates ^{44}Sc, which subsequently transforms to stable ^{44}Ca. Like in the case of the similar ^{68}Ge/^{68}Ga radionuclide generator, it is a secular transformation equilibrium. The parent (P) half-life is much higher than the daughter (D) ($t_{½\ P} \gg t_{½\ D}$, i.e. $\lambda_P \ll \lambda_D$). The parent, ^{44}Ti, radioactivity does not decrease significantly during several daughter half-lives. The ^{44}Ti/^{44}Sc generator system shows a half-life ratio (parent to daughter) of ca. 130 000 [18]. Thus, every 4 h, about 50% of the saturation activity is generated, resulting in identical daily ^{44}Sc batches very close to saturation and generator derived ^{44}Sc activities correspond to daily nominal ^{44}Ti activities. Additionally, the ^{44}Sc produced in this manner is free from the contaminant ^{44m}Sc ($t_{½}$ = 58.61 h) which is co-produced to a varying degree via the direct production routes.

A few strategies to design a ^{44}Ti/^{44}Sc generator were investigated in the 1960s and 1970s, [22–25] based on radiochemical technique with relatively low ^{44}Ti activities and pharmaceutical aspects were not considered. In contrast, a 185 MBq generator was developed in 2009/2010 at the University of Mainz, immediately aimed to routinely provide ^{44}Sc for PET imaging in patients [5]. Later, in addition to the generator development in Mainz, two National US Laboratories (Los Alamos and Brookhaven) were able to accumulate over 10 mCi of ^{44}Ti [26, 27].

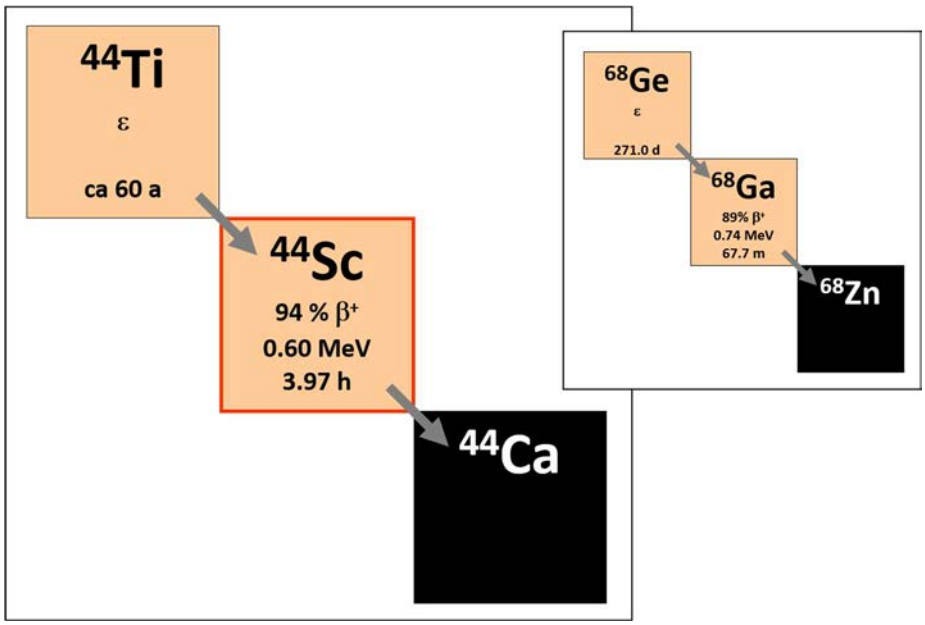

FIG. 5. Decay principle of the $^{44}Ti/^{44}Sc$ generator, as compared to the well known $^{68}Ge/^{68}Ga$ generator (courtesy of F. Rösch, Johannes Gutenberg-Universität Mainz, Germany).

2.1.1.1. ^{44}Ti production via $^{45}Sc(p,2n)^{44}Ti$

While the design of a long lasting robust $^{44}Ti/^{44}Sc$ generator is challenging due to radiochemistry aspects, the high yield production of the generator parent ^{44}Ti itself is a challenge in terms of isotope production. For the choice of nuclear reactions, two principal approaches are of interest: the direct ^{44}Ti production via proton induced reactions on natural scandium, and (p,xnyp) spallation processes on targets such as vanadium. The Sc(p,2n) production pathway on naturally monoisotopic ^{45}Sc appears to be a practicable option, see Fig. 6. Cross sections are reproduced in Fig. 7. Maximum cross sections occur at approximately 22 to 25 MeV. At higher energy, integral yields of ^{44}Ti increase to about twice as high at a proton energy of 30 MeV [28].

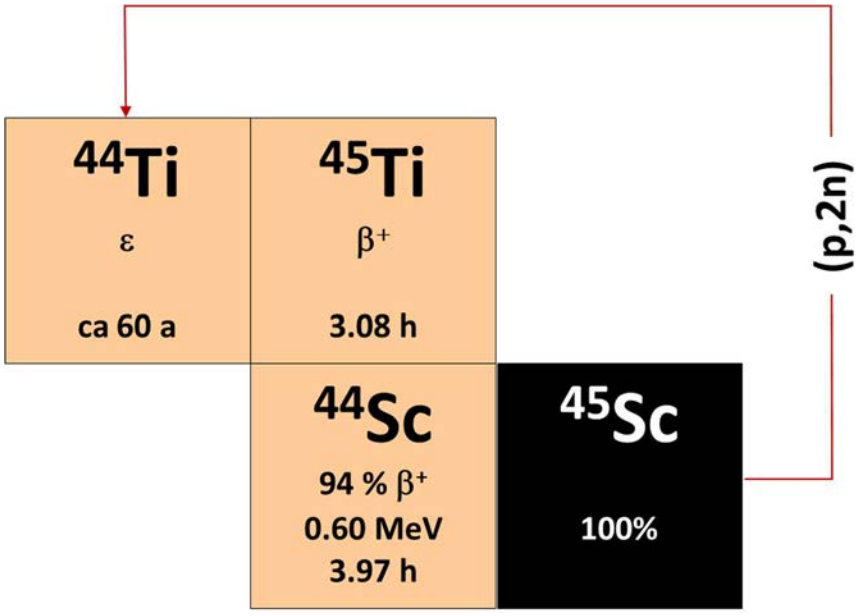

FIG. 6. Production route for ^{44}Ti via $^{45}Sc(p,2n)$ (courtesy of F. Rösch, Johannes Gutenberg-Universität Mainz, Germany)

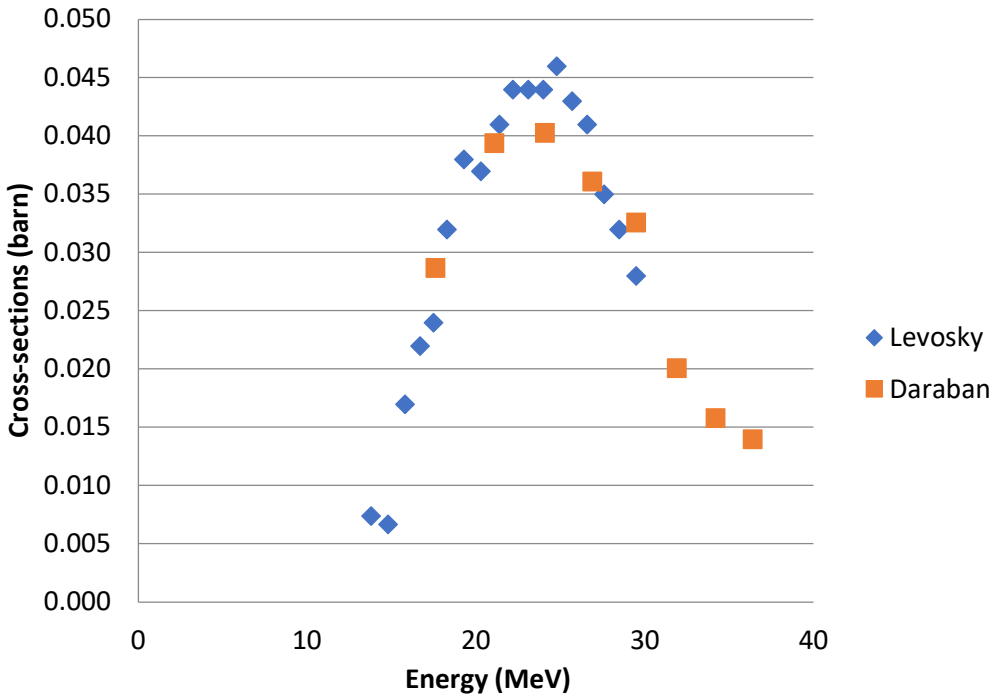

FIG. 7. Production cross section for the $^{45}Sc(p,2n)^{44}Ti$ reaction (courtesy of F. Alves, University of Coimbra, Portugal, and C. Hoehr, TRIUMF, Canada. Raw data adapted from [28, 29]).

The physical half-life of ^{44}Ti is the production rate limiting parameter, where one day or even one week realistic irradiation periods offer low saturation factors (0.000032 and 0.000222, respectively). The only way out of this dilemma is high beam current irradiation. At 1 mA proton beam intensity and 30 MeV proton energy, 560 MBq (15 mCi) of ^{44}Ti would be obtained at a one week irradiation. This nuclear reaction was performed at 200 µA internal proton beam intensity and ca. 25 MeV energy [5]. A metallic Sc target (overall mass of 1.5 g) was melted into 220 µm thick layers onto sophisticated copper backings to withstand the high proton beam flux and provide optimum heat transfer. A silver layer was used in between to minimize the ^{65}Zn contamination. With this target, 185 MBq of ^{44}Ti were obtained and the $^{44}Ti/^{44}Sc$ generator is still in daily use.

Another reported production of ^{44}Ti was performed at Los Alamos (LANL) and Brookhaven National Laboratories (BNL) [26]. High purity natural scandium targets (99.99%) were irradiated at the Isotope Production Facility (IPF) at LANL and Brookhaven Linac Isotope producer (BLIP) resulting in production of 145.4 MBq (3.9 mCi) for 41.8 mAh and 30.7 MBq (0.83 mCi) for 18.3 mAh, respectively. The target consisted of a scandium disk (27 g, d × h 50.8 × 5.1 mm) packed in an Inconel capsule at LANL, while the BNL target was packed in an aluminium capsule (17.5 g, d × h 60.3 × 1.5 mm) ^{44}Ti was accumulated when opportunistic beam time became available at IPF of LANL.

2.1.1.2. Separation of ^{44}Ti from the target ^{45}Sc

The irradiated target at the University of Mainz was dissolved in 2M HCl solution and loaded on a cation exchange chromatography. About 99.9% of the ^{44}Ti was isolated followed by a subsequent chromatography step for complete separation of scandium ($< 10^{-3}$%, about 15 µg of the initial scandium). In this process 99.6% of ^{44}Ti was recovered [5].

For ^{44}Ti produced at LANL and BNL the above reported method was not feasible due to the much larger target masses (27 and 17.5 g, respectively) of scandium targets. An alternative separation approach was applied to remove the bulk scandium mass by using an anion exchange column in concentrated (12.3 M) hydrochloric acid [26]. In these conditions, the produced ^{44}Ti remained on the column and bulk scandium mass was passing through. Subsequently, ^{44}Ti was eluted with diluted 4M HCl and directly loaded onto a cation exchange column for final purification. Finally, ^{44}Ti was purified from co-produced ^{56}Co via an anion exchange in 4M HCl, where titanium was passing through without sorption and ^{56}Co was retained on the resin, see Fig. 8. This procedure resulted in recovery of over 90% of ^{44}Ti with a separation factor over 10^6. Due to co-production of high activities (GBq's) of ^{46}Sc and ^{56}Co all handling was performed remotely in a hot cell environment.

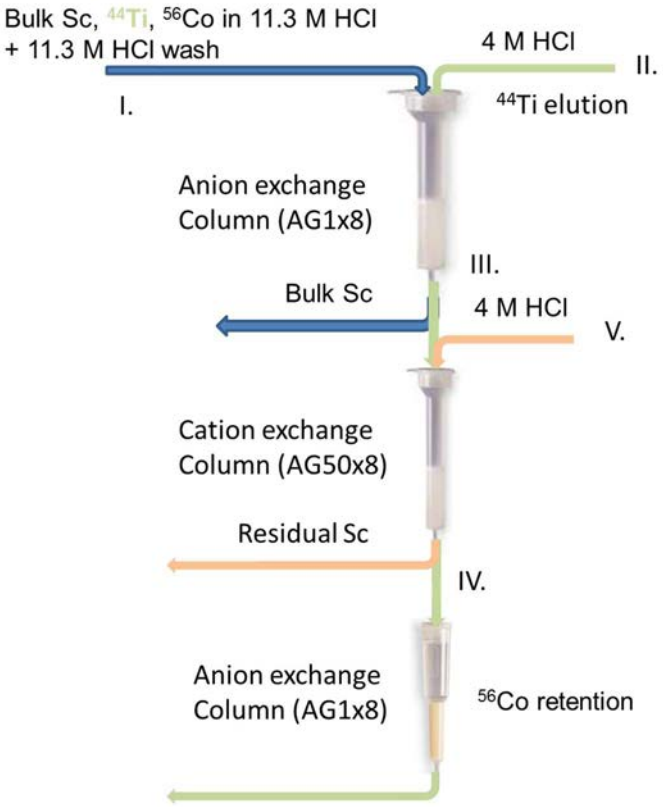

FIG. 8. Schematic of the separation strategy (courtesy of V. Radchenko, TRIUMF, Canada).

Later, an alternative method to simplify and speed up the separation was proposed and successfully tested based on hydroxamate based Zr resin (produced by Triskem International) [27]. This resin enables sorption of titanium while bulk scandium mass is passing through without retention in diluted hydrochloric acid. Finally, ^{44}Ti was eluted in the mixture of hydrochloric acid and hydrogen peroxide. This method provides over 95% of recovery of ^{44}Ti and separation factor of Ti/Sc $\geq 10^5$.

2.1.1.3. The design of ^{44}Ti/^{44}Sc radionuclide generator

In order to prepare a ^{44}Ti/^{44}Sc radionuclide generator [30, 31], several radiochemical criteria should be considered. Effective separation strategies to provide high ^{44}Sc yields with low ^{44}Ti content is the major goal. On the other hand, Sc eluate type should be carefully considered to best adapt to solvent characteristics of the radiolabelling reactions such as low volume, low pH, high purity, etc [30]. There are only a few reports on ^{44}Ti/^{44}Sc generators. A mixture of

0.1M $H_2C_2O_4$ / 0.2M HCl on a Dowex-1 resin, yields 60% to 70% ^{44}Sc elution (in 30–50 ml) [23]. Using a solvent extraction method (1% 1-phenyl-3-methyl-4-capryl-pyrazolone-5 in methyl isobutyl) yielded over 90% Sc recovery (with a Ti contamination of $<10^{-6}$) [23]. In studies using 0.01M HCl as an eluent and ^{44}Ti (adsorbed on inorganic ZrO_2), the elution yields 42–46% were reported (decontamination factor of 5 x 10^4) [24].

For the first medical generator [30–32] an ion exchange system based on HCl/oxalic acid mixtures was optimized. Scandium-III is strongly complexed in oxalic acid solution in oxalate form and in turn the complexes are selectively destroyed by HCl addition [33]. Distribution coefficients K_d of Ti^{IV} and Sc^{III} on various ion exchange resins and mixtures of HCl/oxalic acid were measured systematically. Optimum mixtures for efficient separations to elute ^{44}Sc from AG 1-X8 resins were; 0.2M HCl / 0.1 M$H_2C_2O_4$, 0.125M HCl / 0.025M $H_2C_2O_4$ or 0.06–0.08M HCl / 0.005M $H_2C_2O_4$. The most favoured mixture was shown to be 0.06–0.08M HCl / 0.005M $H_2C_2O_4$ [5].

A polyether ether ketone column (H;150 mm, D;3 mm, V_0;0.55 ml) filled with AG 1-X8 (200-400 mesh, Br^--form) [5] was used for the process. ^{44}Ti was dried using heat and inert gas flow and re-dissolved in 0.1M $H_2C_2O_4$ (20 ml) and packed into the column. The resin was washed with a mixture of 0.005M $H_2C_2O_4$ / 0.07 M HCl. ^{44}Sc (180 MBq) was eluted by a mixture of 0.07M HCl / 0.005M $H_2C_2O_4$ (20 ml), and small ^{44}Ti breakthrough (90 Bq), reflected an excellent separation result (separation factor 2 x 10^6).

2.1.1.4. Reverse ^{44}Ti/^{44}Sc generator scheme

The ^{44}Ti/^{44}Sc generator is designed to work for several years, thus requiring superb long term performance. Assuming that the generator is eluted every working day (up to 250 elutions per year), the overall elution volume will be from 5 to 50 litres. There may be differences for static and dynamic conditions using solid phase based ion exchange separations. ^{44}Ti ions desorbed under elution may migrate and re-adsorb at downstream resin capacities. With several subsequent elutions and/or high volume elutions, the maximum adsorption zone of the parent radionuclide, i.e. ^{44}Ti ions moves gradually. In Fig. 9 you can observe a hypothesized phenomenon for solid phase ion exchange method under static conditions (S) and dynamic conditions (D). Parent radionuclide migration and re-adsorbtion at downstream resin capacities (D2). Parent radionuclide adsorption zone gradual movement with subsequent elutions and/or high volume elutions at larger eluent volumes (D2). Supposing each elution which isolated the daughter is followed by a washing step using a fresh eluent of identical volume in opposite direction (red arrow in D3), the re-distribution of the parent zone is organized. This dual elution mode is referred to as ‘reverse’

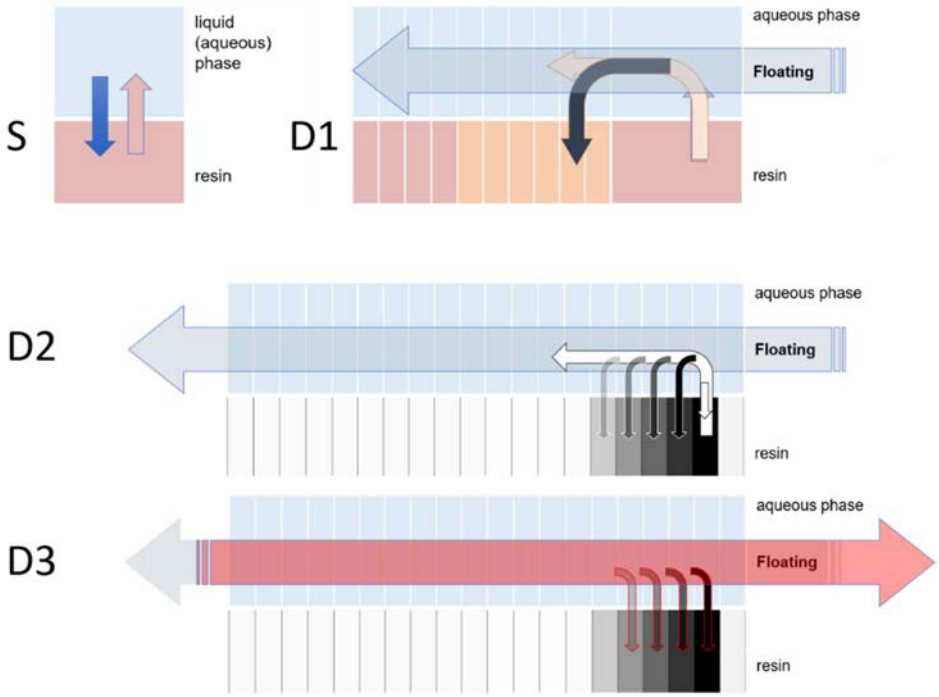

FIG. 9. Schematic mechanism of the parent radionuclide maximum adsorption zone (courtesy of F. Rösch, Johannes Gutenberg-Universität Mainz, Germany).

Figure 10 represents the 5 mCi generator column in a horizontal position (II) to avoid effects due to gravity. Two eluate solution reservoirs are connected to the inlet (I) and the outlet (III) position. Air pressure is applied through filter F to the reservoirs II and III to avoid contaminating the eluate composition by air borne metal contaminants. All parts are connected via tubing and three-way valves. The eluate solution of reservoir (I) (20 ml) is transferred through the radionuclide generator into the vial (IV) which contains ^{44}Sc. The generator is eluted backward ('reverse') followed by each elution, with the same eluate composition using reservoir (III) content. Reservoir (III) content is refreshed routinely, while the eluate in (I) can be used for the subsequent elution. This scheme guarantees safer handling, as it represents an inherently ^{44}Ti closed system. The system achieves ^{44}Sc elution yields of 97% (180MBq). The breakthrough of ^{44}Ti is only 5 x 10^{-5}% (90Bq).

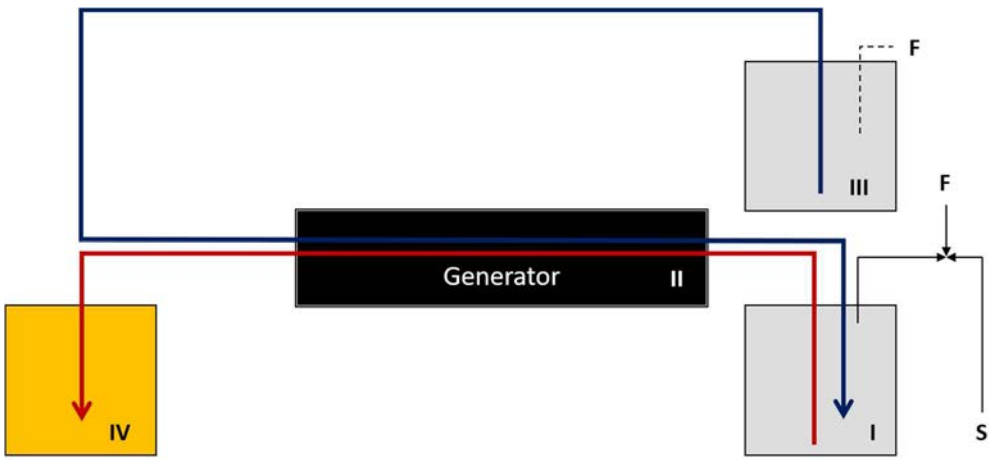

FIG. 10. The post-elution processing scheme of ^{44}Sc-eluates. Generator column I, Eluate reservoirs I and III, ^{44}Sc trap IV, completely closed system: S = syringe, F = filters. Red line is initial elution of ^{44}Sc, blue line is reverse flow of fresh elute solution (courtesy of F. Rösch, Johannes Gutenberg-Universität Mainz, Germany).

An alternative generator based on a Zr resin was tested [27] in direct and reverse elution modes. Direct elution showed breakthrough after approximately 40 resin bed volumes and reverse elution mode provide promising results with no breakthrough even after 65 column volumes. However, more data will be required to show feasibility of this generator scheme.

2.1.1.5. ^{44}Sc post-elution processing in ^{44}Ti/^{44}Sc generator for medical applications

Similar to post-processing ^{68}Ge/^{68}Ga generators approach for radiolabelling, an efficient post-elution processing for ^{44}Sc eluate on the cation-exchange resin was developed [34, 35]. An absorber material was identified and positioned online at the generator outlet to capture the radionuclide, followed by ^{44}Sc elution using a small volume of a suitable solution for subsequent labelling process.

The first step of the pre-concentration adsorbs ^{44}Sc from the generator eluate (0.005 M $H_2C_2O_4$/0.07M HCl mixture) using an appropriate resin. Utilization of the AG 50W-X8 (200–400 mesh, H^+-form) achieves 89% retention of ^{44}Sc. High recovery of ^{44}Sc (~90%) can be obtained using 0.25 M ammonium acetate buffer (for 3 ml, pH4.0 by addition of acetic acid). The schematic diagram of the online generator post-processing module system is illustrated in Fig. 11.

Finally, the 0.25 M ammonium acetate buffer (3 ml, pH4.0), is slowly pressed through the column V (0.7 ml/min). ^{44}Sc is collected in vial (VII) recovering ~90% of ^{44}Sc. The obtained ^{44}Sc solution is ready for labelling chemistry. The ^{44}Ti final content in the final ^{44}Sc fraction (140 to 160 MBq) is around 7 Bq, showing significantly low contamination ($<2 \times 10^{-7}$). The initial breakthrough of 5×10^{-5}% was thus further reduced by a factor of 10 [32].

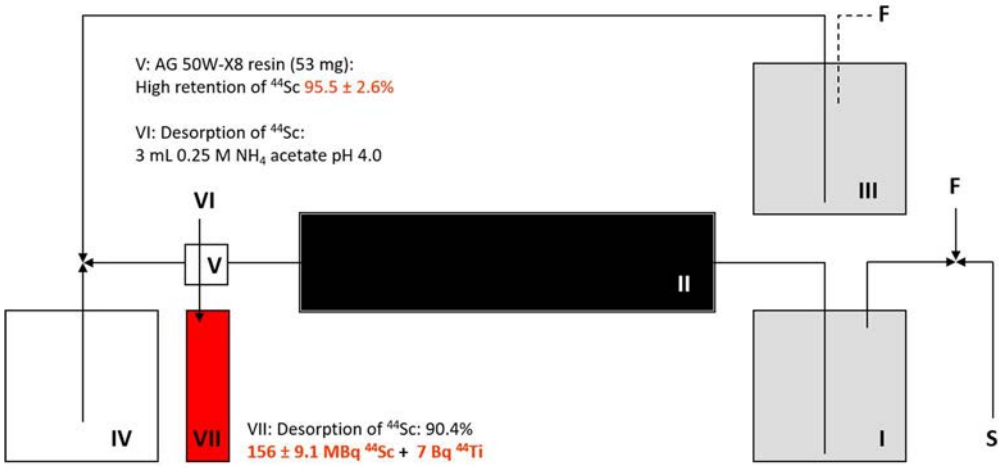

FIG. 11. Final schematic set-up of an on-line generator post-processing module: Miniaturized chromatography column (V) syringe (S) the cationic cartridge (V), waste vial (IV) (courtesy of F. Rösch, Johannes Gutenberg-Universität Mainz, Germany).

2.1.2. $^{43/44}$Sc production from solid Ca target

The direct production of ^{44}Sc is achieved using a Ca target via the Ca(p,n)^{44}Sc nuclear reaction, see Fig. 12. A number of sites have used natural metallic Ca [36, 37], as this offers simple thick target preparation and generally reasonable radioisotopic purity, despite the 2.09% natural abundance of ^{44}Ca. However, if even higher radioisotopic purity is needed, albeit met with challenges in thick target preparation, the use of enriched ^{44}Ca has also been extensively used [38]. From the published cross sections [29, 39, 40] it can be seen that the production cross

section has a maximum of ~650 mb in the 8–13 MeV energy range. Calcium carbonate targets have predominantly been used for target irradiation, but recently pressed CaO targets have also been reported [38]. Here, enriched calcium carbonate material is heated to 900°C to convert the carbonate to oxide form. The resultant powder is pressed as a pellet 6 mm diameter and 0.5 mm thickness (approximately 30 mg), using a two-ton press. The pellet is immediately encapsulated in aluminium, to avoid absorption of moisture from the air. The resultant target is irradiated at ~11 MeV, 50 μA, for 90 min to produce high yields of ^{44}Sc. Up to 50 μA beam intensity on target has been reported and high yields (~ 2 GBq) were obtained on ~10 mg enriched target material when irradiating for up to 90 min [41, 42]. It should be noted that ^{44m}Sc is co-produced as a contaminant using the (p,n) route.

The most popular nuclear reactions for the production of ^{43}Sc are ^{43}Ca(p,n)^{43}Sc and ^{46}Ti(p,α)^{43}Sc routes [43]. Cross-section measurements have shown a maximum of 283 ± 27 mb at a proton energy of 11.6 ± 0.6 MeV [29, 39]. $CaCO_3$ targets were irradiated with 12.0 ± 2.3 MeV and 10.4 ± 2.6 MeV protons, respectively, for 90 to 220 min (50 μA) to produce yields in the range of 250 to 480 MBq. Low impurity levels of ^{44m}Sc, ^{47}Sc and ^{48}Sc (0.34%), from a 57.9% enriched target material were determined using long term γ spectroscopic measurements.

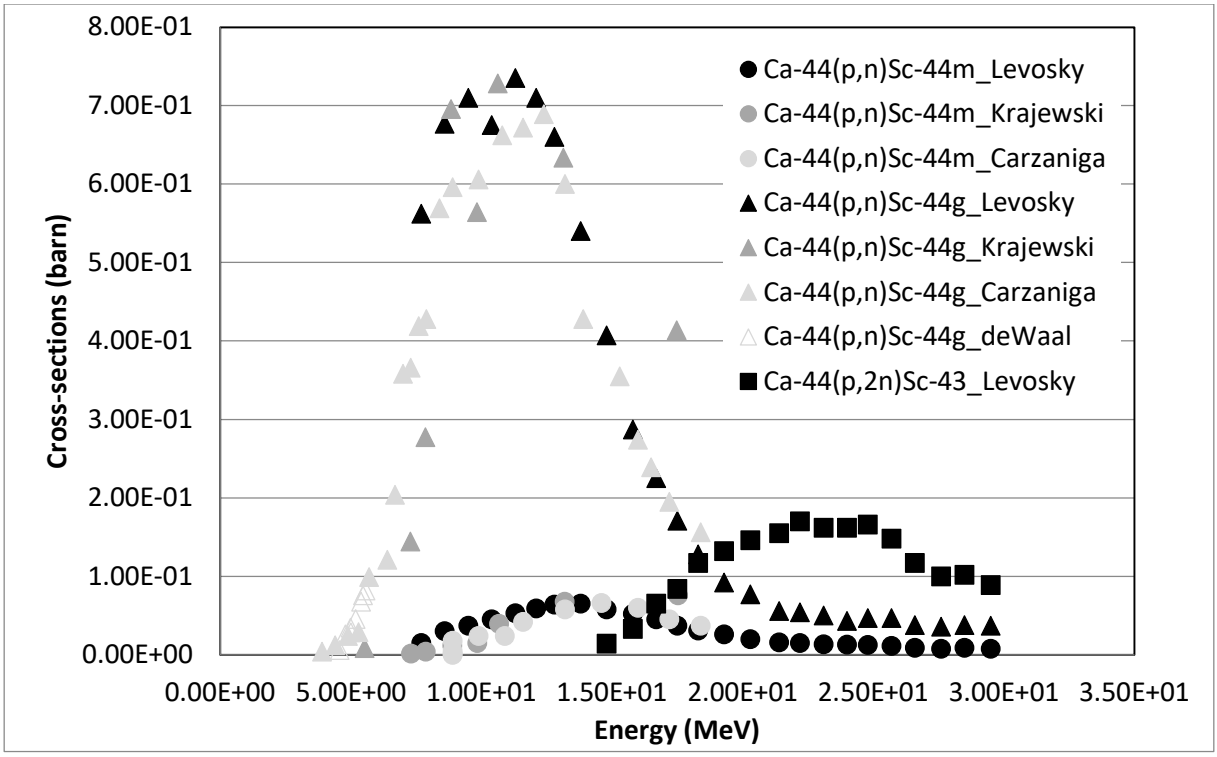

FIG. 12. Relevant calcium-based cross sections for ^{44}Sc production (courtesy of F. Alves, University of Coimbra, Portugal, and C. Hoehr, TRIUMF, Canada. Raw data extracted from [29, 39, 40, 44]).

Another means of producing ^{43}Sc from Ca targets is by taking advantage of the 15 fold higher natural isotopic abundance of ^{44}Ca vs. ^{43}Ca is the irradiation of ^{44}Ca via the (p,2n) nuclear reaction [45]. A concept of irradiating ^{42}Ca targets with deuterons was also suggested, with cross-section measurements being published in this regard [46]. It is suggested that the use of this nuclear reaction could yield good results. The ^{nat}Ca(α,p)^{43}Sc nuclear reaction has also been employed [1]. The ^{43}Sc yield at end of bombardment (EOB) is significantly higher with the ^{43}Ca(p,n)^{43}Sc nuclear reaction compared to ^{46}Ti(p,α)^{43}Sc production route. However, the latter yielded higher radionuclidic purity for ^{43}Sc (98.2% vs 66.6% from the Ca target). It should be noted that perhaps a ^{43}Sc/^{44g}Sc mixture is tolerable, regardless of the ratio, as it will surely be

better than ^{44}Sc alone from a dose/imaging/shielding point of view, and pure ^{43}Sc might not be so practical.

Some experts believe that ^{43}Sc is an attractive radiometal for PET application, however its limiting factor is the production rate and cost of Ca target material, thereby, potentially influencing its future implementation in theranostic applications. In the future, economic considerations have to be taken into account to decide which production route will be most feasible to provide ^{43}Sc in sufficient quantities for clinical applications. High current Ti targets may provide an alternative pathway for this isotope.

2.1.3. $^{43/44}$Sc production from solid Ti target

Scandium-43/44 production via the proton irradiation of Ti targets has been studied at a few institutions. While the reaction rates are typically lower than the (p,n) reactions, these methods can lead to high purity ^{43}Sc, which is not possible with currently available Ca enrichment levels. This method is also attractive as the analogous reaction pathway on ^{50}Ti can lead to the therapeutic ^{47}Sc, thus yielding a true matched pair theranostic approach.

Irradiations have been carried out using both natural and enriched TiO_2 pressed powder targets at 24 MeV up to 30 μA. Approximately 35 or 70 mg of TiO_2 was transferred into a clean 7 mm or 10 mm die and pressed for 5 min at 4 tons pressure on a manual press. Additional TiO_2 was iteratively added and pressed. This process was repeated twice to achieve final target masses of approximately 52 or 110 mg.

Alternatively, Ti metal targets may be used. Reduced ^{46}Ti metal powder (9 to 28 mg) can be placed over graphite powder (~150 mg) and compressed into pills (5 to 7 tons of pressure). The resulting target ranged between 0.4 mm and 0.5 mm thickness, (diameter; 16mm). The pellet was encapsulated in aluminium and irradiated. Using 15.1 ± 1.9 MeV protons, ^{46}Ti targets were irradiated (beam current: 30 μA, 60 to 420min).

Enriched $^{46}TiO_2$ was mixed with excess CaH_2 (2.3 to 4.6 mmol/tablet) followed by grinding into a fine powder (under dry Ar atmosphere). A 10 mm tablet is obtained by placing the ground mixture between two layers of ~ CaH_2 (80mg). The mixture is pressed under three tons pressure (30 to 40 sec). The resultant tablet is then placed into a tantalum container and set inside a Ni tube. The latter tube was evacuated under low pressure (10^{-3}–10^{-5} mbar). A temperature increase program was used to consolidate the enriched mixture (gradually increased from 800 to 1000°C during 60–120 min) and the temperature maintained for 30min. The reduction products were retrieved after cooling, and the metallic ^{46}Ti isolated from the co-produced CaO using dilute acetic acid. For target preparation, the reduced ^{46}Ti metal powder can be directly used.

2.1.4. ^{44}Sc production from liquid Ca target

Alternatively, ^{44}Sc is produced in a liquid target via the ^{44}Ca(p,n)^{44}Sc reaction [47]. The advantage of liquid target production is the familiarity of many medical cyclotron sites with liquid targets, especially if there is no solid target station available. The disadvantage is the relatively lower yield when compared with a solid target due to the reduced starting material density.

In a study up to 54 g of $Ca(NO_3)_2 \cdot 4\ H_2O$ with Ca of natural abundance was dissolved in 25 ml of purified water [47]. The natural abundance of ^{44}Ca is only 2.09%. The density of the solution

was 1.55 ± 0.005 g/ml and the Ca concentration amounted to 0.1800 ± 0.0006g/cm^3. The solution was remotely pushed with He gas into a liquid target with an internal volume of 0.9 ml, identically to the design of an ^{18}F target. 12 MeV protons were used to irradiate the target solution in triplet (beam current: 7.8 ± 0.3 µA, 60 ± 0.5 min). The beam current was limited by the pressure rise in the target due to radiolysis. After the irradiation, the solution was then remotely pushed with He into a vial in a hot cell close to the cyclotron. The activity measured via gamma spectroscopy was found to be 5.7 ± 0.5MBq. This corresponds to a saturation yield of 4.6 ± 0.3MBq/µA. Other observed co-produced isotopes of Sc were ^{43}Sc (3.3% of the ^{44}Sc activity), ^{44m}Sc (0.42%), ^{47}Sc (0.16%) and ^{48}Sc (1.4%). When using enriched ^{44}Ca as the starting material, fifty times more ^{44}Sc can be produced. This will also reduce the amount of co-produced Sc isotopes, except ^{44m}Sc which is being mainly co-produced from ^{44}Ca as well.

2.2. $^{43/44}$Sc PURIFICATION

2.2.1. $^{43/44}$Sc purification, recovery & QC from Ca target

Irradiated $CaCO_3$ solid targets can be dissolved in HCl (3.0 M) and loaded onto a column containing ~80 mg DGA (N,N,N′,N′-tetrakis-2-ethylhexyldiglycolamide) extraction resin (Fig. 13). The desired Sc product was retained by the resin, while the Ca was not adsorbed. The load fraction was segregated from other waste for the target recycling process. The Sc product was eluted from the resin using 0.1M HCl, before loading it onto a small strong cation exchange cartridge such that the Sc product could be concentrated and eluted in a small volume (<1 ml) 4.8M NaCl / 0.1M HCl. A subsequent method was developed, where two columns containing DGA resin were used: the eluant from the first column was concentrated and passed through a smaller second column for concentration purposes. The final product was obtained in 0.05M HCl for use in preclinical studies [42].

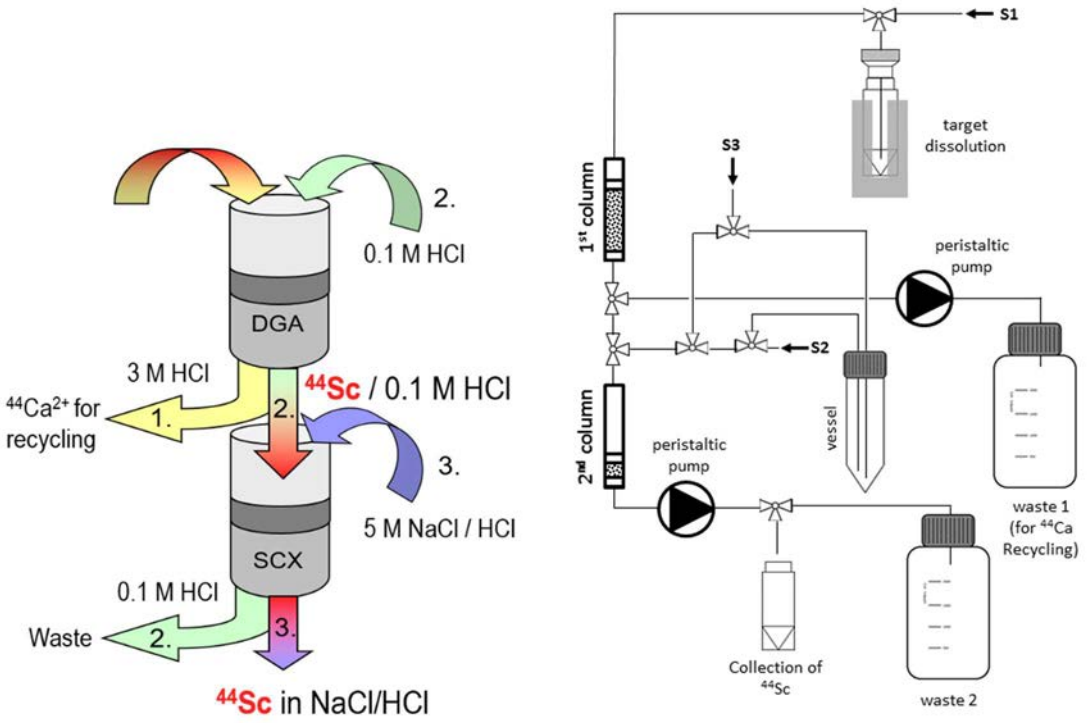

FIG. 13. (Left) Purification schematic of ^{44}Sc from Ca target, (Right) Flow diagram of scandium purification (courtesy of N. Van der Meulen, Paul Scherrer Institut, Switzerland).

The main contaminants that can be expected in the final product include calcium, zinc, iron, and nickel. The latter three elements are strong competitors for DOTA complexation, as their thermodynamic stability constants are similar to that of scandium [37]. As a result, onsite QC of the product can be assessed by radiolabelling of a ligand with a DOTA chelator, as excess of these contaminants will compromise the molar activity of this process. The radiolabelling process is as follows: 2 ml, 0.2 M, pH4, sodium acetate buffer, DOTA-1-Nal3-octreotide (NOC) (70 µl, 0.7 nmol/µl) and the ^{44}Sc product solution (300–600 MBq, pH4.5, ~600 µl) were mixed in a borosilicate vial and heated at 85°C for 15min. QC is assessed using high performance liquid chromatography (HPLC) with a C-18 reversed-phase column (mobile phase: 95% MilliQ water, 0.1% trifluoracetic acid, 5% acetonitrile, 20 min period, flow rate: 1 ml/min). The recycling of the enriched ^{44}Ca material is described in Fig. 14.

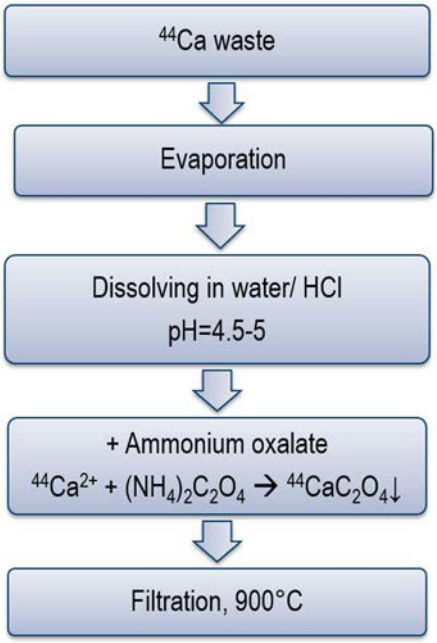

FIG. 14. Method of recycling enriched Ca target material to CaO. It is recommended that more than 50 mg recyclable material is used to ensure high recycling yields (courtesy of N. Van der Meulen, Paul Scherrer Institut, Switzerland).

2.2.2. $^{43/44}$Sc purification and QC, and target recovery from solid Ti target

The irradiated Ti metal target content was initially dissolved in hot, 8.0M HCl, before being diluted to 4.0 M and loaded onto a DGA extraction resin column (1 ml size, ~85 mg resin). Sc(III) is strongly retained on DGA resin at HCl (<6 M) [48], while Ti has negligible sorption under similar conditions. The resin was rinsed with 4.0M HCl to fully remove ^{46}Ti residues, prior to ^{43}Sc elution (4.0 ml, 0.1M HCl). The results was loaded directly onto a second column containing strong cation exchange resin. In the latter column, ^{43}Sc was concentrated and could easily be eluted in small volumes (<1 ml 4.8M NaCl / 0.13M HCl). Although, the theoretical values indicated potentially higher yields, up to 2 340 MBq, the practical yield of product at EOB was lower (60–225 MBq ^{43}Sc). Low activity levels of ^{44m}Sc, ^{46}Sc, ^{47}Sc and ^{48}Sc, were determined using long term γ-spectroscopic measurements [43].

The eluate from the DGA column in the initial load step containing Ti was collected and heated to boiling. The mixture pH was adjusted to 8.0 (using 25% NH_3 solution) to yield a black precipitate. The latter was transformed into TiO_2 powder during a 40 min process. The precipitated mixture was filtered through a glass filter crucible, heated to 400°C and the

temperature maintained for 1 h to ensure complete oxidation. While oxide targets have been used to produce ^{47}Sc [49], the volume of hot, concentrated H_2SO_4 required to dissolve the target material is large.

A recent alternative method was reported for the dissolution of TiO_2. Irradiated TiO_2 targets were dissolved using a mixture of NH_4HF_2/HCl (a perfluoroalkoxyalkane closed flask must be used). Irradiated TiO_2 was transferred into a conical 15 screw-cap vial and mixed with NH_4HF_2 (1:3 ratio). The vial was capped and heated to 230°C for minimum 45 min. After heating, the dry residue was dissolved by adding 5 ml of 12.1M HCl and heating the closed vessel for 45 min in a Si oil bath at 160°C. Using branched N,N,N',N'-tetra-2-ethylhexyldiglycolamide resins, scandium radionuclides were purified via ion exchange chromatography. The final eluate containing the Sc radionuclides was collected into a 10 ml conical vial and evaporated to dryness under vacuum at 100°C. After evaporation, the purified Sc was reconstituted in 0.5M $CH_3CO_2NH_4$ buffer. This resulted in an average ratioscandium recovery of ~95% and nearly quantitative Ti recovery via alkali precipitation with ammonia solution.

2.3. $^{43/44}$Sc RADIOLABELLING EXAMPLES

The trivalent d-element Sc(III) undergoes complex formation with a variety of chelators. Similar to Ga(III), macrocyclic, hybrid and non-macrocyclic chelators have been reported to work efficiently in radio-Sc(III) coordination chemistry. Figure 15 shows the various chelators that have been investigated.

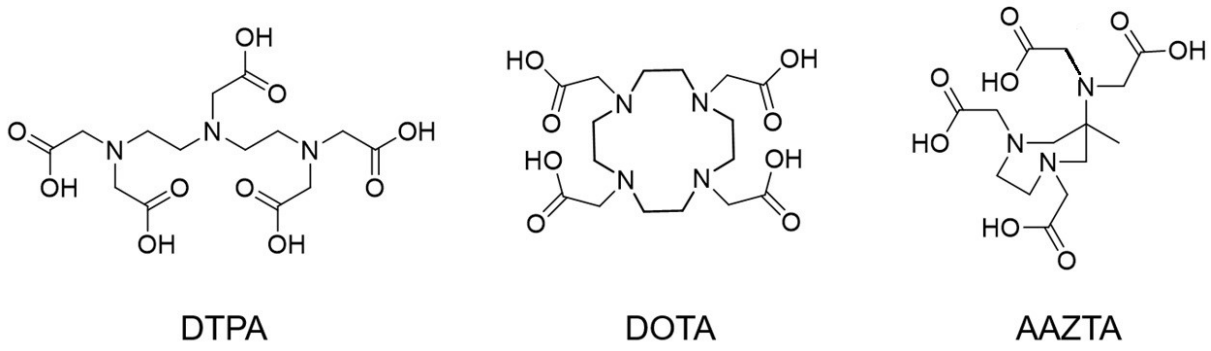

FIG. 15. Various chelators investigated with scandium (courtesy of A. Jalilian, IAEA, Austria).

2.3.1. DOTA, NOTA and other tetraaza-based macrocycles

The thermodynamic stability constants (logK) of the DOTA and other tetraaza-based macrocycles are far higher than open chain chelator analogs, such as EDTA or DTPA. For example, the thermodynamic stability constants of Gd^{III}-DOTA and Gd^{III}-DTPA are logK. 25.8 and 22.1, respectively. Thermodynamic stability constants for Sc^{III}-DOTA and DTPA complexes are logK. 27.0 and 20.99, respectively [50–52], and are thus even more stable than Lu^{III} or Ga^{III} analogues [20].

The DOTA potentials for preparation of peptide conjugates and other targeting vectors with ^{44}Sc was investigated systematically. DOTA-TOC and DOTA-TATE were used as model molecules to evaluate and optimize the labelling procedure for various vectors [31]. Reaction factors (buffer type and conditions, peptide concentrations, pH, temperature and time) have been optimized. Experimental data confirmed the Sc^{III}-DOTA stability. For instance, a specific

amount of DOTA-TOC (21 nmol) can be labelled using processed ^{44}Sc eluate (2 ml) in ammonium acetate buffer (2 ml, pH4.0) in high labelling yields (>98%) in 25 min (oil bath, 95ºC), though the reaction time can be reduced to 3 min by using a microwave oven. The product was stable in various solutions, including 0.9% NaCl, PBS (pH7.4), pure ethanol and interestingly in the presence of metal cations (Fe^{3+}, Ca^{2+}, Cu^{2+}, Mg^{2+}). Even the presence of competitors like EDTA and DTPA did not affect the stability of the product. [^{44}Sc]Sc-DOTA-TOC as synthesized from ^{44}Ti/^{44}Sc generator derived ^{44}Sc was the first ^{44}Sc labelled PET tracer successfully used in human studies [20, 21]. The same compound [^{44}Sc]Sc-DOTA-TOC was also reported in human application based on direct production [53].

Several other DOTA conjugated molecular targeting vectors have been studied, see Table 2 [54–59]. Various clinically important ligands including two new somatostatin analogs [54], prostate specific membrane antigen inhibitor (PSMA)-617 [55], human epidermal growth factor receptor 2 (HER2) antibody [56], cyclic arginine glycine aspartate [57] were labelled with ^{44}Sc using DOTA as a chelator. In addition, DOTA conjugated tetrazine [58] and DTPA [59] were also reported to be labelled with ^{44}Sc. In general, DOTA based compounds were successfully labelled with ^{44}Sc at pH4.0–5.0 at 90ºC. For diagnosis and therapy of prostate cancer PSMA inhibitors, such as DOTA-PSMA-617, were labelled with ^{44}Sc for various purposes, most importantly for patient based dosimetry. For NOTA, the trend is opposite than for DOTA: Sc-NOTA has a logK of 14.8 only [53, 60]. Accordingly, attempts to label NOTA or NODAGA conjugated targeting vectors were of limited success.

TABLE 2. RADIOLABELLING EXAMPLES FOR ^{44}Sc

(courtesy of M. Pandey, Mayo Clinic, United States of America, and C. Hoehr, TRIUMF, Canada)

Chelator	Ligand	Reference
DOTA	PSMA-617	[31, 55, 58, 61–63]
DOTA	Somatostatin analogs	[54, 64]
DOTA/NODAGA	Arginylglycylaspartic acid (RGD) peptides	[42]
DOTA	HER_2 affibodies	[56]
DOTA	A dimeric cyclic-RGD peptide, $(cRGD)_2$	[57]
DOTA	Tetrazine	[58]
DTPA	Cetuximab fab fragment	[59]
DOTA	BN[2-14]NH_2 (Bombesin analog)	[65]
DOTA	Puromycin	[66]
DOTA	*N*-(2-hydroxypropyl)methacrylamide (HPMA)	[67]
DOTA	n.a.	[68]
DOTA	Folate	[69]
DOTA	NAPamide (Alpha- melanocyte stimulating hormone (MSH) analog binds to MC1-R)	[70]
H_4pypa	TRC105 (A monoclonal antibody)	[71]

3. PRODUCTION OF ^{61}Cu

3.1. PHYSICS AND TARGET MATERIAL

Copper has several radioisotopes with complementary nuclear decay characteristics. Namely, there are four positron emitting copper radioisotopes with half-lives suitable for PET applications – i.e. ^{60}Cu, ^{61}Cu, ^{62}Cu, ^{64}Cu and a long lived β^- emitter suitable for therapy – i.e. ^{67}Cu. Each of these copper isotopes can be used either on their own, or, they may be used as a theranostic pair for patient selection and dosimetry estimation prior to radiotherapy, see Table 3.

TABLE 3. LIST OF COPPER ISOTOPES

(Courtesy of F. Alves, University of Coimbra, Portugal, and K. Gagnon, GE Healthcare, Sweden)

Radioisotope	Half-life	Decay mode	Intensity	β energy (keV)		γ energy (keV) and intensity
			(%)	maximum	mean	Most abundant γ-line
Cu-60	23.7 min	β+	93	3773.5	970	467.3 (3.52%) 826.4 (21.7%) 1332.5 (88.0%) 1791.6 (45.4%)
Cu-61	3.339 h	β+	61	1215.58	500	282.956 (12.7%) 656.008 (10.4%)
Cu-62	9.673 min	β+	97.83	2936.9	1319.0	1172.97 (0.342%)
Cu-64	12.701 h	β+	17.60	653.03	278.21	1345.77 (0.475%)
		β-	38.5	579.4	190.70	
Cu-67	2.58 days	β-	100	561.7	141	91.266 (7.00%) 93.311 (16.10%) 184.577 (48.7%)

Of the positron emitting copper radioisotopes, ^{64}Cu is currently the most commonly used in clinical settings (see Fig. 16). This is perhaps due to its relatively longer half-life of 12.701 h which therefore enables distribution to distant application centres. Although ^{60}Cu ($t_{½}$ = 23.7 m) and ^{62}Cu ($t_{½}$ = 9.673 min) may have applicability at selected sites, their short half-lives make the large scale adoption of these isotopes a challenge. On the other hand, ^{61}Cu presents an interesting high potential as a viable PET radionuclide (see Fig. 17), for the production cross sections. Its moderate 3.339 h half-life enables regional distribution and it is especially suited to study kinetics of tracers that show maximum uptake 4 to 8 h post injection, thus filling the gap between the 110 m half-life of widely used ^{18}F and the longer 12.7 h of ^{64}Cu, making it ideal for labelling with peptides. In addition, ^{61}Cu offers an approximate three fold higher positron branching ratio when compared with ^{64}Cu (i.e. 61 vs 17.60%), resulting in higher signal images with potentially lower patient dose [72].

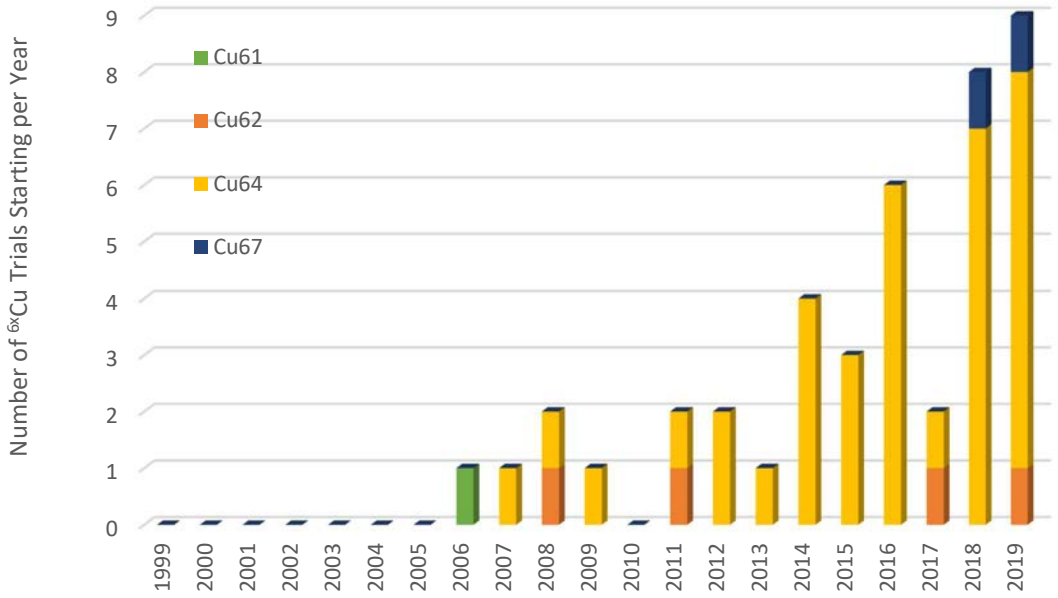

FIG. 16. The number of ^{6x}Cu clinical trials starting per year (courtesy of K. Gagnon, GE Healthcare, Sweden, data compiled from several reports accessed at https://clinicaltrials.gov/).

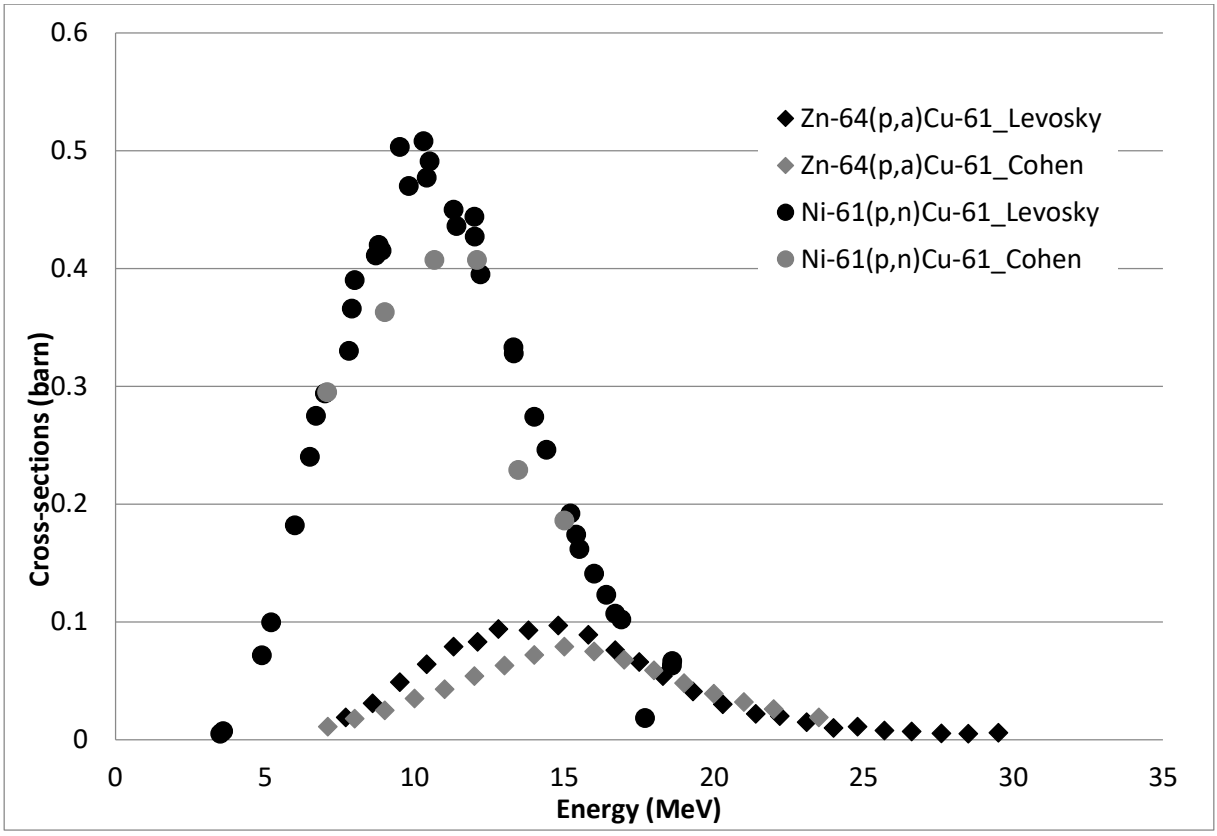

FIG. 17. Proton induced production cross sections for ^{61}Cu (courtesy of F. Alves, University of Coimbra, Portugal, and C. Hoehr, TRIUMF, Canada. Raw data extracted from [29, 72]).

In the context of ^{61}Cu production, one additional advantage when compared with ^{64}Cu is that it is possible to obtain relatively high radioisotopic purity by irradiation of natural abundance targets, including proton irradiation of natural zinc or deuteron irradiation of natural nickel. By changing to enriched target materials, yields can be scaled accordingly. Table 4 lists relative thick target yields for select examples, assuming similar irradiation parameters (13.0 MeV as

proton energy and 8.4 MeV as deuteron energy incident on the target, respectively). The use of both liquid and solid targets using zinc or nickel have been explored as routes to ^{61}Cu production as described below.

TABLE 4. DIFFERENT PRODUCTION ROUTES FOR ^{61}Cu ISOTOPE
(*Courtesy of K. Gagnon, GE Healthcare, Sweden. Calculated using the IAEA medical isotope browser*)

Route	Natural abundance (%)	Recycle?	Relative Thick Target Yield (%)
^{nat}Zn(p,α)	100	No	4
^{64}Zn(p,α)	49.17	Not necessary	9
^{nat}Ni(d,n)	100	No	4
^{60}Ni(d,n)	26.223	Not necessary	15
^{61}Ni(p,n)	1.1399	Yes	100

3.1.1. ^{61}Cu production from solid Ni target

In considering the production of copper from nickel targets, the most common strategy for target preparation is by electroplating of nickel. As the techniques for electroplating are agnostic to the isotope of nickel which is being electroplated, and given the vast literature reporting on ^{64}Ni target preparation in the context of ^{64}Cu production, we refer here to Section 2.3 of the IAEA Radioisotopes and Radiopharmaceuticals Reports No.1 [16] which extensively describes nickel quality requirements, nickel target backing materials, electrode and electroplating conditions, and further, gives three different step by step examples. Nevertheless, in the context of nickel target preparation for ^{61}Cu, there are select unique considerations as related to target thickness requirements. If considering proton irradiation, since protons have a longer range in matter when compared with deuterons of the same energy, significantly thicker nickel targets will be required if aiming to stop the full proton beam energy. However, due to the low natural isotopic abundance, thick ^{61}Ni targets may be prohibitively expensive. To this end, it is often strategic to decrease the incident irradiation energy in order to maximize the yields for a reaction and target thickness. To demonstrate this, Table 5 provides four different ^{61}Ni(p,n)^{61}Cu irradiation scenarios (normalized to Scenario A) with relative yields calculated using the IAEA Medical Isotope Browser[1] [73].

TABLE 5. THE RELATIVE YIELDS AND MATERIALS USED FOR FOUR DIFFERENT ^{61}Ni(p,n)^{61}Cu IRRADIATION SCENARIOS, NORMALIZED TO SCENARIO A
(*courtesy of K. Gagnon, GE Healthcare, Uppsala, Sweden. Calculated using IAEA medical isotope browser and SRIM [64])*

Scenario	Energy range (MeV)	Yield	Material use
A	17 → 0	100%	100%
B	13 → 0	73%	63%
C	13 → 7	64%	41%
D	17 → 13	27%	37%

[1] The IAEA Medical Isotope Browser can be accessed at https://www-nds.iaea.org/relnsd/isotopia/isotopia.html.

It can be seen in Table 5 that it is possible to maintain nearly two thirds of the yield, with only ~40% of the ^{61}Ni target material, provided the energy is appropriately selected to maximize the area under the curve. Scenarios C and D are also noted graphically in Fig. 18 [74], for which a clear benefit of decreasing the energy is noted in order to maximize the area under the excitation function.

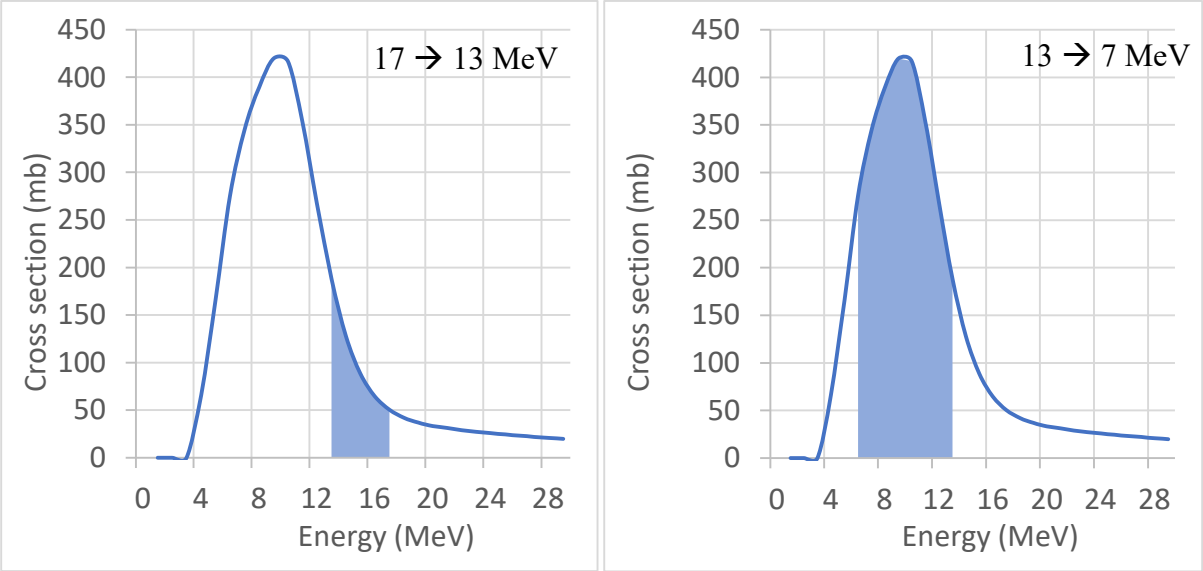

FIG. 18. A comparison of ^{61}Cu production for 17 → 13 and 13 → 7 MeV noting a benefit for maximizing the area under the excitation function (cross sections taken from TENDL-2015 (courtesy of K. Gagnon, GE Healthcare, Sweden).

3.1.2. ^{61}Cu production from solid Zn target

Production of ^{61}Cu is readily possible using proton irradiation of natural zinc at the specific energy range based on calculations using ALICE code [75] as well as some other experimental data. It was calculated that 22–12 MeV proton range is optimum beam energy to produce ^{61}Cu with the highest thick target yield and the least radionuclidic impurities. Based on SRIM calculations, an 80 mm zinc layer was enough target thickness in production [73]. A layer of natural zinc, electroplated on a gold layered (50 µm), copper backing was used to prevent leaching of the natural copper support during radiochemical separation (Fig. 19). In order to prepare an electrodeposition bath, an ultrapure pure (99.99%) metallic gold sample (3.00 g), was dissolved in aqua regia (60 ml) and heated at 50°C to reduce the volume to 10%. The residue was re-dissolved in conc. HCl (25 ml) and heated to 100°C. Distilled water (30 ml) was added to the residue and evaporated (twice). Ammonium hydroxide solution (1 ml, 25%) was added until a brown precipitate formed. To the latter, solid KCN (1–2 g) was added portion wise to prepare a colourless transparent liquid. To a stirring mixture of KH_2PO_4 (45 g), citric acid (45 g) and KCN (30 g) in distilled water (100 ml), the latter transparent liquid was added and the mixture was reconstituted to 450 ml by the addition of distilled water. For electroplating using this bath, a current density of 1.2 A/dm^2 at 60°C was used (pH6.0, using 0.1M KOH). A platinum anode was used to obtain a 50 µm gold layer on the copper backing after 20h.

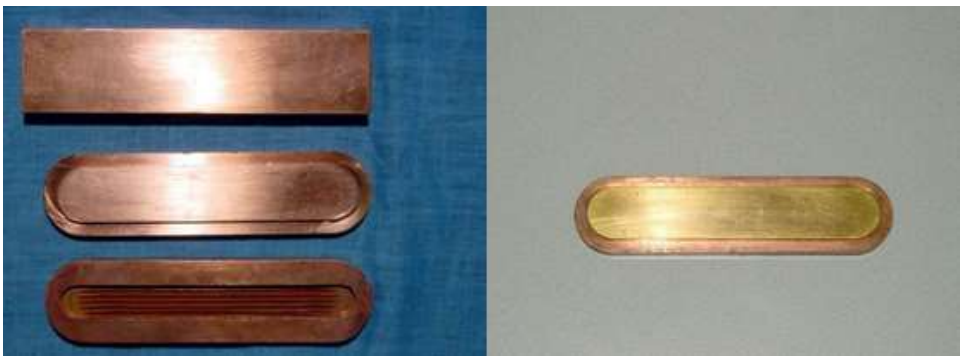

FIG. 19. (Left) The copper target body surfaces (unfinished target (up), electroplating surface (middle) and water-cooled surface (below) and (right) gold-plated target used for zinc electroplating (courtesy of A. Jalilian, IAEA, Austria).

After preparing the copper backing with the gold layer, the natural zinc was electroplated onto the backing with a calculated thickness enough to reduce the proton energy to the desired range (from 22 MeV to 12 MeV). For electroplating, a natural zinc bath solution was prepared by the dissolution of ZnO (twice the required electroplated mass) in 0.05 N HCl. As the reducing agent hydrazine dihydrochloride (2 ml) was added and electrodeposition performed using this bath solution (conditions: pH2.5–3, cell volume: 480 ml, accurate density:35 mA/cm^2, Pt; anode). The process resulted appropriate zinc target layer (100 µm) on the gold coated copper backing (3.5h). The target can provide multi-curie activity at EOB.

3.1.3. ^{61}Cu production from liquid Ni target

The production of radiometals using liquid targets [9, 13, 47, 76] underwent remarkable progress in recent years, mainly fostered by the growth of its application to the production of ^{68}Ga [14, 76]. The production of ^{61}Cu using the ^{61}Ni(p,n)^{61}Cu nuclear reaction [77] was explored in a liquid target at Mayo Clinic using natural $Ni(NO_3)_2{\cdot}6H_2O$ on a BruceTech TS-1650 target with a 0.16 mm thick Nb target window, see Fig. 20 [78]. The target solution was prepared by dissolving natural $Ni(NO_3)_2{\cdot}6H_2O$ (1.48 g, 1.7 M, 3 ml) in varying concentrations of nitric acid (0.001 N – 1.0 N) to mitigate the formation insoluble $Ni(OH)_2$ during proton irradiation due to the radiology of water and subsequent reaction with metal [9]. Nickel nitrate

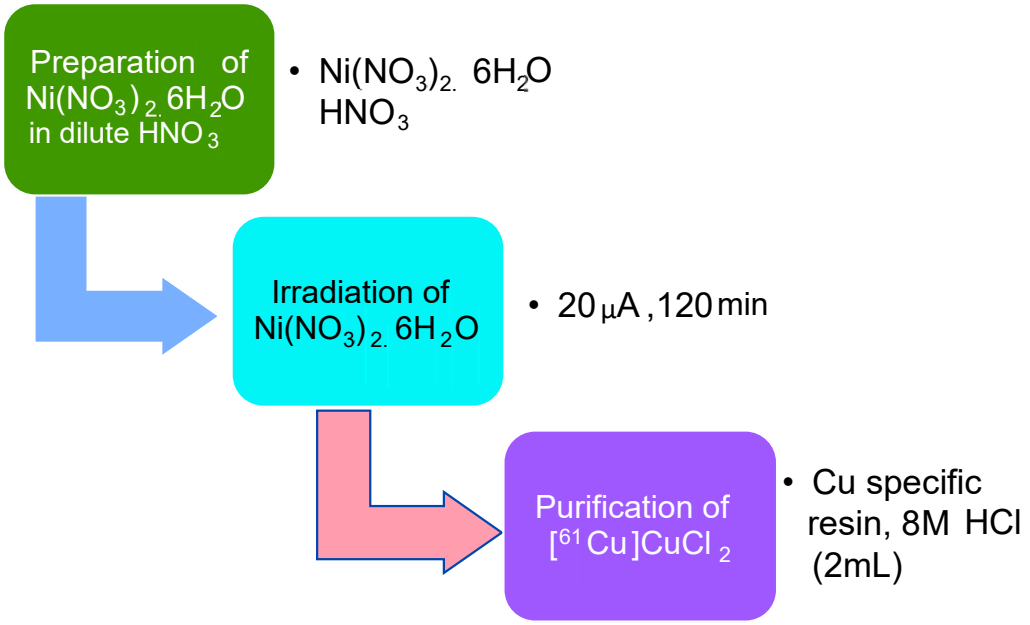

FIG. 20. Outline of ^{61}Cu production using natural nickel in liquid target (courtesy of M. Pandey, Mayo Clinic, United States of America).

solution in dilute nitric acid was irradiated at 20 μA for 2 h using PET trace cyclotron. The lowest concentration of nitric acid (0.001 N) was found to be sufficient to prevent the formation of insoluble $Ni(OH)_2$.

3.1.4. ^{61}Cu production from liquid Zn target

In addition, the liquid target methodology using the $^{64}Zn(p,\alpha)^{61}Cu$ nuclear reaction has been successfully demonstrated as a convenient production method for ^{61}Cu [79], using inexpensive ^{nat}Zn, benefiting from 48.6% natural abundance of ^{64}Zn, and thus leading to a cost efficient alternative to the use of alternative nuclear reaction $^{61}Ni(p,n)^{61}Cu$, characterized by prohibitive prices of ^{61}Ni (natural abundance 1.14%).

^{nat}Zn or enriched ^{64}Zn target solutions are commercially available from specialized vendors or can be prepared on site by the dissolution of ^{nat}Zn or ^{64}Zn in nitric solution followed by dilution in 10 mM nitric acid [79]. High Zn concentrations, up to 250 mg/ml can be used, leading to the production of up to 300 MBq of ^{61}Cu in a 45 min irradiation of 3 ml of ^{nat}Zn target solution [80]. Scaling up total production amount can be achieved by the use of enriched ^{64}Zn – which also result in the reduction of impurities originating from the irradiation of other isotopes of Zn – and/or longer irradiations [80].

3.2. ^{61}Cu PURIFICATION

3.2.1. ^{61}Cu purification, (recovery) & QC from solid Ni target

^{6x}Cu are commonly produced from electroplated Ni targets, where extensive information regarding production of ^{64}Cu from both Ni and Zn materials are reviewed in sections 2.5.1 and 2.5.2 of the IAEA Radioisotopes and Radiopharmaceuticals Reports No.1 [16], respectively. In the context of ^{64}Cu purification from Ni targets, the noted report discusses target dissolution, the importance of using high quality reagents, two anion exchange based purification schemes, subsequent cation purification, and automation. These discussions serve as an excellent basis for ^{61}Cu purification and thus are not repeated here since methods developed for ^{64}Cu purification are generally applicable for ^{61}Cu. However, there are some differences which should be highlighted as noted below.

First, when evaluating which purification method to employ, a method that is faster might be preferred for ^{61}Cu due to its shorter, 3.3 h half-life vs. ^{64}Cu ($t_{½}$ = 12.7h). Next, when producing ^{61}Cu from Ni, while recycling enriched ^{61}Ni is likely desired from a cost perspective, depending on a site's expertise/setup, etc., recycling may or may not prove cost effective when using ^{60}Ni as the target material.

Finally, in considering radiocobalt impurities, the $^{64}Ni(p,\alpha)$ reaction produces ^{61}Co ($t_{½}$ = 1.649h), with other radiocobalt impurities (e.g. ^{55}Co, etc.) arising largely from the small quantities of other ($A \neq 64$) Ni isotopes in the isotopically enriched starting material. In the context of ^{61}Cu, however, among other reactions on other Ni isotopes, the dominant $^{61}Ni(p,\alpha)$ and $^{60}Ni(d,\alpha)$ reactions will give rise to long lived ^{58}Co ($t_{½}$ = 70.86 d). For example, McCarthy et al. [3] and Strangis et al. [81] noted that 0.05% and 0.11% of produced ^{58}Co relative activity compared with ^{61}Cu, respectively. As such, efficient purification from radiocobalt by-products may prove to be even more important in the context of ^{61}Cu purification.

In considering QC of ^{61}Cu, Section 2.6 of the IAEA Radioisotopes and Radiopharmaceuticals Reports No. 1 [16] presents in great detail on ^{64}Cu radionuclidic purity, apparent molar activity

(previously referred to as effective specific activity), and cold metal analysis via ion chromatography, ICP-OES, X ray fluorescence, and voltammetry. Other than a different radiocobalt impurity profile, and an emphasis on the importance of assessing such contaminants with regards to radionuclidic purity, the QC discussion presented in the earlier publication is directly applicable to ^{61}Cu, and thus not repeated here. We do, however, present an additional test method (applicable to both ^{61}Cu and ^{64}Cu) for cold metal analysis which was not presented in the earlier publication.

One fast and inexpensive method to assess cold contaminants without having sophisticated equipment, or shipping samples to a third party (which is often a challenge with radioactivity), is by using commercially available semi-quantitative test strips or kits that exist for several elements. These strips and kits are especially useful for screening during development efforts as they provide instant, visual feedback. The main drawback with these analysis methods are their large sample consumption (particularly for the kits) which do not render suitable for routine QC, and/or, may require sample dilution or scaling down of test volumes. Furthermore, there is sometimes quite a wide range between the visual comparison points (colour card/chart).

It should be noted that these tests may not replace routine chemical purity tests for radionuclide production for ultimate use in human subject or animals, however, these tests may prove quite useful for select applications, during the development of appropriate chemical separation methods. The kits can enable sub ppm analysis of the sample which is a valuable tool. Shown in Fig. 21, there are three examples colorimetric test strips and a commercial test kit for:

— Cu strips (Scale: 10-30-100-300 mg/L);
— Co^{2+} strips (Scale: 10-30-100-300-1000 mg/L);
— Ni strips (Scale: 10-25-100-250-500 mg/L);
— Ni kit (Scale: 0.02-0.04-0.07-0.10-0.15-0.2-0.3-0.4-0.5 mg/L).

FIG. 21. Commercially available semi-quantitative metal detection test strips and colour card comparator kit (courtesy of K. Gagnon, GE healthcare, Sweden).

In order to separate the ^{61}Cu following solid target irradiation, see Fig. 22, the irradiated target was dissolved in HCl (10 M, 15 ml, H_2O_2 added) and the dissolved product was transferred onto a cation exchange resin (AG 50W, mesh 200–400, H^+ form, h ¼ 10 cm, +¼ 1.3 cm), preconditioned with 9M HCl (25ml). The cation exchange resin was then washed by 9M HCl (by 25 ml, flow rate:1 ml/min) to remove copper and zinc ions. In the next step, water (30 ml) and 6M HCl solution (100 ml) were added to the eluate and the final solution was transferred onto another exchange resin for final ^{61}Cu elution. The resin was AG1X-8 Cl form, 100–200 mesh) and loaded in a column (h ¼ 25 cm, +¼ 1.7 cm) pre-treated with HCl (6 M, 100 ml). [^{61}Cu]$CuCl_2$ was eluted using 2M HCl (50 ml) (whole process time was 60min).

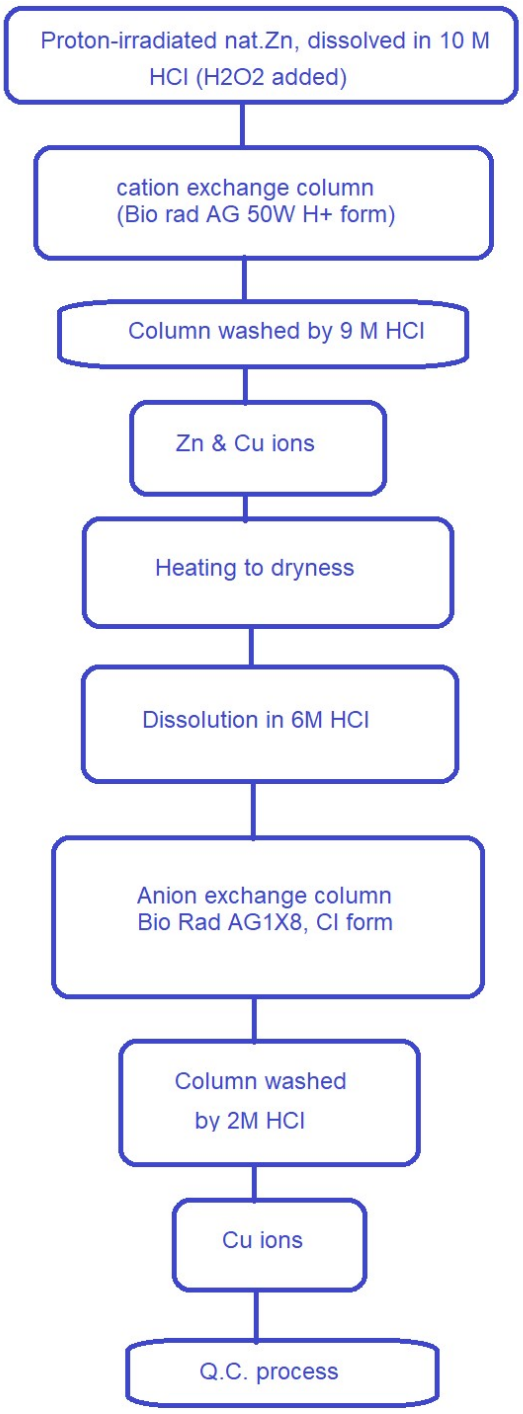

FIG. 22. Schematic steps for the separation of ^{61}Cu from the irradiated Zn target (courtesy of A. Jalilian, IAEA, Austria).

3.2.2. ^{61}Cu purification & QC from solid Zn target

For the QC of the product, radionuclidic purity was checked by γ spectroscopy of the final sample using a high purity germanium (HPGe) detector equipped with a multi-channel analyser (1 000 sec) (Fig. 23). The next most abundant γ lines (keV) are 283, 373, 511, 565 and 1186 keV which are related to the product showing significantly high radionuclidic purity (>99%).

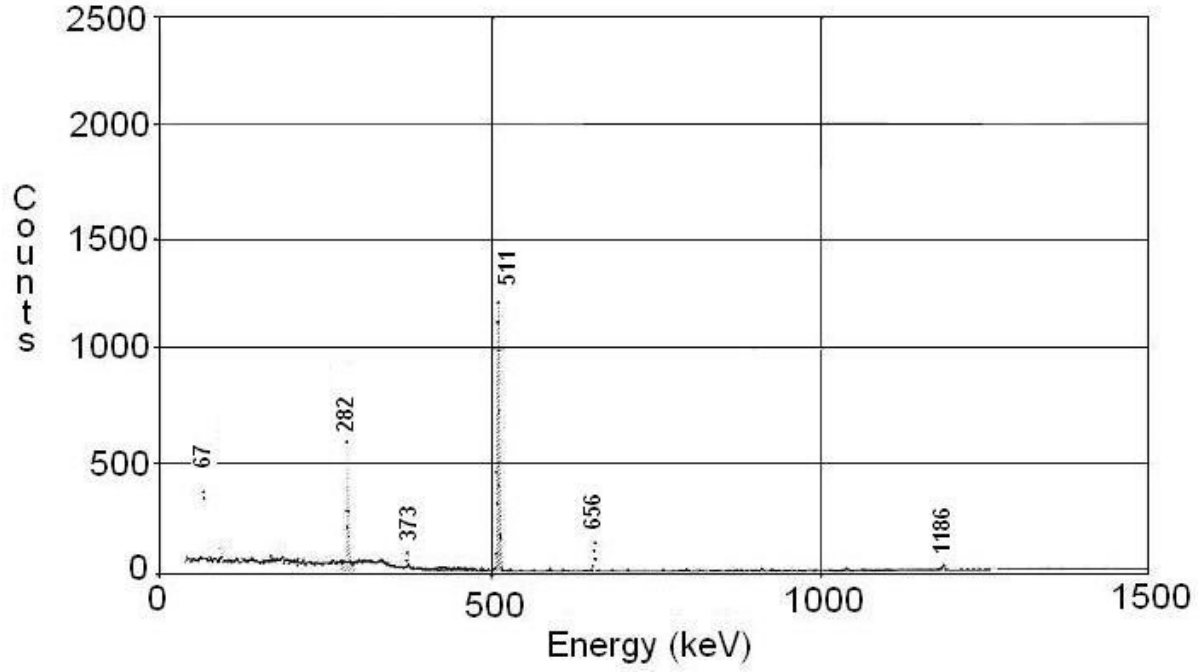

FIG. 23. Gamma spectroscopy of the final [^{61}Cu]$CuCl_2$ sample using an HPGe detector (courtesy of A. Jalilian, IAEA, Austria).

The presence of zinc, copper, iron and some other metals were detected by inductively coupled plasma mass spectroscopy (ICP-MS) method for chemical purity determination. The amount of all metals was less than 100ppb. It is worthwhile mentioning that in case of peptide radiolabelling use of iron free environment as well as iron free solvents and acids is highly recommended. However, for radiolabelling small molecules such as bis-thiosemicarbazones, routine reagents can be used. In some cases, RCP of ^{61}Cu cation can be checked by instant thin iTLC and/or TLC using DTPA (1 mM, pH5.5) solution (R_f 0.8) as well as ammonium acetate 10%: Methanol (1:1) solution (R_f 0.1).

3.2.3. ^{6X}Cu purification & QC from liquid Ni target

After irradiation of the $Ni(NO_3)_2$ solution, the pH of the obtained solution was adjusted by either diluting with water or by using small quantities of 1M Na_2CO_3 to achieve optimal pH of the solution before separation. Two different separation methods were evaluated: Chelex100 (5.0 g), pH(1.22–1.69) [82, 83], or Cu specific resin (50–200 mg resin, Eichrom Technologies Inc, IL), pH3.5–4.0. Using aforementioned separation conditions, ^{61}Ci was selectively trapped on both resins, whereas Ni and ^{55}Co (formed during irradiation) passed though the resins. Due to an extremely tight pH range required for the Chelex resin, this method was not continued. Alternatively, ^{61}Cu was eluted from Cu specific resin with 2 ml of 8M HCl after washing the resin with 0.01N HNO_3. A small quantity of ^{61}Cu was detected after irradiation of natural nickel solution along with ^{55}Co and ^{57}Ni. The produced isotopes were characterized using an HPGe detector (Canberra). The purpose of the developed method was to use natural nickel as a surrogate for ^{64}Cu production in liquid target. Therefore, production yield was not optimized.

3.2.4. ^{61}Cu purification & QC from liquid Zn target

Purification of radiometals produced through the irradiation of a liquid target is a critical step leading to their effective use in radiopharmaceutical development. It must involve separation of the desired radionuclide from the irradiated target material as well as purification from other elements in the target solution, most remarkably the ones resulting from proton induced nuclear reactions. Production of ^{61}Cu by the irradiation of Zn in liquid targets, unless isotopically pure ^{64}Zn is used, involves the irradiation of the whole range of stable Zn isotopes, which mainly leads to the production of gallium radioisotopes as impurities.

A method to purify ^{61}Cu produced following irradiation of Zn liquid targets has been recently described [84]. It consists of two major steps. The first step aims the separation of ^{61}Cu from the different isotopes of zinc and gallium, the major contaminants resulting from the production process. For this step, a Cu resin (Triskem International, Bruz, France) is used. The solution resulting from this first step is very acidic, and a second step is used to dissolve copper into a more suitable solvent. This second step uses the anion exchange TK200 resin (Triskem International, Bruz, France) which simultaneously concentrates the copper in the final [^{61}Cu]$CuCl_2$ solution and may therefore increase its purity. These two steps and have been optimized to guarantee the best yield of copper in the final solution while minimizing the concentration of contaminants, e.g. Ga and Zn isotopes. Figure 24 illustrates the process, describing the conditions employed for all the resins during the purification process.

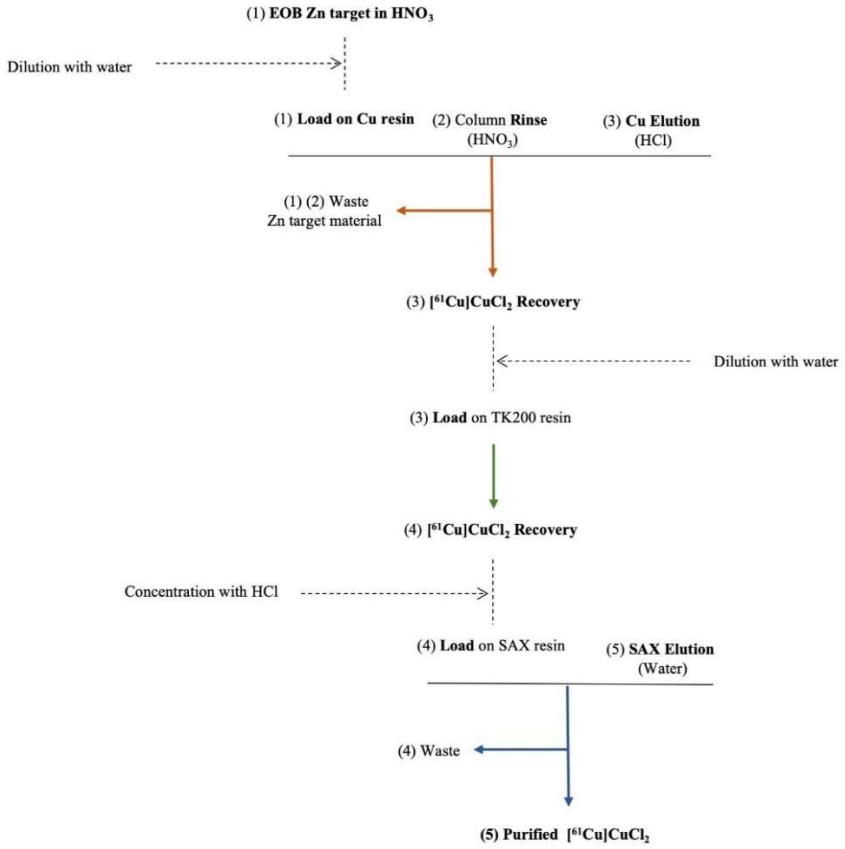

FIG. 24. Schematic representation of ^{61}Cu purification methodology. Numbers represent the sequential order of the purification process and solutions passing through the resins. Each coloured arrow represents the flux through a different resin: Cu resin (Orange arrows), TK200 (Green arrow) and SAX resin (Blue arrows), whereas dashed arrows represent dilution or concentration of the different solutions during the process (courtesy of F. Alves, University of Coimbra, Portugal).

This purification process has successfully been automated [84] using commercial synthesis modules (IBA Synthera® Extension, Louvain-la-Neuve, Belgium) and the methodology described elsewhere [11]. Automation leads to quality controlled radiopharmaceutical production methodology, routine scale in compliance with good manufacturing practice (GMP) guidelines and reproducible results, while ensuring radioprotection of the operators. Figure 25 and Fig. 26 illustrate layouts of the synthesis module software for the first and second step, respectively. In Fig. 25 all components used are shown, including the two different resins used, CU and TK200, a 20 ml syringe (Syr) and five different vials. All these components are connected through inert silicone tubes and PP connectors, held in position on a reusable cassette support. The valves are identified with numbers (from 1 to 10), except for the inert gas valve, controlling a stream of nitrogen gas into the circuit. In Fig. 26 all components are connected through inert silicone tubes and PP connectors, held in position on a reusable cassette support. Valves are identified with numbers (from 1 to 10), as well as the inert gas valve, which allows for a stream of nitrogen gas into the circuit. The whole purification process is achieved in 60 min, leading to purified [^{61}Cu]$CuCl_2$ in 5 mL of 1M HCl. Purification yields above 80% decay corrected are achieved.

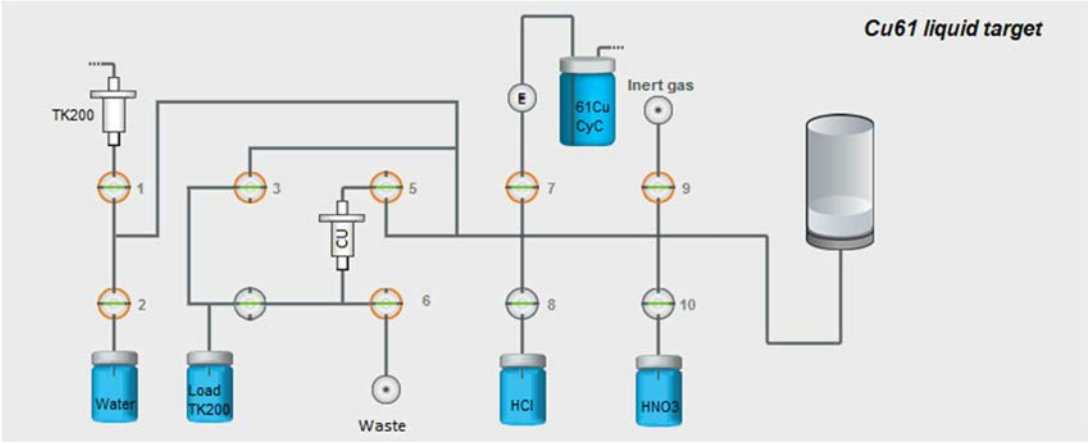

FIG. 25. Layout of an extension module for the first stage of the automated purification process (courtesy of F. Alves, University of Coimbra, Portugal).

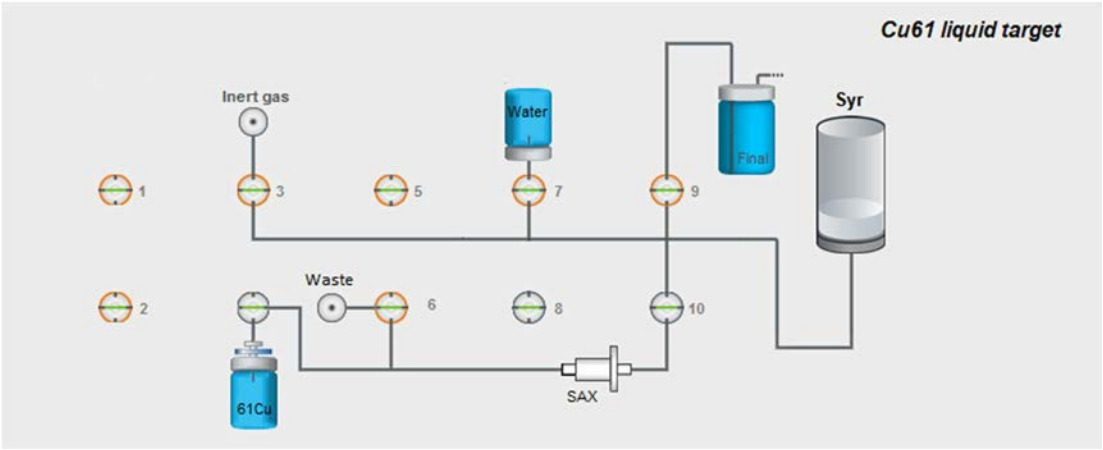

FIG. 26. Software layout illustrating a flowchart of an extension module for the second stage of the automated purification process. SAX resin, a syringe (Syr) and three different vials are shown (courtesy of F. Alves, University of Coimbra, Portugal).

Assessment of QC parameters of the final compound, based on predefined criteria, is mandatory to ensure the quality of the final solution, compliance with GMP and efficient labelling. Half-life is an essential parameter in the assessment of radionuclidic identity: when the determined

half-life value is within a 10% range of the known radionuclide half-life its identity is generally confirmed. The half-life can be measured using a common dose calibrator.

Gamma spectroscopy also allows the confirmation of the radionuclidic identity, using a HPGe detector system and correlating the [^{61}Cu]$CuCl_2$ gamma ray spectrum at the end of purification process, as the one shown in Fig. 27. with the known gamma peaks of ^{61}Cu.

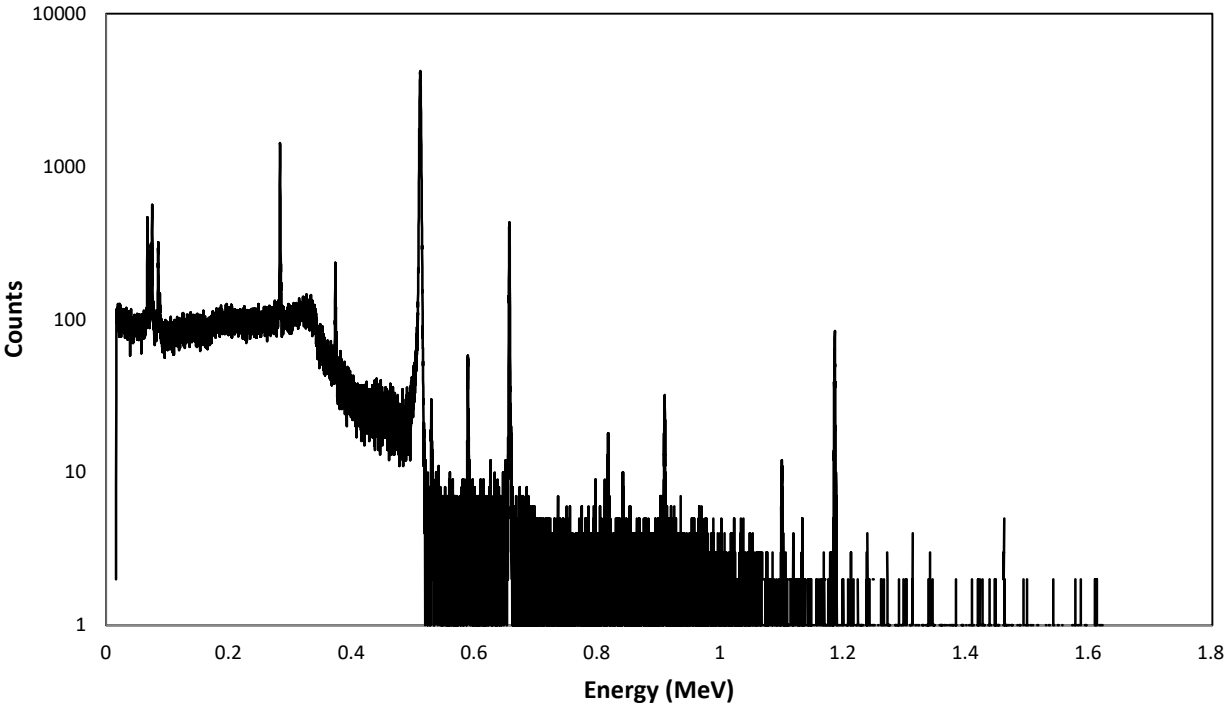

FIG. 27. Gamma spectrum of the [^{61}Cu]$CuCl_2$ solution at the end of purification (courtesy of F. Alves, University of Coimbra, Portugal).

Additionally, since chemical purification processes do not allow separation of ^{61}Cu from other Cu isotopes, measurement of ^{64}Cu and ^{67}Cu characteristic peaks should be performed to assess the level of these Cu impurities in the purified solution. Using natural Zn, the presence of these long lived radioisotopic impurities, which are produced from cross-reactions on stable Zn isotopes, may have a significant impact on long term radionuclidic purity of the final purified compound. A ^{61}Cu radionuclidic purity over 97% and absence of Ga radioisotopes has been reported from gamma spectroscopy analysis at the end of the purification process [80].

The RCP can be analysed using iTLC, a quick and highly sensitive method used to separate the [^{61}Cu]$CuCl_2$ from the Cu colloidal form. iTLC analysis uses a simple cellulose strip and 5 μL of the sample applied on the bottom of that strip. 1:4 v/v MeOH:buffer (0.1 M sodium acetate) is typically used as mobile phase. A typical run is illustrated in Fig. 28.

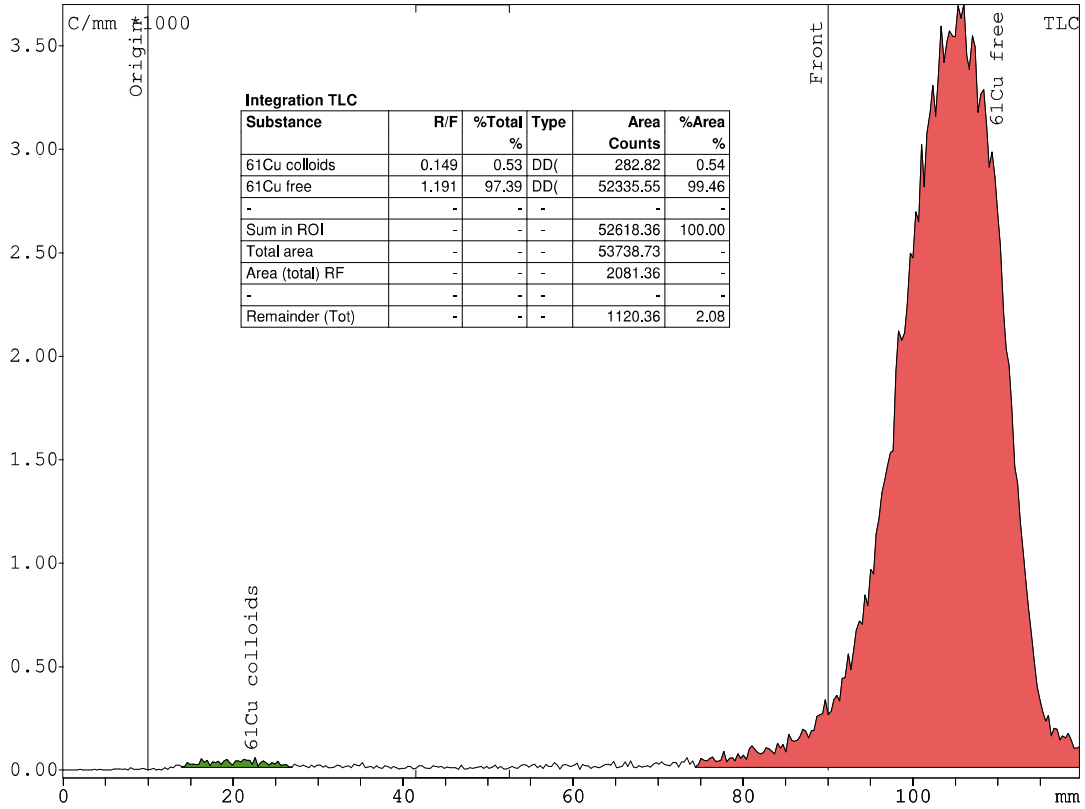

FIG. 28. Typical iTLC chromatogram of the purified [^{61}Cu]$CuCl_2$ using a Raytest miniGita detector. Stationary phase: Cellulose strips; Mobile phase: 1:4 v/v MeOH:buffer (0.1 M sodium acetate) (courtesy of F. Alves, University of Coimbra, Portugal).

Chemical purity should be periodically assessed, mainly for other metal impurities such as Zn and Fe in the final purified solution. Since even trace concentrations of metal impurities can influence ^{61}Cu labelling processes, a highly sensitive analytical technique like ICP-MS or 'atomic absorption spectroscopy' is able to determine with great precision (at the ppm or below range) the concentration of most metal elements in a given sample that should be used. These high precision techniques can also be used to determine specific activity (in GBq/µg), by using the measurement of the total mass of Cu present in the final purified solution.

3.3. ^{61}Cu RADIOLABELLING EXAMPLES

A number of ^{61}Cu tracers have been developed for the detection of various malignancies and biological processes. Considering the physical and biological half-life of the radionuclide and carrier molecules, some tracers possess higher potentials for translation into human applications with completed preclinical experiments such as [^{61}Cu]Cu-DOTA-NOC [85] [^{61}Cu]Cu-diacetyl-di(N^4-methylthiosemicarbazone (ATSM) [86] and [^{61}Cu]Cu-PTSM [87]. Additional extended information on preparation of these latter two reactions is provided in Annex I.

On the other hand, many other molecules have been investigated in a research setting, with efforts underway to further assess/demonstrate the potential effectiveness for future applications. Table 6 provides a non-exhaustive list of various additional ^{61}Cu tracers with some additional details.

TABLE 6. EXAMPLE OF RADIOTRACERS LABELLED WITH ^{61}Cu
(*courtesy of A. Jalilian, IAEA, Austria*)

Radiolabelled ligand	Chelator	Target	Model	Ref
IgG M75	phosphinate	human carbonic anhydrase epitope	mice with inoculated colorectal cancer	[88]
TRC105 (anti CD105 Fab)	NOTA	CD105/endoglin	4T1 tumor	[89]
Tagged VEGF121	NOTA	VEGFR	4T1 tumor	[90]
Bleomycin	direct	Fibrosarcoma tumor	Fibrosarcoma bearing mice	[91]
Doxorubicin	direct	Fibrosarcoma tumor	fibrosarcoma bearing mice	[92]
tri(methanephosphonic acid)derivative	Triethylenetetramine	Bone hydroxy appatite	Normal rodent	[93]
2-acetylpyridine thiosemicarbazone	direct	ribonucleotide reductase	Normal rodents	[94]
octreotide	Triethylenetetramine	Somatostatin receptors	Animal model	[3]
DTPA	direct	Red blood cells	Human blood	[95]
oxinate	Direct	White blood cells	Human blood	[96]
NHAG	Direct	Fibrosarcoma tumors	fibrosarcoma bearing mice	[97]
PQTS	Direct	Fibrosarcoma tumors	fibrosarcoma bearing mice	[98]

3.3.1. Radiolabelling example with [^{61}Cu]$CuCl_2$ from liquid target production and separation methodology: [^{61}Cu]Cu-DOTA-NOC

The highly chemically and radiochemically pure solution of [^{61}Cu]$CuCl_2$ obtained after liquid target production of ^{61}Cu and subsequent automated separation/purification method is ready to be used in a labelling reaction, which can – in compliance with GMP guidelines – lead to the production of ^{61}Cu based radiopharmaceuticals for both research and clinical routine use.

In the example of DOTA-NOC labelling, [^{61}Cu]$CuCl_2$ purified solution is mixed with 50 μg of DOTA-NOC acetate peptide in sodium acetate, with the pH fixed between 4 and 4.5, for 10 min at 90ºC. This reaction allows over 95% radiochemical yield of the final [^{61}Cu]Cu-DOTA-NOC labelled compound.

Prior to QC of final [^{61}Cu]Cu-DOTA-NOC, 'cold' Cu-DOTA-NOC should be independently identified using the HPLC method, under specific conditions, to allow confirmation of radiochemical identity of the radiolabelled [^{61}Cu]Cu-DOTA-NOC. Figure 29 shows a UV chromatogram of standard Cu-DOTA-NOC. The standard reference time (Rt: 7.53 min) will be subsequently compared to the reference time of the final radiolabelled compound ([^{61}Cu]Cu-DOTA-NOC). Both iTLC and HPLC analysis are used to confirm the RCP of the final labelled compound. Figure 30 and 31 are examples of such analysis, in which over 99% RCP of the final [^{61}Cu]Cu-DOTA-NOC is reported.

The pH is another essential parameter which, for [^{61}Cu]$CuCl_2$, might influence the labelling reaction, or, in the context of a ^{61}Cu labelled radiopharmaceutical, pH is also important to ensure an adequate safety profile for clinical use. pH can be measured by using pH paper (test strips),

by colorimetric evaluation or by using an analytical pH meter. Ideally, concerning DOTA-NOC labelling, pH values of the final compound ranges from 4.0 to 4.5.

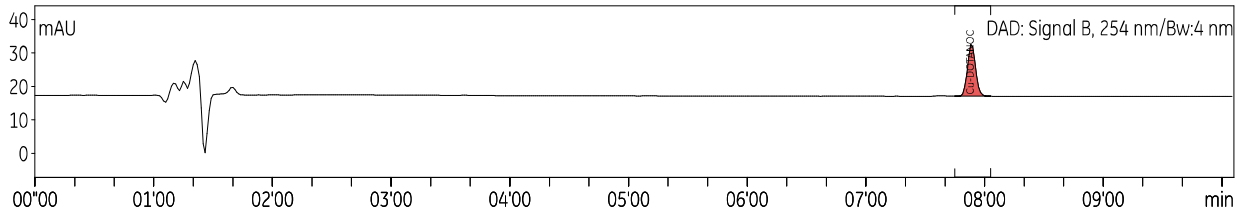

Integration DAD: Signal B, 254 nm/Bw:4 nm

Substance	R/T s	Type	Area mAU*s	%Area %
Cu-DOTANOC	07'53	BB(M)	73,92216	100,00
Sum in ROI	-	-	73,92216	100,00

FIG. 29. Analytical UV-HPLC (254 nm) of Cu-DOTA-NOC (Rt: 7.53 min) using an Agilient 1200 Series analytical HPLC on an ACE® HPLC column (courtesy of F. Alves, University of Coimbra, Portugal).

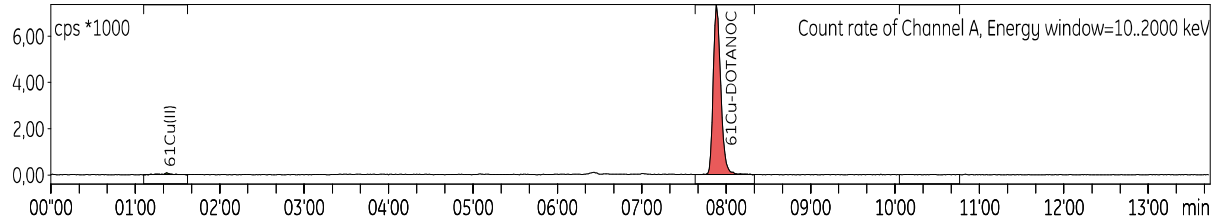

Integration Count rate of Channel A, Energy window=10..2000 keV

Substance	R/T s	Type	Area Counts	%Area %
61Cu(II)	01'23	DD(M)	403,49	0,90
61Cu-DOTANOC	07'53	DD(M)	44292,79	99,10
Sum in ROI	-	-	44696,28	100,00
Area (total)	-	-	47394,47	-
BKG1 (CPS)	-	-	15,791	-
Remainder	-	-	2698,19	5,69

FIG. 30. Typical iTLC chromatogram of the [^{61}Cu]Cu-DOTA-NOC (Rf: 0.27) labelled compound using a Raytest miniGita detector. Stationary phase: cellulose strips; mobile phase: 1:4 v/v MeOH:buffer (0.1 M sodium acetate) (courtesy of F. Alves, University of Coimbra, Portugal).

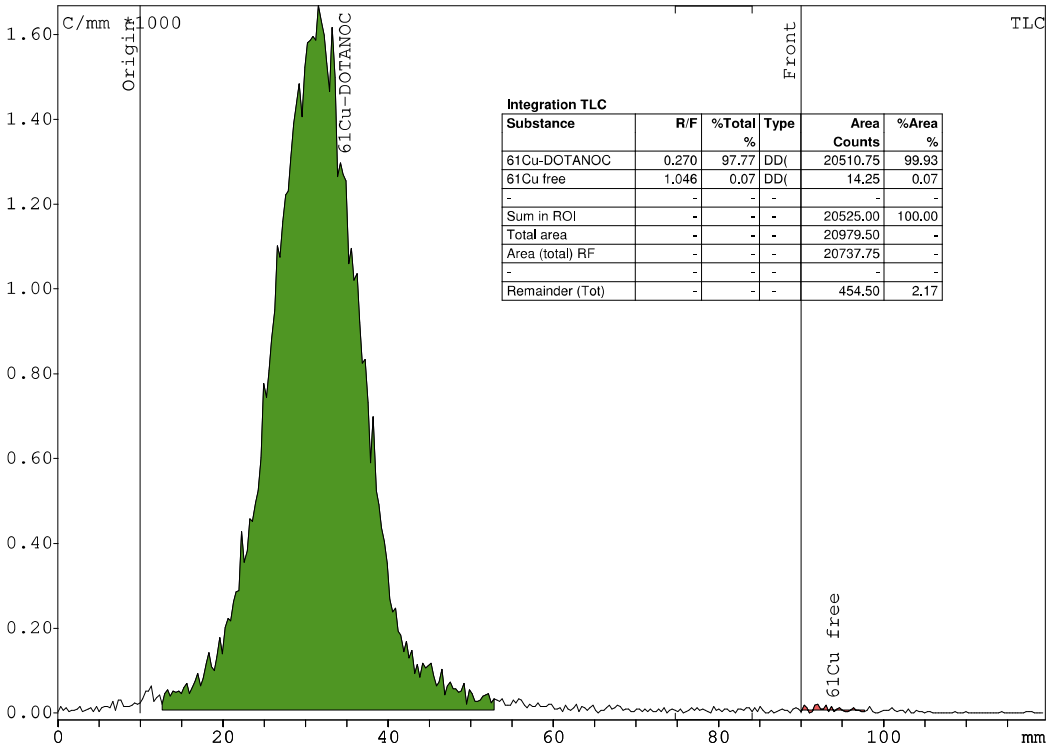

FIG. 31. Analytical HPLC chromatogram of the [^{61}Cu]Cu-DOTA-NOC (Rt: 7.53 min) labelled compound using an Agilient 1200 Series analytical HPLC on an ACE® HPLC column (courtesy of F. Alves, University of Coimbra, Portugal).

4. PRODUCTION OF ^{86}Y

Theranostics concept entails a therapy accompanying diagnosis aimed at patient specific treatment. Desirable diagnostic radiopharmaceuticals identify and stage the disease for an individual patient. Its biodistribution may also verify that a particular targeting vector is matched to and selective for the individual patient's disease.

Before ^{177}Lu (and ^{225}Ac), the β^- emitting therapeutic radionuclide ^{90}Y ($t_{½}$ = 64.053 h) was the most important therapeutic radiometal for many indications; for certain indications it still is. One of its key advantages is its availability as carrier-free nuclide from the ^{90}Sr/^{90}Y generator system. On the other hand, imaging of ^{90}Y labelled tracers was impossible for a long time, which is a substantial drawback in terms of the philosophy of theranostics. Only recently have bremsstrahlung imaging and internal pair produced based PET imaging been introduced, but these techniques struggle to achieve image quantification that is useful in theranostic applications. Thus, the pharmacodynamics and pharmacokinetics of ^{90}Y labelled therapeutic tracers in vivo were not accessible; the treated patient in question appeared to be a 'black box'. Consequently, the Jülich team decided to apply the β^+ emitter ^{86}Y ($t_{½}$ = 14.7 h) for imaging [4]. The isotope pair ^{86}Y/^{90}Y for PET/CT and therapy, see Fig. 32, represents the chemical ideal of a theranostic pair.

Following demonstration of the potential of the ^{86}Y/^{90}Y theranostic isotope pair and the success of therapies employing ^{90}Y, ^{86}Y has been recognized as the ideal choice for PET imaging of radiopharmaceuticals designed for ^{90}Y radiotherapy [99–102].

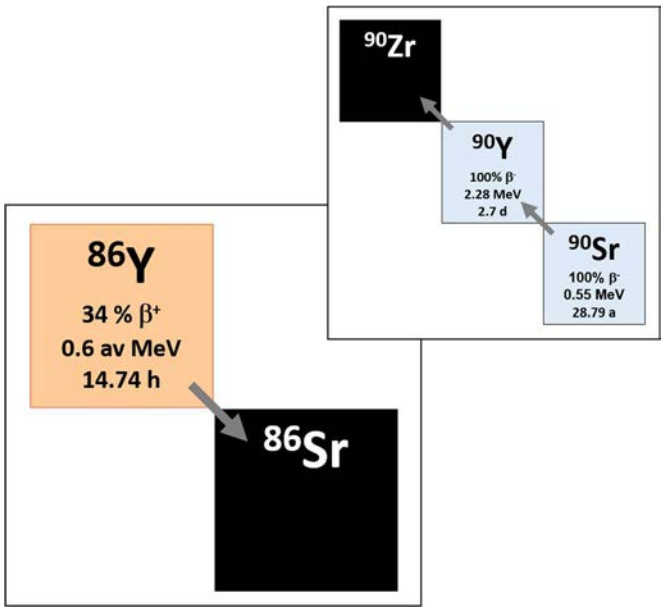

FIG. 32. The isotope pair ^{86}Y vs. ^{90}Y (courtesy of F. Rösch, Johannes Gutenberg-Universität Mainz, Germany).

Thanks to an extended half-life compared with other trivalent radiometals such as ^{68}Ga ($t_{½}$ = 67.71. min) or ^{44}Sc ($t_{½}$ = 3.97 h), ^{86}Y ($t_{½}$ = 14.74 h) allows PET/CT imaging over 48 to 72 h, and accurate pharmacokinetic profiling of radiopharmaceuticals with prolonged biological half-lives such as nano-microparticles (labelled spheres) [102, 103], long circulating small molecules [104–107], antibodies [108–111] and antibody fragments [112]. This facilitates quantitative image based determination of patient specific activity distributions of radiopharmaceuticals, which enables pretherapeutic treatment planning and the accurate estimation of absorbed doses to maximize efficacy and mitigate radiation toxicity.

Application of ^{86}Y as a PET imaging surrogate has been expanded beyond its ^{90}Y congener. Due to remarkable chemical similarities between Y(III) ions and the lanthanide series, $^{86}Y^{3+}$ has demonstrated its utility a PET imaging surrogate of Lu(III) and Gd(III). Hernandez and colleagues [107] recently reported the utilization of ^{86}Y as a PET companion for a ^{177}Lu labelled therapeutic small molecule, and demonstrated equivalent biodistribution of both Y and Lu labelled compounds, facilitating the implementation of the theranostic approach. Another interesting application employed ^{86}Y as a Gd(III) substitute to assess the long term stability and retention of Gd-based MRI contrast agents (GBCAs) in vivo [113]. These examples are evidence of the versatility of ^{86}Y as radiometal for PET and portend future expansion of ^{86}Y in biomedical applications.

4.1. ^{86}Y PHYSICS & TARGET MATERIALS

Yttrium-86 gross features of the decay scheme are well known [19, 114–117], as it decays via electron capture and β^+ emission (six positron groups) with various end point energies and intensities (total β^+ emission intensity: 32%). Uncertainties in this value require new measurement improved methods of detection and quantification [116, 117]. The primary emissions are followed by emission of γ rays and re-evaluation of the ^{86}Y whole decay scheme has been recommended [118].

For production routes, see Table 7. The most relevant nuclear reactions towards ^{86}Y at small to medium sized cyclotrons include ^{86}Sr(p,n)^{86}Y; ^{86}Sr(d,2n)^{86}Y; ^{88}Sr(p,3n)^{86}Y; ^{nat}Rb(^{3}He,xn)^{86}Y [119]; ^{85}Rb(α,3n)^{86}Y; ^{90}Zr(p,αn)^{86}Y and ^{nat}Zr(p,x)^{86}Y nuclear reactions [120–123], though

other possible reactions exist with very low cross sections. Figure 33 illustrates the most reliable pathway and Fig. 34 shows the relevant cross sections for the (p,n) reactions.

TABLE 7. PRODUCTION ROUTES FOR ^{86}Y
(courtesy of F. Alves, University of Coimbra, Portugal)

Projectile	Target material	Reaction	Energy range	Production yield (MBq/uAh)	References
Protons	^{86}Sr	(p,n)	15.1–0	48 ± 8	[124][124]
			16–10	175	[125]
			15	240	[126]
			14 – 7	371 [a]	[127]
			15	111	[128]
			15	139 [a]	[128]
			15–6	215.5 [a]	[129]
			13.8–10.4	155	[6]
			12.0–8.0	86	[6]
			16–12	150	[130]
			14.5	166 ± 10	[131]
			11	44.4	[132]
			13.8	74	[133]
			15.2	100 ± 15	[134]
			14.2–8.4	146 ± 6	[135]
			16	80	[136]
				33 [a]	[137]
			16	32.1 [b]	[138]
	^{nat}Sr	(p,n)	2	1.44 [a]	[13]
			16	3.6 [a]	[138]
	^{88}Sr	(p,3n)	43–33	1005 [b]	[127]
			45.1–38.9	407	[139]
	^{nat}Sr	(p,3n)	66.4–44.6	377.4	[139]
			45.5–37.2	514.3	[139]
	^{nat}Zr	(p,x)	43–28		[127]
			40–25	50 [a]	[17]
	^{89}Y	(p,4n)^{86}Zr->	70–45	970	[140]
Deuterons	^{86}Sr	(d,2n)	19–15	91.7 [b]	[129]
	^{nat}Sr(d,x)				[141]
Alfa-particles	^{85}Rb	(a,3n)	60–32	200 [b]	[142]
^{3}He	^{85}Rb	(^{3}He,2n)	24–12	192.4 [b]	[119]
			15–10	1.76 [b]	[129]

[a] *Liquid target*
[b] *predicted*

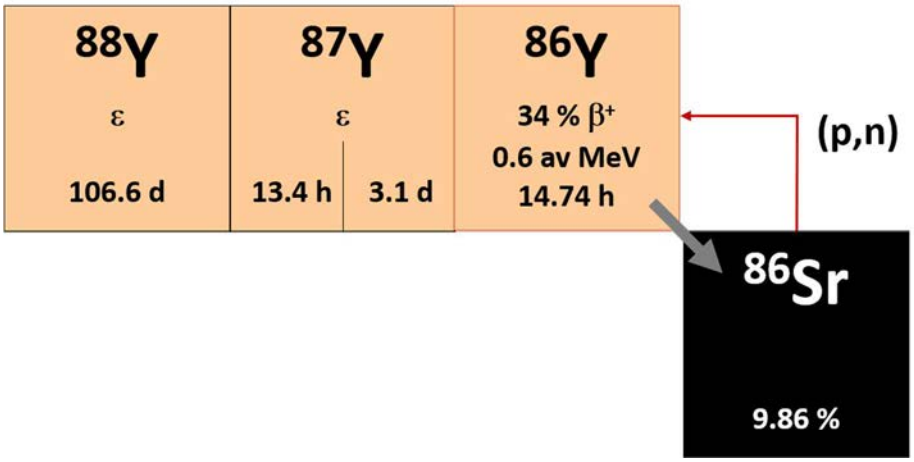

FIG. 33. The $^{86}Sr(p,n)^{86}Y$ pathway to produce ^{86}Y (courtesy of F. Rösch, Johannes Gutenberg-Universität Mainz, Germany).

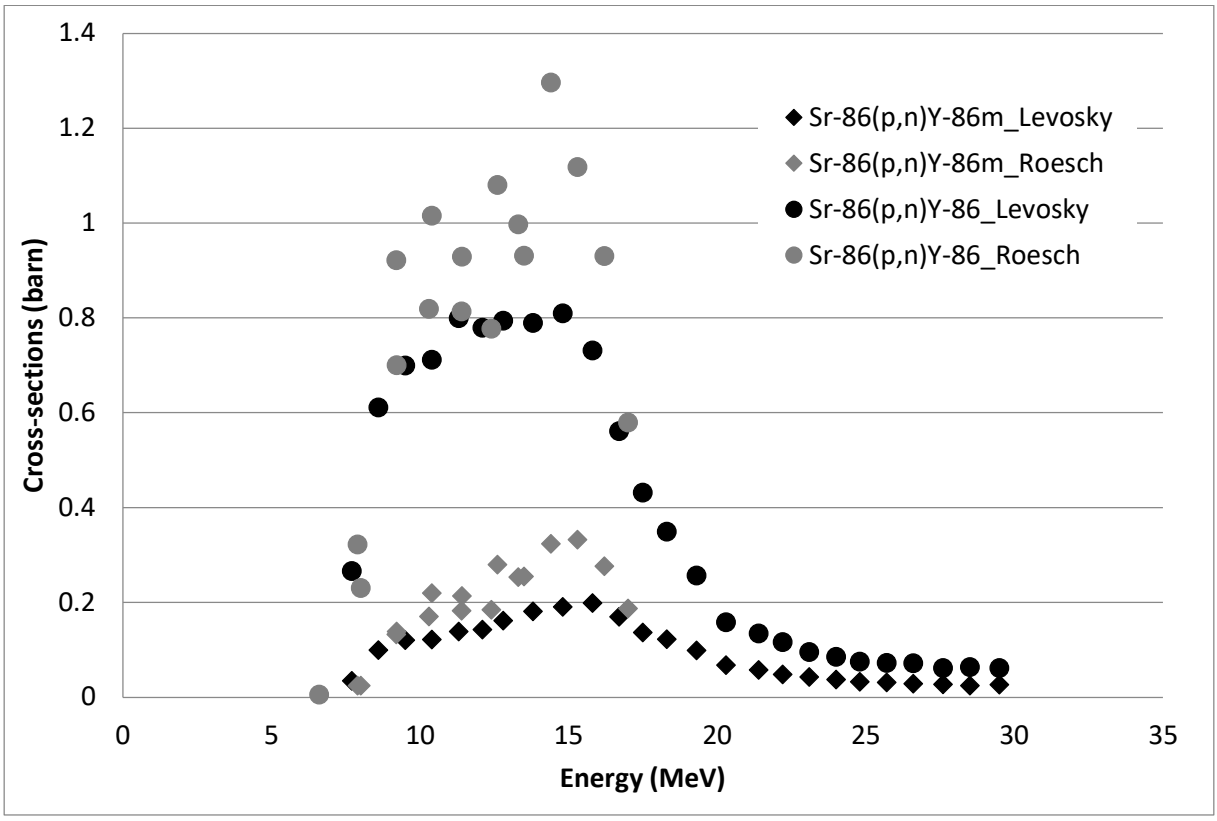

FIG. 34. The (p,n) production cross sections for ^{86}Y (courtesy of F. Alves, University of Coimbra, Portugal and C. Hoehr, TRIUMF, Canada. Raw data extracted from [29, 119]).

Early on, cross-section data for some of these reactions had been published [6, 29, 143, 144] and the $^{86}Sr(p,n)^{86}Y$ reaction was employed using a high enrichment target [6]. Recently, a more comprehensive study was published [145]. It should be noted that if the incident proton energy is larger than 25 MeV, when using the $^{nat}Zr(p,x)^{86}Y$ route, the ^{87}Y impurity (via the $^{90}Zr(p,\alpha)^{87}Y$) is minimized, since the $^{90}Zr(p,\alpha n)^{86}Y$ reaction is favoured.

4.1.1. ^{86}Y production from solid Sr carbonate

In order to produce ^{86}Y, most of the initial attempts focused on the $^{86}Sr(p,n)^{86}Y$ reaction at low energy cyclotrons ($E_p \leq 18$ MeV) using highly enriched [^{86}Sr]$SrCO_3$ [6] and continued later on

[124–126, 128, 130–133, 135, 146, 147], except for [^{86}Sr]SrO [131]. The target material is pressed and transferred in appropriate target holders. The Jülich team targetry employed a thin metal foil cover, for water-cooling at the back during a few hours irradiations (beam current: about 5 μA) using 16 MeV protons [6, 131, 135]. Similarly, the [^{86}Sr]$SrCO_3$ pellet was placed into a groove in a Al-made target holder sealed by a sliding lid [125] and cooled in a 4π target head, similar to [148], withstanding beam currents of up to 10 μA. However, a nominal current of about 6 μA, was used during long production runs. Proton beam energies were 19 MeV degraded at the target front to 16 MeV, see Fig. 35.

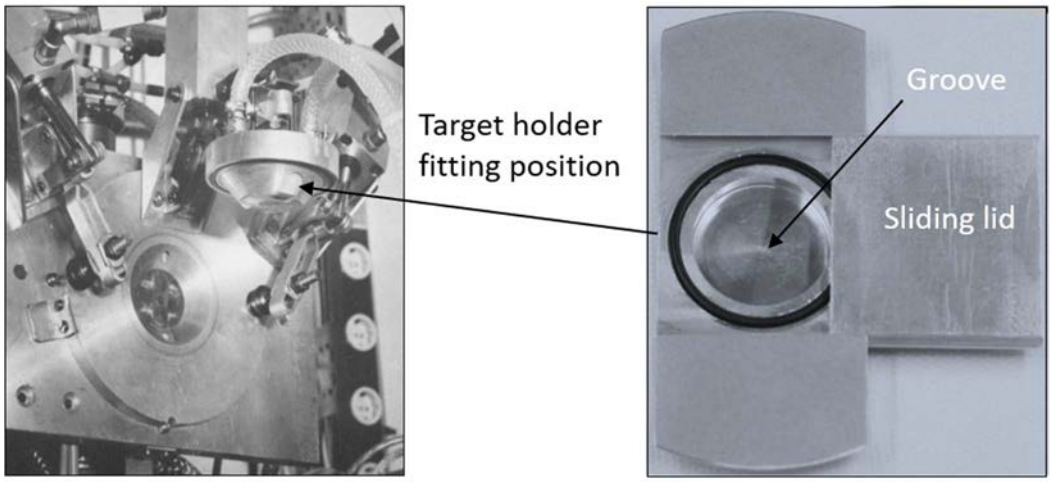

FIG. 35. Photo of the 4π water cooled target head at the Forschungszentrum Jülich [148] (left); and Al target holder with a groove for the [^{86}Sr]$SrCO_3$ pellet (right). The target head was remotely opened after irradiation to deliver the target holder in a transport containment (courtesy of F. Rösch, Johannes Gutenberg-Universität Mainz, Germany).

In another version [132], front target chilled He cooling was applied in addition to water cooling at the back, while irradiation currents of up to 15 μA of 11 MeV protons were applied. In a separate try, the target material was irradiated with 15 MeV protons (inclined angle: 6°–15°) in a jet water cooled target holder [124, 128, 131, 147]. Though, the target may withstand higher currents, a beam current of 10 μA was employed [124, 128, 131, 147] (n=6).

At the University of Wisconsin, ^{86}Y is produced via the nuclear reaction ^{86}Sr(p,n)^{86}Y using enriched [^{86}Sr]$SrCO_3$ targets in a 16 MeV GE PET trace cyclotron within the energy range E_p = 14.1–7.1 MeV (Fig. 36). Before irradiation, approximately 150 mg of [^{86}Sr]$SrCO_3$ is pressed into a niobium crucible and covered with a 12.7 μm thick niobium foil to encase the target material and degrade the beam energy to 14.1 MeV. Typical irradiations are carried out at 5 μA for up to 2 h with direct water jet cooling on the back of the crucible (Fig. 36 (c)). Under these conditions, ^{86}Y is produced with an EOB physical yield of 0.11 ± 0.02 GBq/μAh [149].

The solid target production yield of ^{86}Y is limited so far to about 3.5 GBq per batch, since progress in high current targetry is limited [125]. For newer target designs, in particular liquid targets, see 4.1.2.

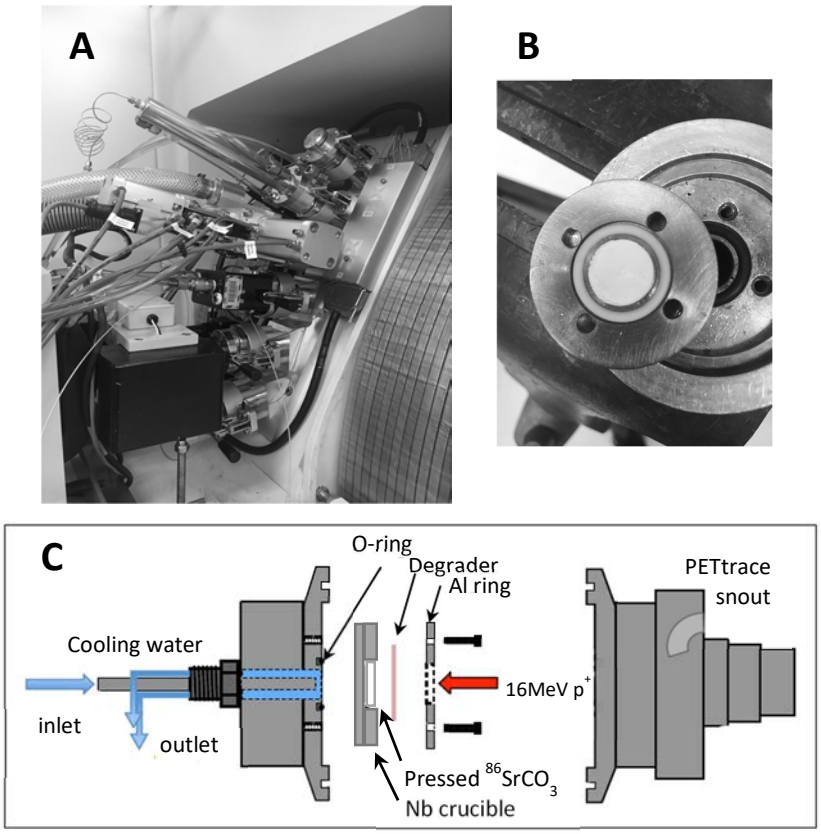

FIG. 36. Magnification of the target ports of the 16 MeV GE PETtrace cyclotron at the University of Wisconsin-Madison, USA (A); pressed [^{86}Sr]SrCO3 target (a niobium crucible; 12.2 mm diameter, 1.2 mm deep pocket (B); schematic of the solid target port used for ^{86}Y production at UW-Madison (C)(courtesy of J. Engle, University of Wisconsin, United States of America).

4.1.2. ^{86}Y production from liquid Sr target

Production of ^{86}Y from cyclotron using liquid target was first attempted by Vogg et al. [138], where authors used aqueous solution of natural strontium nitrate salt and irradiated with proton beam at 6 µA for 60min. By irradiating aqueous solution of natural strontium nitrate salt under aforementioned condition authors reported 21.6 MBq of ^{86}Y isotope decay corrected to EOB. Ráliš et al. [137] reported irradiated enriched [^{86}Sr]Sr$(NO_3)_2$ solutions with typical irradiation conditions of 10 to 15 µA for 1 to 2h. Physical yields of 33 MBq/µAh were reported, and successful [^{86}Y]Y-DOTA-TOC labelling was demonstrated following precipitation based [^{86}Y]YCl_3 purification. However, based on the findings reported [9], by directing the use of nitrate salt in dilute nitric acid for a successful production of radiometals in liquid target, Oehlke et al. [13] demonstrated production of ^{86}Y using natural strontium nitrate solution in 1 M nitric acid.

Later, Pandey and DeGrado at Mayo Clinic Rochester used enriched strontium nitrate (96%) and dissolved in 0.2N HNO_3 and irradiated at 40 µA beam current for 30 min. Authors reported 337 MBq (9.11 mCi) of [^{86}Y]YCl_3 after purification decay corrected to the end of the bombardment. The irradiation time, concentrations of enriched strontium nitrate solution and nitric acid can be changed appropriately to achieve highest quantity of pure [^{86}Y]YCl_3. Details of producing [^{86}Y]YCl_3 from cyclotron using liquid target are mentioned below.

4.2. ^{86}Y PURIFICATION

4.2.1. ^{86}Y purification & QC from solid Sr carbonate

Several ^{86}Y purification techniques from an irradiated strontium targets ($SrCO_3$, SrO or $SrCl_2$) have been proposed, involving ion exchange, co-precipitation, electrodeposition, single and multiple column chromatography, solvent extraction, target element precipitation and extraction chromatography, each having its own advantages and disadvantages.

Rösch et al. [6] developed combined co-precipitation and ion exchange method initially, where the irradiated [^{86}Sr]$SrCO_3$ was dissolved in minimum volume of HCl, and no-carrier-added ^{86}Y coprecipitated using $La(OH)_3$ (NH_4OH solution added). The precipitate was later centrifuged off and redissolved in HCl (a few drops). Yttrium-86 was isolated from cold La via cation exchange chromatography/α-hydroxyisobutyric acid [6, 125] yielding GBq amounts of ^{86}Y in only 150µl volume.

The radionuclidic purity was performed via gamma spectroscopy and ICP-MS was used for the chemical purity assessment [125]. In a modified method [126], the radioyttrium co-precipitation was done using $Fe(OH)_3$, while the final radioyttrium purification was performed using ion specific resin chromatography.

Reischl et al. [124] developed an electrodeposition method, which was later optimized by Yoo et al. [131] and Lukic et al. [135]. In brief, the target material was dissolved in dilute HNO_3 and electrolysed (2 A current, Pt electrodes) followed by electrodes removal from the cell. The electrodes were then transferred to another glass vial containing freshly prepared dilute HNO_3. By a second electrodeposition step, using a platinum wire electrode (at 200–400 mA), ^{86}Y was collected on the Pt wire, followed by its recovery with 0.05M HCl (250µl).

Kandil et al. [130] investigated the single column chromatography method for the separation of ^{86}Y. The team used both the cation exchanger (Dowex 50W-X8, H form) and the anion exchanger (Dowex 21k, Cl^- form). In brief, the irradiated [^{86}Sr]$SrCO_3$ was dissolved in HCl (6 M) and the mixture was evaporated and re-dissolved in citrate buffer (0.1 M, pH4) for the cation exchanger method. For the anion exchanger route, the residue was dissolved in citrate buffer (0.1 M, pH5) followed by elution with citrate buffer (0.1 M, pH4). In the first case, ^{86}Y flowed through the resin while strontium was retained on the resin column, while in the latter case it is opposite.

Garmestani et al. [133] introduced the multiple column chromatographic method, which was further developed by Park et al. [146]. Briefly, the target was transferred to the hot cell and was dissolved using 4 N nitric acid completely and loaded over a strontium selective resin. The resin was washed further with 4N HNO_3 and radioyttrium was removed and adsorbed on a 2nd RE-SPEC column. Thereafter, the column was eluted by 0.1N HCl and the eluate was re-adsorbed on a third resin column (Aminex A5) connected in sequence. In the last step, Finally, using 3N HCl ^{86}Y was eluted from the column and concentrated. The final product was taken up in 200 µl of 0.1N HNO_3 or any suitable radiolabelling buffer.

Kandil et al. [130] also developed a solvent extraction method for ^{86}Y separation from a carbonate target. The irradiated target was dissolved in 1M HCl and transferred to an extraction funnel and shaken for 3 min with a mixture of 10% (v/v) diethylhexyl phosphoric acid:n-heptane (equal volumes for 2 phases). The organic phase was separated and washed with

1M HCl (200 ml) for 2 min. Back extraction into the aqueous phase was performed using 9M HCl to recover ^{86}Y, followed by drying the solution and re-dissolving the residue in dilute HCl.

Avila-Rodriguez et al. [132] developed a simple target element precipitation method for ^{86}Y separation of from irradiated [^{86}Sr]$SrCO_3$. The dissolved target material in 6M HCl (0.5 ml) was alkalized by the addition of 1M NH_4OH (5 ml) and filtered through Whatman 42 filter paper under vacuum. Using 1M HCl, the no-carrier-added ^{86}Y was washed out from the filter paper. Sadeghi et al. [150] also applied the same technique with modifications using $^{nat}SrCO_3$ target dissolved in 8M HCl. In the first step, Cu and Zn impurities were removed via AEX, followed by the gradual sulfuric acid addition to the $^{86\text{-}88}$Y/Sr mixture solution at 50°C. Finally, $SrSO_4$ precipitate was filtered while the majority of the radioyttrium passed through the filtrate.

Recently, Alucio-Sarduy [149] reported a new approach, briefly, the [^{86}Sr]$SrCO_3$ irradiated target was dissolved 9M HCl, and an extraction resin functionalized with N,N,N′,N′-tetrakis-2-ethylhexyldiglycolamide was used to isolate ^{86}Y based on the differential affinities of Sr^{2+} and Y^{3+} for the resin. The enriched material recovery was performed by combining the load fraction and the initial acidic column rinse. Trace metal impurities (e.g. Zn, Cu, and Fe) were removed with a subsequent 15 ml 0.5M HNO_3 rinse, and the no-carrier-added ^{86}Y was almost completely eluted from the resin column as [^{86}Y]YCl_3 in 0.1M HCl (0.6 ml). A separation factor of 10^5 with a high radiochemical yield (96 ± 2%) was achieved. The isotopically enriched target material was recovered as [^{86}Sr]$SrCO_3$ by adding saturated $(NH_4)_2CO_3$ to the collected solutions (efficiency of 98 ± 1%).

4.2.1.1. Comparison of separation methods

The co-precipitation of ^{86}Y with $La(OH)_3$, method including cation exchange chromatography, led to pure batch production, sufficient for the first clinical applications [6], while the solvent extraction method using $^{nat}SrCO_3$ was modest. Enriched ^{86}Sr carbonate was used in all other cases, and the method was further optimized on the targetry and chemical separation techniques sides [125], leading to the batch yield increase and the highest chemical purity. The two step electrodeposition process was also successful, and clinical scale batches were reported [124, 131, 135]. The chemical impurity test on Sr content demonstrated higher contents than co-precipitation/cation exchange route. Naturally, the multiple column chromatography methods have shown somewhat lower separation efficiency than the other methods, while the single column cation exchange chromatography affords similar results as the electrodeposition method. In this publication, though the chemical impurities were not checked, the ^{86}Y was utilised in the labelling of two agents with satisfactory results. On the other hand, the simple precipitation/filtration technique showed to be effective both for the separation and batch yield, however, the chemical impurities were rather high. In the case of extraction chromatography, the method allowed the highest reported radiochemical yield. The chemical purity and apparent molar activity were comparable to other reports, and suitable for radiopharmaceutical formulations. This method is quite attractive for the separation of no-carrier-added ^{86}Y from ^{86}Sr targets due to the speed, simplicity, cost effectiveness and compatibility with automated approaches.

4.2.1.2. Radionuclidic purity

Considering the latter section and discussions, application of a medical cyclotron with the energy range of $E_p = 14 \rightarrow 7$ MeV and the ^{86}Sr(p,n)^{86}Y reaction is the method of choice for ^{86}Y production. Since, all research groups used similar target enrichment percentage (95.6–

97%), ^{87}Y (~0.4%) and ^{87m}Y (<3%) were the major impurities. Just to note that if highly enriched ^{86}Sr (~99%) would be used, the ^{87m}Y impurity could be considerably reduced.

4.2.2. ^{86}Y purification & QC from liquid Sr target

The energy range and interesting application of ^{86}Y has attracted some interests for the clinics equipped with medical cyclotrons to install new solid target systems [117] or install/modify appropriate liquid target systems [13, 138]. For liquid targets, usually the yields (including ^{86}Y) is low but it may be enough for local use [13].

Enriched ^{86}Sr comes in the chemical form of carbonate salt and can be purchased from Isoflex. In brief, 2.0 g of [^{86}Sr]$SrCO_3$ was dissolved in 10.0 ml concentrated nitric acid. After complete dissolution, the solution was dried in vacuum on a rotary evaporator at 50.0°C. The resulting dry powder was reformulated in 0.9M [^{86}Sr]$Sr(NO_3)_2$, 0.2N HNO_3 solution. This solution was loaded into the cyclotron target using an automated loading station as described by Pandey et al. [9] and irradiated at 40 µA for 30min. The target pressure was measured during irradiation (60–80 psi). The irradiated target solution was transferred to a hot cell containing 5 ml of 1M NH_4OH solution in a receiving vial. The target was rinsed with one load of water, which was collected in the same receiving vial. After collecting the rinse load, the entire solution was pushed through a filter paper (Whatman grade 42) kept in a cartridge following the method by Avila-Rodriguez [132]. The collection vial was rinsed with an additional 5 ml of 1M NH_4OH and loaded onto the same cartridge, washed with 10 ml of water, and the ^{86}Sr was eluted as [^{86}Sr]$SrCl_2$ in 2 ml of 1M HCl solution with >99% elution efficiency. For an overview of the steps involved, see Fig. 37.

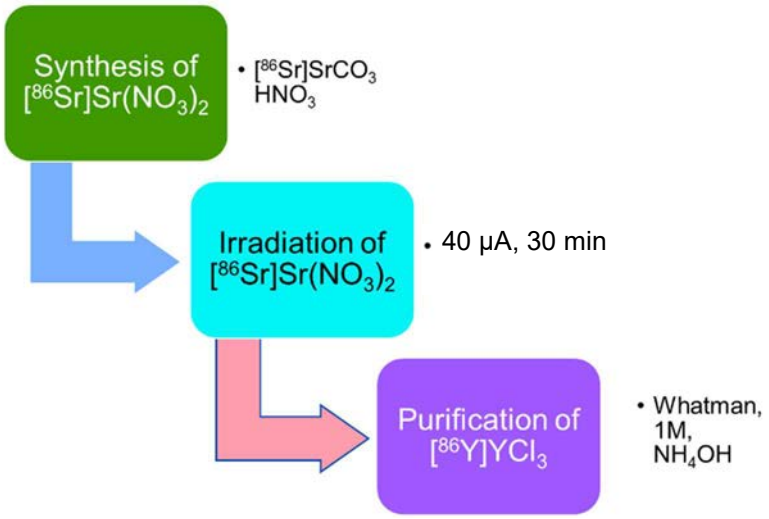

FIG. 37. Steps involved in cyclotron production and purification of ^{86}Y using liquid target (courtesy of M. Pandey, Mayo Clinic, United States of America).

4.3. ^{86}Y RADIOLABELLING EXAMPLES

First radiolabelling studies with ^{86}Y were focused on theranostic investigations of [^{90}Y]Y-citrate and [^{90}Y]Y-EDTMP as radiotherapeutics for disseminated bone metastases. Both ligands, citrate and EDTMP, allow rapid and quantitative complex formation at room temperature [4, 151].

The macrocyclic chelator DOTA was adopted for ^{86}Y labelling of peptidic targeting vectors. High yields are achieved at temperatures about 95°C, similar to all other trivalent radiometals.

This was first demonstrated for [^{86}Y]Y-DOTA-TOC [151–156] in the context of the establishment of routine clinical use of [^{90}Y]Y-DOTA-TOC. This was later adopted in several studies [13, 157, 158].

Since the initial use for DOTA-TOC labelling, a number of other DOTA conjugated targeting vectors haven been described for ^{86}Y, including small molecules and peptides [104–107, 159–161]. Leveraging the 14.7 h half-life of ^{86}Y, which allows for theranostics with radiopharmaceuticals of long biological half-lives, various examples of peptides and antibodies were labelled with ^{86}Y using DOTA as chelator such as octreotide [162], and TRC105 [108].

Despite the advantages of DOTA, due to a need for mild conditions for antibody or antibody fragment labelling, chelators like EDTA or DTPA are often favoured due to satisfactory performance at room temperature, including quantitative labelling and excellent in vitro and in vivo stability. Examples of antibodies and antibody fragments labelled with ^{86}Y using these chelators include the clinically relevant herceptine [133], trastuzumab [163], cetuximab [164], metaiodobenzyl guanidine [165], bevacizumab [111], among others [109–112, 146, 161, 163, 164, 166–168]. In all instances, ^{86}Y was successfully used as imaging surrogate for dosimetry estimation, therapy planning, and verifying treatment effectiveness with ^{90}Y and ^{177}Lu. These findings confirm the potential of ^{86}Y as a PET companion not only for ^{90}Y, but also for lanthanides such as ^{177}Lu.

Aside from theranostic applications, ^{86}Y-DOTA and ^{86}Y-DTPA based molecules were used to quantify the whole body pharmacokinetics of GBCA by PET imaging. The results showed that $^{86}Y^{3+}$ is an excellent surrogate for Gd^{3+}, and that ^{86}Y labelled GBCAs represents a new tool for the detection of residual GBCA in vivo, which could potentially be translated to humans [113]. There are also several reviews on ^{86}Y labelling chemistry and ^{86}Y PET tracers, see for example [99–102].

More recently, long circulating small molecules, including EB-PSMA-617 [104], a PSMA ligand conjugated to an albumin binding moiety, and the alkylphosphocholine analog NM600 [105–107] were radiolabeled with ^{86}Y via chelation with DOTA, to guide the implementation of targeted radionuclide therapy agents. For a non-exhaustive list of radiolabeling examples, see Table 8.

TABLE 8. RADIOLABELLING EXAMPLES FOR ^{86}Y
(courtesy of M. Pandey, Mayo Clinic, United States of America)

Chelator	Tracer/Receptor Ligand	Reference
DTPA	Panitumumab	[111, 169]
DTPA	Cetuximab	[164]
DTPA	Antibody fragment derived from a single antimindin/RG-1 mAb	[112]
DTPA	Herceptine	[133]
DTPA	Octreotide	[170]
DOTA	PSMA ligands	[158]
DOTA	Oligonucleotide (L-RNA)	[171]
DOTA	Arginylglycylaspartic acid (RGD) Peptides	[172]
DOTA	Ammonium-functionalized carbon nanotubes (fCNT)	[173]

TABLE 8. RADIOLABELLING EXAMPLES FOR ^{86}Y (‘cont.’)

DOTA	[Pro^{1},Tyr^{4}]-Bombesin[1-14]	[174]
DOTA	ReCCMSH(Arg(11)) a cyclic analogue of alpha-melanocyte stimulating hormone (alpha-MSH)	[160]
H_4pypa	TRC105 (A monoclonal antibody)	[71]
Citrate	Citrate/transferrin receptor	[4]

CONCLUSION

While the classical organic positron emitters ^{18}F, ^{11}C, ^{13}N and ^{15}O have dominated clinical PET for decades, with [^{18}F]FDG being the working horse of PET/CT, there was and is a permanent search for new positron emitting nuclides to add value to the diagnoses of diseases that are not fully assessed by the traditional radiopharmaceuticals. Obviously, there have been extremely successful examples such as ^{68}Ga, ^{82}Rb and ^{89}Zr, which addressed several very important clinical needs. A larger number of candidates are ‘in the pipeline’ and there are excellent non-conventional positron emitters.

Based on the characteristics of ^{61}Cu, ^{43,44}Sc and ^{86}Y radioisotopes, and rapidly evolving theranostic radiopharmaceutical chemistry, the authors and the IAEA felt that this publication comes at an opportune time. The nuclear data, cross sections and excitation functions for these radionuclides have been extensively studied in recent decades, and significant advances in targetry, separation chemistries, and labelling strategies have been reported. The key, however, to routine clinical application lies in the robust availability of the nuclides at high batch yields, sufficient radionuclidic purity, and production in means suitable for clinical use. It is this context which makes the publication timely: as noted above, the barrier-to-entry in transferring of basic science to routine application has been lowered in recent years thanks to technology advances which include, but are not limited to, commercial solid target systems as well as development and commercial availability of unique resins which simplify purification processes, and can be readily mixed and matched depending on known impurities. Furthermore, yields may be reduced by more than an order of magnitude vs. solid targets due to significant interaction of the particle beam with water, for sites which do not have solid target infrastructure, or, perhaps require only low quantities of radioactivity, solution targets can be irradiated by dissolving an appropriate salt. ^{61}Cu can be produced in high specific activity and yields using a medical cyclotron starting inexpensive natural target material, while available ^{64}Cu radiopharmacy [175] experiences can be perfectly translated for development of appropriate ^{61}Cu radiopharmaceuticals. The intermediate half-life and interesting decay properties allow for better image quality and possibly lower radiation dose to patients.

On the other hand, ^{86}Y is the best surrogate/pair known for the interesting therapeutic generator based radionuclide, i.e. ^{90}Y. The suitable half-life and decay properties support the logic of its applications for radioimmunoscintigraphy, especially during the development of ^{90}Y therapeutic monoclonal antibodies. And last but not the least ^{43,44}Sc radioisotopes, both within the 4 h half-life range, are interesting candidates for peptide receptor PET imaging and possible surrogates for ^{47}Sc radiopharmecuticals with respect to recent IAEA activities for this theranostic scandium radioisotope [176].

REFERENCES

[1] WALCZAK, R., et al., Cyclotron production of ^{43}Sc for PET imaging, EJNMMI Phys. **2** (2015) 33.

[2] KOUMARIANOU, E., PAWLAK, D., KORSAK, A., MIKOLAJCZAK, R., Comparison of receptor affinity of nat Sc-DOTA-TATE versus nat Ga-DOTA-TATE, J. Nucl. Med. **14** (2011) 85.

[3] MCCARTHY, D.W., et al., High purity production and potential applications of copper-60 and copper-61, Nucl. Med. Biol. **26** (1999) 351.

[4] HERZOG, H., et al., Measurement of pharmacokinetics of yttrium-86 radiopharmaceuticals with PET and radiation, J. Nucl. Med. **34** (1993) 2222.

[5] FILOSOFOV, D.V., LOKTIONOVA, N.S., RÖSCH, F., A ^{44}Ti/^{44}Sc radionuclide generator for potential application of 44Sc-based PET-radiopharmaceuticals, Radiochim. Acta **98** (2010) 149.

[6] RÖSCH, F., QAIM, S.M., STÖCKLIN, G., Production of the positron emitting radioisotope ^{86}Y for nuclear medical application, Appl. Radiat. Isot. **44** (1993) 677.

[7] SADEGHI, M., et al., Cyclotron production of ^{68}Ga via proton-induced reaction on ^{68}Zn target, Nukleonika **54** (2009) 25.

[8] JENSEN, M., CLARK, J., Direct Production of Ga-68 from Proton Bombardment of Concentrated Aqueous Solutions of [Zn-68] Zinc Chloride, 13th International Workshop on Targetry and Target Chemistry, Danmarks Tekniske Universitet, Risø Nationallaboratoriet for Bæredygtig Energi, Roskilde, Denmark (2011) 288–292.

[9] PANDEY, M.K., ENGELBRECHT, H.P., BYRNE, J.F., PACKARD, A.B., DEGRADO, T.R., Production of ^{89}Zr via the ^{89}Y (p, n) ^{89}Zr reaction in aqueous solution: effect of solution composition on in-target chemistry, Nucl. Med. Biol. **41** (2014) 309.

[10] LIN, M., WALIGORSKI, G.J., LEPERA, C.G., Production of curie quantities of ^{68}Ga with a medical cyclotron via the ^{68}Zn (p, n) ^{68}Ga reaction, Appl. Radiat. Isot. **133** (2018) 1.

[11] ALVES, V.H., DO CARMO, S.J., ALVES, F., ABRUNHOSA, A.J., Automated purification of radiometals produced by liquid targets, Instrum. **2** (2018) 17.

[12] PANDEY, M.K., BYRNE, J.F., SCHLASNER, K.N., SCHMIT, N.R., DEGRADO, T.R., Cyclotron production of ^{68}Ga in a liquid target: Effects of solution composition and irradiation parameters, Nucl. Med. Biol. **74** (2019) 49.

[13] OEHLKE, E. et al., Production of Y-86 and other radiometals for research purposes using a solution target system, Nucl. Med. Biol. **42** (2015) 842.

[14] INTERNATIONAL ATOMIC ENERGY AGENCY, Gallium-68 Cyclotron Production, IAEA-TECDOC-1863, Vienna (2019) 66.

[15] COUNCIL OF EUROPE. Gallium (^{68}Ga) Chloride (accelerator produced) solution for radiolabelling, PA/PH/Exp. 14/T (18) 13 ANP, Pharmeuropa No. 30.4 (2018).

[16] INTERNATIONAL ATOMIC ENERGY AGENCY, Cyclotron produced radionuclides: Emerging positron emitters for medical applications: ^{64}Cu and ^{124}I, Radioisotopes and Radiopharmaceuticals Reports 1, IAEA, Vienna (2016) 63.

[17] RÖSCH, F., HERZOG, H., QAIM, S., The beginning and development of the theranostic approach in nuclear medicine, as exemplified by the radionuclide pair ^{86}Y and ^{90}Y, Pharmaceuticals **10** (2017) 56.

[18] ROESCH, F., Scandium-44: benefits of a long-lived PET radionuclide available from the ^{44}Ti/^{44}Sc generator system, Curr. Radiopharm. **5** (2012) 187.

[19] BROOKHAVEN NATIONAL LABORATORY, ENSDF Database, NNDC National Nuclear Data Center, http://www.nndc.bnl.gov/ensarchivals/.

[20] RÖSCH, F., BAUM, R.P., Generator-based PET radiopharmaceuticals for molecular imaging of tumours: on the way to theranostics, Dalton Trans. **40** (2011) 6104.

[21] ZHANG, J., et al., From bench to bedside: The bad Berka experience with first-in-human studies, Semin. Nucl. Med. **49** (2019) 422.
[22] GREENE, M.W., HILLMAN, M., A scandium generator, Int. J. Appl. Radiat. Isot. **18** (1967) 540.
[23] MIRZA, M.Y., AZIZ, A., A scandium generator, Radiochim. Acta **11** (1969) 43.
[24] SEIDL, E., LIESER, K.H., Die Radionuklidgeneratoren, ^{113}Sn/^{113m}In, ^{68}Ge/^{68}Ga und ^{44}Ti/^{44}Sc, Radiochim. Acta **19** (1973) 196.
[25] HOSAIN, F., SYED, I.B., SPENCER, R.P., The role of positron emitters in nuclear medicine with special reference to scandium-44, J. Label. Compd. Radiopharm. **13** (1977) 272.
[26] RADCHENKO, V., et al., Proton-induced production and radiochemical isolation of ^{44}Ti from scandium metal targets for ^{44}Ti/^{44}Sc generator development, Nucl. Med. Biol. **50** (2017) 25.
[27] RADCHENKO, V., et al., Separation of ^{44}Ti from proton irradiated scandium by using solid-phase extraction chromatography and design of ^{44}Ti/^{44}Sc generator system, J. Chromatogr. A. **1477** (2016) 39.
[28] DARABAN, L., REBELES, R.A., HERMANNE, A., TARKANYI, F., TAKACS, S., Study of the excitation functions for ^{43}K, $^{43, 44, 44m}$Sc and ^{44}Ti by proton irradiation on ^{45}Sc up to 37 MeV, Nucl. Instrum. Methods Phys. Res., B **267** (2009) 755.
[29] LEVKOVSKII, V.N. Activation cross sections for nuclides of average masses (A = 40–100) by protons and alpha-particles with average energies (E = 10–50 MeV); Experiments and systematics. Inter-Vesy, Moscow (1991).
[30] RÖSCH, F., KNAPP, F.F., "Radionuclide Generators", Handbook of Nuclear Chemistry, 2nd edition, (VÉRTES, A., NAGY, S., KLENCSÁR, Z., LOVAS, R., RÖSCH, F., Eds), Springer Science, Boston (2011) 1935.
[31] PRUSZYŃSKI, M., MAJKOWSKA-PILIP, A., LOKTIONOVA, N.S., EPPARD, E., ROESCH, F., Radiolabeling of DOTATOC with the long-lived positron emitter ^{44}Sc, Appl. Radiat. Isot. **70** (2012) 974.
[32] PRUSZYŃSKI, M., LOKTIONOVA, N.S., FILOSOFOV, D.V., RÖSCH, F., Post-elution processing of ^{44}Ti/^{44}Sc generator-derived ^{44}Sc for clinical application, Appl. Radiat. Isot. **68** (2010) 1636.
[33] WALTER, R.I., Anion exchange studies of Sc (III) and V (IV). Separation of scandium, titanium and vanadium, J. Inorg. Nucl. Chem. **6** (1958) 58.
[34] ZHERNOSEKOV, K.P., et al., Processing of generator-produced ^{68}Ga for medical application, J. Nucl. Med. **48** 10 (2007) 1741.
[35] ASTI, M., et al., Validation of ^{68}Ge/^{68}Ga generator processing by chemical purification for routine clinical application of ^{68}Ga-DOTATOC, Nucl. Med. Biol. **35** (2008) 721.
[36] SEVERIN, G.W., ENGLE, J.W., VALDOVINOS, H.F., BARNHART, T.E., NICKLES, R.J., Cyclotron produced ^{44g}Sc from natural calcium, Appl. Radiat. Isot. **70** (2012) 1526.
[37] VALDOVINOS, H.F., et al., Separation of cyclotron-produced ^{44}Sc from a natural calcium target using a dipentyl pentylphosphonate functionalized extraction resin, Appl. Radiat. Isot. **95** (2015) 23.
[38] VAN DER MEULEN, N., HASLER, R., VERMEULEN, C., Targetry Developments for ^{44}Sc Production Using Nriched CaO, Coimbra, Portugal (2018) 78.
[39] CARZANIGA, T.S., et al., Measurement of ^{43}Sc and ^{44}Sc production cross-section with an 18 MeV medical PET cyclotron, Appl. Radiat. Isot. **129** (2017) 96.
[40] KRAJEWSKI, S., et al., Cyclotron production of ^{44}Sc for clinical application, Radiochim. Acta **101** (2013) 333.
[41] VAN DER MEULEN, N.P., et al., Cyclotron production of ^{44}Sc: From bench to bedside, Nucl. Med. Biol. **42** (2015) 745.

[42] DOMNANICH, K.A., et al., ^{44}Sc for labeling of DOTA- and NODAGA-functionalized peptides: Preclinical in vitro and in vivo investigations, EJNMMI Radiopharm. Chem. **1** (2017) 8.
[43] DOMNANICH, K.A., et al., Production and separation of ^{43}Sc for radiopharmaceutical purposes, EJNMMI. Radiopharm. Chem. **2** (2017) 14.
[44] DE WAAL, T.J., PEISACH, M., PRETORIUS, R., Activation gross sections for deuteron-induced reactions on calcium isotopes up to 5.5 MeV, Radiochim. Acta **15** (1971) 123.
[45] VAN DER MEULEN, N., HASLER, R., The possibility of producing ^{43}Sc from ^{44}Ca via the (p, 2n) nuclear reaction, Nucl. Med. Biol. **72** (2019) S9.
[46] CARZANIGA, T.S., et al., Measurement of the ^{43}Sc production cross-section with a deuteron beam, Appl. Radiat. Isot. **145** (2019) 205.
[47] HOEHR, C., et al., Production of radiometals in a liquid target, Nucl. Med. Biol. **41** (2014) 401.
[48] POURMAND, A., DAUPHAS, N., Distribution coefficients of 60 elements on TODGA resin: application to Ca, Lu, Hf, U and Th isotope geochemistry, Talanta **81** (2010) 741.
[49] ROTSCH, D.A., et al., Electron linear accelerator production and purification of scandium-47 from titanium dioxide targets, Appl. Radiat. Isot. **131** (2018) 77.
[50] MASUDA, Y., OKADA, Y., MURASE, I., SEKIDO, E., Complex formation of scandium (III) with polyaminopolycarboxylic acids and isotachophoretic separation of scandium using complexation equilibria, Japan Analyst **40** (1991) 215.
[51] MAJKOWSKA-PILIP, A., BILEWICZ, A., Macrocyclic complexes of scandium radionuclides as precursors for diagnostic and therapeutic radiopharmaceuticals, J. Inorg. Biochem. **105** (2011) 313.
[52] HUCLIER-MARKAI, S., et al., Chemical and biological evaluation of scandium (III)-polyaminopolycarboxylate complexes as potential PET agents and radiopharmaceuticals, Radiochim. Acta **99** (2011) 653.
[53] SINGH, A., et al., First-in-human PET/CT imaging of metastatic neuroendocrine neoplasms with cyclotron-produced ^{44}Sc-DOTATOC: A proof-of-concept study. Cancer Biother. Radiopharm. **32** (2017) 124.
[54] YAKUSHEVA, A., et al., From octreotide to shorter analogues: Synthesis, radiolabeling, stability, J. Labelled Comp. Radiopharm. **62** (2019) 718.
[55] UMBRICHT, C.A., et al., ^{44}Sc-PSMA-617 for radiotheragnostics in tandem with ^{177}Lu-PSMA-617 – preclinical investigations in comparison with ^{68}Ga-PSMA-11 and ^{68}Ga-PSMA-617, EJNMMI Res. **7** (2017) 9.
[56] HONARVAR, H., et al., Evaluation of the first ^{44}Sc-labeled Affibody molecule for imaging of HER2-expressing tumors, Nucl. Med. Biol. **45** (2017) 15.
[57] HERNANDEZ, R., et al., ^{44}Sc: An attractive isotope for peptide-based PET imaging, Mol. Pharmaceutics **11** (2014) 2954.
[58] EDEM, P.E., et al., Evaluation of the inverse electron demand Diels-Alder reaction in rats using a scandium-44-labelled tetrazine for pretargeted PET imaging, EJNMMI Res. **9** (2019) 49.
[59] CHAKRAVARTY, R., et al., Matching the decay half-life with the biological half-life: ImmunoPET imaging with ^{44}Sc-labeled cetuximab fab fragment, Bioconjugate Chem. **25** (2014) 2197.
[60] MAJKOWSKA-PILIP, A., BILEWICZ, A., Macrocyclic complexes of scandium radionuclides as precursors for diagnostic and therapeutic radiopharmaceuticals. J. Inorg. Biochem. **105** (2011) 313.
[61] EPPARD, E., et al., Clinical translation and first in-human use of [^{44}Sc] Sc-PSMA-617 for PET imaging of metastasized castrate-resistant prostate cancer, Theranostics **7** (2017) 4359.

[62] KHAWAR, A., et al., Prediction of normal organ absorbed doses for [^{177}Lu]Lu-PSMA-617 using [^{44}Sc]Sc-PSMA-617 pharmacokinetics in patients with metastatic castration resistant prostate carcinoma, Clin. Nucl. Med. **43** (2018) 486.
[63] KHAWAR, A., et al., [^{44}Sc]Sc-PSMA-617 Biodistribution and dosimetry in patients with metastatic castration-resistant prostate carcinoma, Clin. Nucl. Med. **43** (2018) 323.
[64] KILIAN, K., et al., Separation of ^{44}Sc from natural calcium carbonate targets for synthesis of ^{44}Sc-DOTATATE, Molecules **23** (2018).
[65] KOUMARIANOU, E., et al., ^{44}Sc-DOTA-BN[2-14]NH2 in comparison to ^{68}Ga-DOTA-BN[2-14]NH2 in pre-clinical investigation. Is ^{44}Sc a potential radionuclide for PET?, Appl. Radiat. Isot. **70** (2012) 2669.
[66] EIGNER, S., et al., ^{44}Sc-DOTO-Puromycin: μPET-imaging of protein synthesis, J. Nucl. Med **52** (Suppl. 1) (2011) 566.
[67] EPPARD, E., et al., Labeling of DOTA-conjugated HPMA-based polymers with trivalent metallic radionuclides for molecular imaging, EJNMMI Res. **8** (2018) 16.
[68] KERDJOUDJ, R., et al., Scandium(iii) complexes of monophosphorus acid DOTA analogues: A thermodynamic and radiolabelling study with ^{44}Sc from cyclotron and from a ^{44}Ti/^{44}Sc generator, Dalton Trans. **45** (2016) 1398.
[69] MÜLLER, C., et al., Promising prospects for ^{44}Sc/^{47}Sc based theragnostics: Application of ^{47}Sc for radionuclide tumor therapy in mice, J. Nucl. Med. **55** (2014) 1658.
[70] NAGY, G., et al., Preclinical evaluation of melanocortin-1 receptor (MC1-R) specific ^{68}Ga and ^{44}Sc labeled DOTA-NAPamide in melanoma imaging, Eur. J. Pharm. Sci. **106** (2017) 336.
[71] LI, L., et al., Coordination chemistry of [Y(pypa)]− and comparison immuno-PET imaging of [^{44}Sc]Sc- and [^{86}Y]Y-pypa-phenyl-TRC105, Dalton Trans. **49** (2020) 5547.
[72] COHEN, B.L., NEWMAN, E., CHARPIE, R.A., HANDLEY, T.H., (p, pn) and (p, αn) Excitation Functions, Phys. Rev. **94** (1954) 620.
[73] ZIEGLER, J.F., BIERSACK, J.P., LITTMARK, U., The stopping and range of ions in matter (SRIM Code), Software (2000).
[74] KONING, A.J., et al., TENDL: Complete nuclear data library for innovative nuclear science and technology, Nucl. Data Sheets **155** (2019) 1.
[75] BLANN, M., Statistical model code system with fission competition, ALICE-91, PACKAGE PSR-146 (1991).
[76] ALVES, F., et al., Production of copper-64 and gallium-68 with a medical cyclotron using liquid targets, Mod. Phys. Lett. **32** (2017) 1740013.
[77] MCCARTHY, D.W., et al., Efficient production of high specific activity ^{64}Cu using a biomedical cyclotron, Nucl. Med. Biol. **24** (1997) 35.
[78] ENGELBRECHT, F., et al., Oral presentation in "20th International Symposium on Radiopharmaceutical Sciences", J. Label. Compd. Radiopharm. **56** (2013) S38.
[79] DO CARMO, S.J.C., ALVES, V.H.P., ALVES, F., ABRUNHOSA, A.J., Fast and cost-effective cyclotron production of ^{61}Cu using a Nat Zn liquid target: An opportunity for radiopharmaceutical production and R&D, Dalton Trans. **46** (2017) 14556.
[80] DO CARMO, S.J., SCOTT, P.J., ALVES, F., Production of radiometals in liquid targets, EJNMMI Radiopharm. Chem. **5** (2020) 1.
[81] STRANGIS, R., LEPERA, C.G., Production of ^{61}Cu by Deuteron Irradiation of Natural Ni, 18th International Conference on Cyclotrons and Their Applications, Catania, Italy (2007).
[82] FAN, X., et al., A simple and selective method for the separation of Cu radioisotopes from nickel, Nucl. Med. Biol. **33** (2006) 939.
[83] WATANABE, S., et al., Chelating ion-exchange methods for the preparation of no-carrier-added ^{64}Cu, Nucl. Med. Biol. **36** 6 (2009) 587.

[84] FONSECA, A.I.S., Labelling and Validation of [^{61}Cu] DOTA-NOC for Somatostatin Receptors Imaging, Universidade de Coimbra (2019).
[85] ALVES, F., Unpublished, Institute for Nuclear Science Applied to Health, University of Coimbra, Portugal (unpublished data).
[86] JALILIAN, A., et al., Preclinical studies of [^{61}Cu]ATSM as a PET radiopharmaceutical for fibrosarcoma imaging, Acta Pharm. **59** (2009) 45.
[87] JALILIAN, A., ROWSHANFARZAD, P., SABET, M., Preparation of [^{61}Cu]pyruvaldehyde-bis (N4-methylthiosemicarbazone) complex as a possible PET radiopharmaceutical, Radiochim. Acta **94** (2006) 113.
[88] ČEPA, A., et al., Radiolabeling of the antibody IgG M75 for epitope of human carbonic anhydrase IX by ^{61}Cu and ^{64}Cu and its biological testing, Appl. Radiat. Isot. **143** (2019) 87.
[89] ZHANG, Y., et al., PET imaging of CD105/endoglin expression with a $^{61/64}$Cu-labeled Fab antibody fragment, Eur. J. Nucl. Med. Mol. Imaging **40** 5 (2013) 759.
[90] ZHANG, Y., et al., Positron emission tomography imaging of vascular endothelial growth factor receptor expression with ^{61}Cu-Labeled lysine-tagged VEGF121, Mol. Pharmaceutics **9** (2012) 3586.
[91] JALILIAN, A., et al., Preparation and biological evaluation of [^{61}Cu] bleomycin complex as a possible PET radiopharmaceutical in normal and fibrosarcoma-bearing animals, Nukleonika **54** (2009) 135.
[92] JALILIAN, A., HASSAN, Y., REZA, F., Preparation, quality control and biodistribution of [^{61}Cu]-doxorubicin for PET imaging, NSETEC **20** (2009) 157.
[93] RUANGMA, A., et al., Three-dimensional maximum a posteriori (MAP) imaging with radiopharmaceuticals labeled with three Cu radionuclides, Nucl. Med. Biol. **33** (2006) 217.
[94] JALILIAN, A.R., ROWSHANFARZAD, P., SABET, M., SHAFIEE, A., Preparation of [^{61}Cu]-2-acetylpyridine thiosemicarbazone complex as a possible PET tracer for malignancies, Appl. Radiat. Isot. **64** (2006) 337.
[95] JALILIAN, A., ROWSHANFARZAD, P., SABET, M., KAMALIDEHGHAN, M., Preparation of [^{61}Cu]DTPA complex as a possible PET tracer, Nukleonika **51** (2006) 111.
[96] JALILIAN, A., et al., Preparation, quality control and biodistribution studies of two [^{111}In]-rituximab immunoconjugates, Scientia Pharmaceutica **76** (2008) 151.
[97] JALILIAN, A., et al., Synthesis and preclinical studies of [^{61}Cu]-N-(2-hydroxyacetophenone) glycinate as a possible PET radiopharmaceutical, Sci. Pharm. **76** (2008) 637.
[98] JALILIAN, A., et al., Radiosynthesis and evaluation of [^{61}Cu]-9, 10-phenanthrenequinone thiosemicarbazone in fibrosarcoma-bearing animals for PET imaging, Radiochim. Acta **98** (2010) 175.
[99] NAYAK, T.K., BRECHBIEL, M.W., ^{86}Y based PET radiopharmaceuticals: radiochemistry and biological applications, Med. Chem. **7** (2011) 380.
[100] MIKOLAJCZAK, R., VAN DER MEULEN, N.P., LAPI, S.E., Radiometals for imaging and theranostics, current production, and future perspectives, J. Labelled Comp. Radiopharm. **62** (2019) 615.
[101] ALUICIO-SARDUY, E., et al., PET radiometals for antibody labeling, J. Labelled Comp. Radiopharm. **61** (2018) 636.
[102] HUANG, J., CUI, L., WANG, F., LIU, Z., PET tracers based on ^{86}Y, Curr. Radiopharm. **4** (2011) 122.
[103] SCHILLER, E., et al., Yttrium-86-labelled human serum albumin microspheres: relation of surface structure with in vivo stability, Nucl. Med. Biol. **35** (2008) 227.

[104] WANG, Z. et al., Single low-dose injection of evans blue modified PSMA-617 radioligand therapy eliminates prostate-specific membrane antigen positive tumors, Bioconjug. Chem. **29** (2018) 3213.
[105] HERNANDEZ, R., et al., ^{90}Y-NM600 targeted radionuclide therapy induces immunologic memory in syngeneic models of T-cell Non-Hodgkin's Lymphoma, Commun. Biol. **2** (2019) 79.
[106] GRUDZINSKI, J.J., et al., Preclinical characterization of $^{86/90}$Y-NM600 in a variety of murine and human cancer tumor models, J. Nucl. Med. **60** (2019) 1622.
[107] HERNANDEZ, R., et al., ^{177}Lu-NM600 targeted radionuclide therapy extends survival in syngeneic murine models of triple-negative breast cancer, J. Nucl. Med. **61** (2020) 1187.
[108] EHLERDING, E.B., et al., $^{86/90}$Y-based theranostics targeting angiogenesis in a murine breast cancer model, Mol. Pharm. **15** (2018) 2606.
[109] LÖVQVIST, A., et al., PET imaging of ^{86}Y-labeled anti-Lewis Y monoclonal antibodies in a nude mouse model: Comparison between ^{86}Y and ^{111}In radiolabels, J. Nucl. Med. **42** (2001) 1281.
[110] NAYAK, T.K., GARMESTANI, K., MILENIC, D.E., BAIDOO, K.E., BRECHBIEL, M.W., HER1-targeted ^{86}Y-panitumumab possesses superior targeting characteristics than ^{86}Y-cetuximab for PET imaging of human malignant mesothelioma tumors xenografts, PloS one **6** (2011) e18198.
[111] NAYAK, T.K., GARMESTANI, K., BAIDOO, K.E., MILENIC, D.E., BRECHBIEL, M.W., Preparation, biological evaluation, and pharmacokinetics of the human anti-HER1 monoclonal antibody panitumumab labeled with ^{86}Y for quantitative PET of carcinoma, J. Nucl. Med. **51** (2010) 942.
[112] SCHNEIDER, D.W., et al., In vivo biodistribution, PET imaging, and tumor accumulation of ^{86}Y and ^{111}In-antimindin/RG-1, engineered antibody fragments in LNCaP tumor-bearing nude mice, J. Nucl. Med. **50** (2009) 435.
[113] MARIANE, L.E., et al., Yttrium-86 PET imaging in rodents to better understand the biodistribution and clearance of gadolinium-based contrast agents used in MRI., J. Nucl. Med. **60** supp. 1 (2019) 346.
[114] LEDERER, C.M., SHIRLEY, V.S. (Eds), V. S. Shirley, Eds.,"Table of Isotopes," 7th ed., John Wiley and Sons, Inc., New York (1978).
[115] ECKERMAN, K.F., ENDO, A., Radionuclide Decay Data and Decay Schemes, SNM MIRD Committee, Reston, VA, USA (2007).
[116] QAIM, S.M., Decay data and production yields of some non-standard positron emitters used in PET, Q. J. Nucl. Med. Mol. Imaging **52** (2008) 111.
[117] QAIM, S.M., Development of novel positron emitters for medical applications: Nuclear and radiochemical aspects, Radiochim. Acta **99** (2011) 611.
[118] QAIM, S.M., Nuclear data for production and medical application of radionuclides: Present status and future needs, Nucl. Med. Biol. **44** (2017) 31.
[119] RÖSCH, F., QAIM, S.M., STÖCKLIN, G., Nuclear data relevant to the production of the positron emitting radioisotope ^{86}Y via the ^{86}Sr (p, n)-and natRb (3He, xn)-processes, Radiochim. Acta **61** (1993) 1.
[120] UDDIN, M.S., et al., Excitation functions of the proton induced nuclear reactions on natural zirconium, Nucl. Instrum. Methods Phys. Res., B **266** (2008) 13.
[121] KHANDAKER, M.U., et al., Experimental determination of proton-induced cross-sections on natural zirconium, Appl. Radiat. Isot. **67** (2009) 1341.
[122] SZELECSÉNYI, F., et al., Excitation functions of natZr+ p nuclear processes up to 70 MeV: New measurements and compilation, Nucl. Instrum. Methods Phys. Res., B **343** (2015) 173.

[123] TÁRKÁNYI, F., et al., New activation cross section data on longer lived radio-nuclei produced in proton induced nuclear reaction on zirconium, Appl. Radiat. Isot. **97** (2015) 149.
[124] REISCHL, G., RÖSCH, F., MACHULLA, H.J., Electrochemical separation and purification of yttrium-86, Radiochim. Acta **90** (2002) 225.
[125] KETTERN, K., LINSE, K.H., SPELLERBERG, S., COENEN, H.H., QAIM, S.M., Radiochemical studies relevant to the production of ^{86}Y and ^{88}Y at a small-sized cyclotron, Radiochim. Acta **90** (2002) 845.
[126] FINN, R.D., et al., Low Energy Cyclotron Production and Separation of Yttrium-86 for Evaluation of Monoclonal Antibody Pharmacokinetics and Dosimetry, AIP Conference Proceedings, Vol. 475, American Institute of Physics (1999) 991–993.
[127] ZANEB, H., HUSSAIN, M., AMJED, N., QAIM, S., Nuclear model analysis of excitation functions of proton induced reactions on ^{86}Sr, ^{88}Sr and natZr: Evaluation of production routes of ^{86}Y, Appl. Radiat. Isot. **104** (2015) 232.
[128] SADEGHI, M., ABOUDZADEH, M., ZALI, A., MIRZAII, M., BOLOURINOVIN, F., Radiochemical studies relevant to ^{86}Y production via ^{86}Sr(p,n)^{86}Y for PET imaging, Appl. Radiat. Isot. **67** (2009) 7.
[129] SADEGHI, M., ZALI, A., MOKHTARI, L., Calculations of Y-86 production via various nuclear reactions, Nucl. Sci. Tech. **20** (2009) 369.
[130] KANDIL, S., SCHOLTEN, B., HASSAN, K., HANAFI, H., QAIM, S., A comparative study on the separation of radioyttrium from Sr-and Rb-targets via ion-exchange and solvent extraction techniques, with special reference to the production of no-carrier-added ^{86}Y, ^{87}Y and ^{88}Y using a cyclotron, J. Radioanal. Nucl. Chem. **279** (2009) 823.
[131] YOO, J., et al., Preparation of high specific activity ^{86}Y using a small biomedical cyclotron, Nucl. Med. Biol. **32** (2005) 891.
[132] AVILA-RODRIGUEZ, M.A., NYE, J.A., NICKLES, R.J., Production and separation of non-carrier-added ^{86}Y from enriched ^{86}Sr targets, Appl. Radiat. Isot. **66** (2008) 9.
[133] GARMESTANI, K., MILENIC, D.E., PLASCJAK, P.S., BRECHBIEL, M.W., A new and convenient method for purification of ^{86}Y using a Sr (II) selective resin and comparison of biodistribution of ^{86}Y and ^{111}In labeled Herceptin^{TM}, Nucl. Med. Biol. **29** (2002) 599.
[134] VALDOVINOS, H.F., GRAVES, S., BARNHART, T., NICKLES, R.J., Simplified and reproducible radiochemical separations for the production of high specific activity ^{61}Cu, ^{64}Cu, ^{86}Y and ^{55}Co, AIP Conference Proceedings **1845** (2017) 020021.
[135] LUKIĆ, D., et al., High efficiency production and purification of ^{86}Y based on electrochemical separation, Appl. Radiat. Isot. **67** (2009) 523.
[136] SCHMITZ, J., The production of [^{124}I] iodine and [^{86}Y] yttrium, Eur. J. Nucl. Med. Mol. Imaging **38** (2011) 4.
[137] RÁLIŠ, J., LEBEDA, O., KUČERA, J., Liquid Target System for Production of ^{86}Y, Proceedings of the 13th International Workshop on Targetry and Target Chemistry, Vol. 42, Roskilde, Denmark (2010) 234.
[138] VOGG, A.T.J., et al., Cyclotron production of radionuclides in aqueous targets matrices as alternative to solid targets. Production of ^{86}Y as example, Aachen, Germany (2004) 318.
[139] MEDVEDEV, D.G., MAUSNER, L.F., SRIVASTAVA, S.C., Irradiation of strontium chloride targets at proton energies above 35 MeV to produce PET radioisotope Y-86, Radiochim. Acta **99** (2011) 755.
[140] BAIMUKHANOVA, A., et al., Utilization of (p, 4n) reaction for ^{86}Zr production with medium energy protons and development of a ^{86}Zr → ^{86}Y radionuclide generator, J. Radioanal. Nucl. Chem. **316** (2018).

[141] TÁRKÁNYI, F., et al., Investigation of activation cross sections for deuteron induced reactions on strontium up to 50 MeV, Applied Radiation and Isotopes **127** (2017) 16.
[142] TÁRKÁNYI, F.T., et al., Recommended nuclear data for medical radioisotope production: diagnostic positron emitters, J. Radioanal. Nucl. Chem. **319** (2019) 533.
[143] SACHDEV, D.R., PORILE, N.T., YAFFE, L., Reactions of ^{88}Sr with protons of energies 7–85 MeV, Can. J. Chem. **45** (1967) 1149.
[144] KANTELO, M.V., HOGAN, J.J., Charged-particle emission in reactions of ^{90}Zr with 10-86-MeV protons, Phys. Rev. C **14** (1976) 64.
[145] UDDIN, M. et al., Accurate determination of production data of the non-standard positron emitter ^{86}Y via the ^{86}Sr(p,n)-reaction, Radiochim. Acta **1** (2020).
[146] PARK, L.S., et al., Semi-automated ^{86}Y purification using a three-column system, Nucl. Med. Biol. **31** (2004) 297.
[147] SADEGHI, M., ABOUDZADEH, M., ZALI, A., ZEINALI, B., ^{86}Y production via ^{86}Sr(p,n) for PET imaging at a cyclotron, Appl. Radiat. Isot. **67** (2009) 1392.
[148] MICHAEL, H., et al., Some technical improvements in the production of ^{123}I via the ^{124}Te(p, 2n) ^{123}I reaction at a compact cyclotron, Int. J. Appl. Radiat. Isot. **32** (1981) 581.
[149] ALUICIO-SARDUY, E., et al., Simplified and automatable radiochemical separation strategy for the production of radiopharmaceutical quality ^{86}Y using single column extraction chromatography, Appl. Radiat. Isot. **142** (2018) 28.
[150] SADEGHI, M., ZALI, A., AVILA, M., A novel method for radiochemical separation of radioyttrium from Sr targets using precipitation technique, Radiochim. Acta **98** (2010) 437.
[151] RÖSCH, F., et al., Radiation doses of yttrium-90 citrate and yttrium-90 EDTMP as determined via analogous yttrium-86 complexes and positron emission tomography, Eur. J. Nucl. Med. **23** (1996) 958.
[152] FÖRSTER, G.J., et al., Preliminary data on biodistribution and dosimetry for therapy planning of somatostatin receptor positive tumours: Comparison of ^{86}Y-DOTATOC and ^{111}In-DTPA-octreotide, Eur. J. Nucl. Med. **28** (2001) 1743.
[153] HELISCH, A., et al., Pre-therapeutic dosimetry and biodistribution of ^{86}Y-DOTA-Phe 1-Tyr 3-octreotide versus ^{111}In-pentetreotide in patients with advanced neuroendocrine tumours, Eur. J. Nucl. Med. Mol. Imaging **31** (2004) 1386.
[154] JAMAR, F., et al., ^{86}Y-DOTA 0-d-Phe 1-Tyr 3-octreotide (SMT487)—a phase 1 clinical study: Pharmacokinetics, biodistribution and renal protective effect of different regimens of amino acid co-infusion, Eur. J. Nucl. Med. Mol. Imaging **30** (2003) 510.
[155] BARONE, R., et al., Therapy using labelled somatostatin analogues: Comparison of the absorbed doses with ^{111}In-DTPA-D-Phe1-octreotide and yttrium-labelled DOTA-D-Phe1-Tyr3-octreotide, Nucl. Med. Commun. **29** (2008) 283.
[156] STOLZ, B., et al., Somatostatin receptor-targeted radiotherapy—Preclinical proof of concept, Octreotide: The Next Decade; BioScientifica Ltd., Lamberts, UK (1999).
[157] FORRER, F., WALDHERR, C., MAECKE, H.R., MUELLER-BRAND, J., Targeted radionuclide therapy with ^{90}Y-DOTATOC in patients with neuroendocrine tumors, Anticancer Res. **26** (2006) 703.
[158] BANERJEE, S.R., et al., Preclinical evaluation of ^{86}Y-labeled inhibitors of prostate-specific membrane antigen for dosimetry estimates, J. Nucl. Med. **56** (2015) 628.
[159] BIDDLECOMBE, G.B., et al., Molecular imaging of gastrin-releasing peptide receptor-positive tumors in mice using ^{64}Cu and ^{86}Y-DOTA-(Pro1,Tyr4)-bombesin(1-14), Bioconjug. Chem. **18** (2007) 724.
[160] MCQUADE, P., et al., Imaging of melanoma using ^{64}Cu and ^{86}Y−DOTA−ReCCMSH(Arg11), a cyclized peptide analogue of α-MSH, J. Med. Chem. **48** (2005) 2985.

[161] CHEAL, S.M., et al., Theranostic pretargeted radioimmunotherapy of colorectal cancer xenografts in mice using picomolar affinity ^{86}Y or ^{177}Lu-DOTA-Bn binding scFv C825/GPA33 IgG bispecific immunoconjugates, Eur. J. Nucl. Med. Mol. Imaging **43** (2016) 925.
[162] RÖSCH, F., et al., Uptake kinetics of the somatostatin receptor ligand [^{86}Y]DOTA-DPhe1- Tyr3-octreotide ([^{86}Y]SMT487) using positron emission tomography in non-human primates and calculation of radiation doses of the ^{90}Y-labelled analogue, Eur. J. Nucl. Med. **26** (1999) 358.
[163] PALM, S. et al., Pharmacokinetics and biodistribution of ^{86}Y-Trastuzumab for ^{90}Y dosimetry in an ovarian carcinoma model: Correlative MicroPET and MRI, J. Nucl. Med. **44** (2003) 1148.
[164] NAYAK, T.K., et al., PET imaging of HER1-expressing xenografts in mice with ^{86}Y-CHX-A''-DTPA-cetuximab, Eur. J. Nucl. Med. Mol. Imaging **37** (2010) 1368.
[165] LOPCI, E., et al., Matched pairs dosimetry: ^{124}I/^{131}I metaiodobenzylguanidine and ^{124}I/^{131}I and ^{86}Y/^{90}Y antibodies, Eur. J. Nucl. Med. Mol. Imaging **38** (2011) 28.
[166] WEI, L., et al., Melanoma imaging using ^{111}In, ^{86}Y and ^{68}Ga-labeled CHX-A''-Re(Arg11)CCMSH, Nucl. Med. Biol. **36** (2009) 345.
[167] WONG, K.J., et al., In vitro and in vivo pre-clinical analysis of a F(ab')(2) fragment of panitumumab for molecular imaging and therapy of HER1 positive cancers, EJNMMI Res. **1** (2011).
[168] MCDEVITT, M.R., et al., PET imaging of soluble yttrium-86-labeled carbon nanotubes in mice, PLoS ONE **2** (2007) e907.
[169] CHOPRA, A., "^{111}In/^{86}Y-Labeled F (ab') 2 fragment of panitumumab, a fully human monoclonal antibody directed against the extracellular domain III of the epidermal growth factor receptor", Molecular Imaging and Contrast Agent Database (MICAD), National Center for Biotechnology Information, Bethesda, US (2012).
[170] WESTER, H.J. et al., PET-pharmacokinetics of ^{18}F-octreotide: A comparison with ^{67}Ga-DFO- and ^{86}Y-DTPA-octreotide, Nucl. Med. Biol. **24** (1997) 275.
[171] SCHLESINGER, J., et al., An ^{86}Y-labeled mirror-image oligonucleotide: Influence of Y-DOTA isomers on the biodistribution in rats, Bioconjug. Chem. **19** (2008) 928.
[172] BANDARA, N., et al., Matched-pair, ^{86}Y/^{90}Y-labeled, bivalent RGD/bombesin antagonist, [RGD-Glu-[DO3A]-6-Ahx-RM2], as a potential theranostic agent for prostate cancer, Nucl. Med. Biol. **62** (2018) 71.
[173] ALIDORI, S., et al., Carbon nanotubes exhibit fibrillar pharmacology in primates, PLoS ONE **12** (2017) e0183902.
[174] CHENG, K.T., LEWIS, J.S., BIDDLECOMBE, G.B., "^{86}Y-DOTA-[Pro1, Tyr4]-Bombesin", Molecular Imaging and Contrast Agent Database (MICAD), National Center for Biotechnology Information, Bethesda, US (2008).
[175] INTERNATIONAL ATOMIC ENERGY AGENCY, Copper-64 Radiopharmaceuticals for Theranostic Applications, CRP F22067, IAEA, Vienna (2020).
[176] INTERNATIONAL ATOMIC ENERGY AGENCY, Therapeutic Radiopharmaceuticals Labelled with New Emerging Radionuclides (^{67}Cu, ^{186}Re, ^{47}Sc), CRP F22053, IAEA, Vienna (2020).

ANNEX I. PRODUCTION OF ^{61}Cu CHLORIDE THROUGH SOLID TARGET: EXPERIENCE FROM A 30 MeV IBA FACILITY

I.1. IMAGING OF [^{61}Cu]Cu-ACETATE IN WILD TYPE RATS

The production and purification of ^{61}Cu at a 30 MeV cyclotron facility is described in section I.3. To assess the biodistribution of free ^{61}Cu cations in rats for further studies and to compare with other ^{61}Cu radiolabelled compounds, an isotonic solution of [^{61}Cu]Cu-acetate was prepared and administered to rats. The batch of [^{61}Cu]$CuCl_2$ (3700 MBq, pH2) was diluted using a 1 M solution of sodium acetate and shaken for 5 min at ambient temperature to obtain a solution of [^{61}Cu]Cu-acetate with appropriate acidity (pH>5.5) for i.v. injection. To each rat, the solution (containing 3.7 MBq) was injected through their tail vein and a biodistribution study was performed using co-incidence imaging, see Fig. I.1.

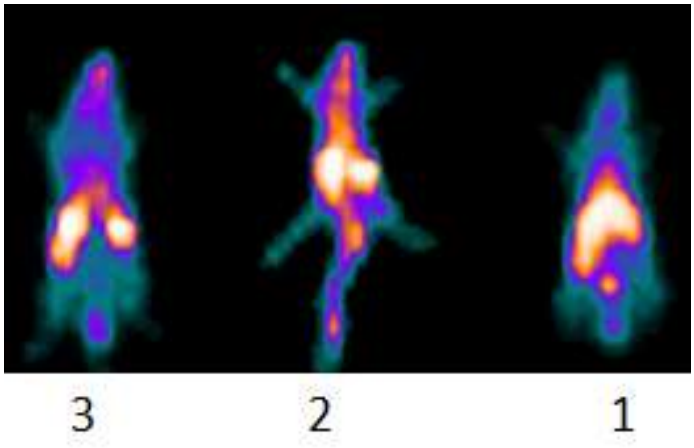

I.1. Co-incidence images for [^{61}Cu]Cu-acetate uptake, 20 (1), 45 (2) and 120 (3) min post injection in normal rats (courtesy of A. Jalilian, IAEA, Austria).

Many compounds were radiolabelled using ^{61}Cu prepared. Two tracers with possible/potential clinical relevance, i.e. [^{61}Cu]Cu-ATSM and [^{61}Cu]Cu-PTSM, are shown in Fig. I.2.

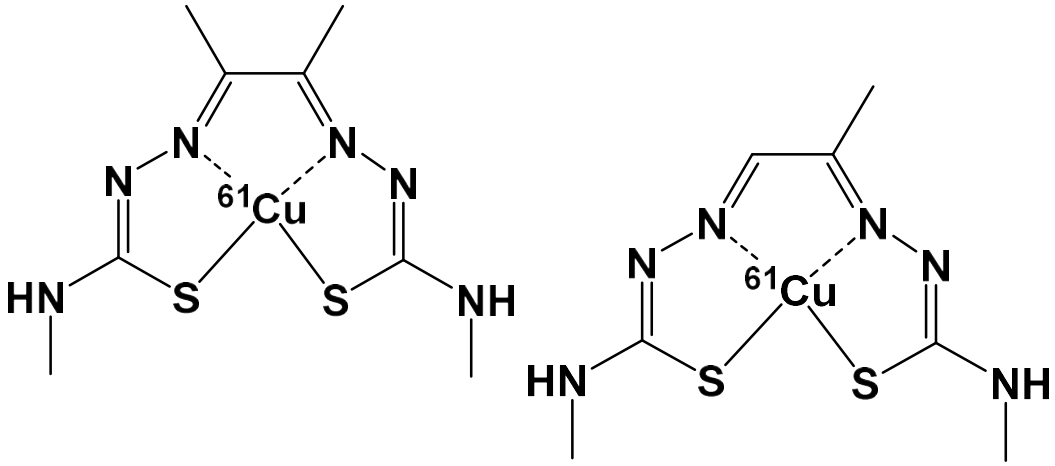

I.2. (Left)^{61}Copper(II) diacetyl-di(N^4-methylthiosemicarbazone ([^{61}Cu]Cu-ATSM). (Right) ^{61}Copper(II)-pyruvaldehyde-bis(N4-methylthiosemicarbazone) ([^{61}Cu]Cu-PTSM) (courtesy of A. Jalilian, IAEA, Austria).

I.1.2. Production of [^{61}Cu]Cu-ATSM

The radiolabelled compound was produced using an in-house synthesized and structurally approved H_2 ATSM sample and copper acetate. A freshly prepared [^{61}Cu]$CuCl_2$ (370 MBq) sample produced from the separation step (in 0.1M HCl, 2 ml) was added in a borosilicate V-shape vial containing 3M sodium acetate solution (0.1 M, 4 ml). The resulting mixture stirred for 2 min contains a [^{61}Cu]Cu-acetate solution. A fresh ATSM stock solution in dry DMSO was prepared and filtered, and a volume (containing 4 mg ATSM) was added to the [^{61}Cu]Cu-acetate solution and shaken at 50°C (1 min). The mixture was then cooled in an ice bath and then loaded onto a C_{18} Sep-Pak. The Sep-Pak was already pre-treated by eluting with 5 ml of ethanol and 2 ml of water respectively prior to purification process. The loaded column is then washed with ultrapure water (4 ml) and then purged with a stream of dry N_2. [^{61}Cu]Cu-ATSM is then eluted from the column by 0.2 ml portions of pure absolute ethanol (n=5). The fractions were counted and the ones with maximum radioactivity (usually fractions 2 and 3) were mixed and diluted to a 5% alcoholic solution by the addition of NaCl 0.9%. Alternatively, if more activity concentration is required the ethanolic fractions can be concentrated in heat/vacue followed by formulation to 5% ethanolic solution. The final formulation was then passed through a 0.22 micron filter. The pH was checked (usually between 5.5–7) and if not within the range can be adjusted by the addition of 3 M L1 sodium acetate buffer.

I.1.3. RCP

The RCP of the [^{61}Cu]Cu-ATSM solution was assessed using TLC on polymer backed silica gel layers. Dry ethyl acetate was used as the mobile phase (Fig. I.3). High performance chromatography was also performed to determine the chemical content, see Fig. I.4.

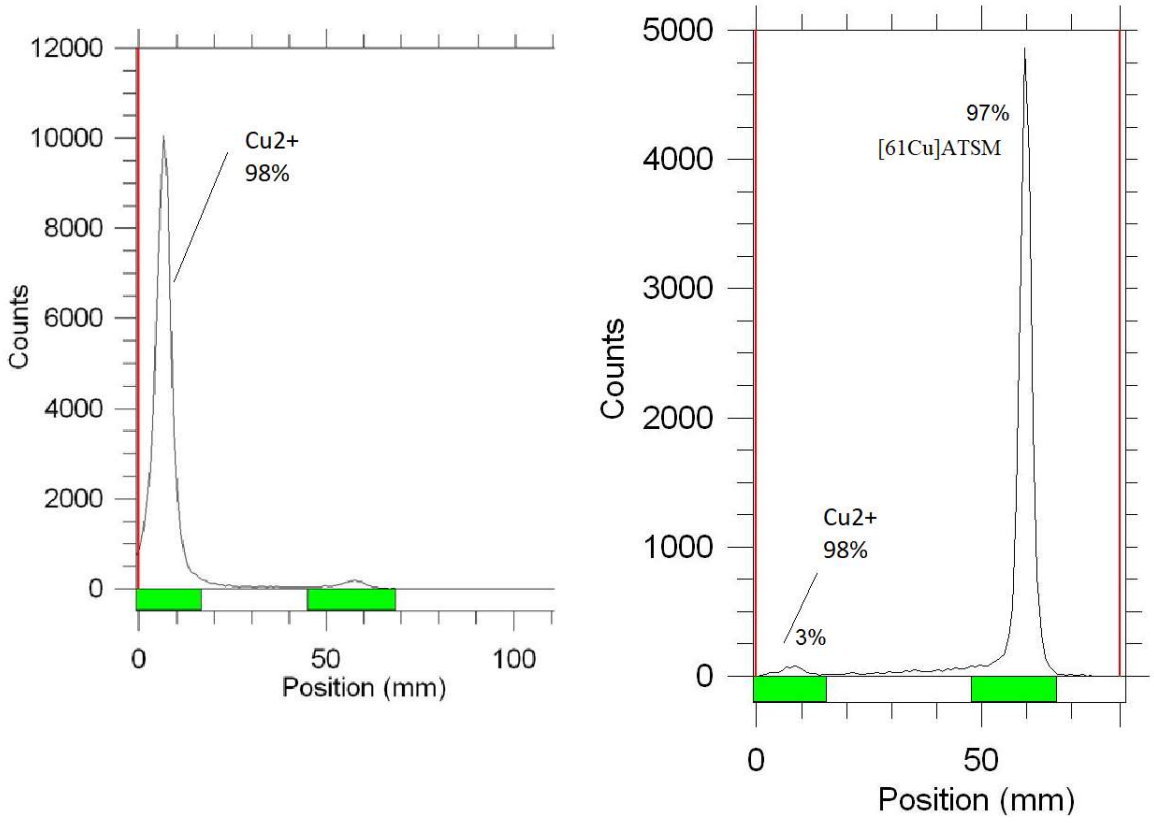

I.3. Radiochromatograms of the starting [^{61}Cu]Cu-acetate (left) and [^{61}Cu]Cu-ATSM (right) (courtesy of A. Jalilian, IAEA, Austria).

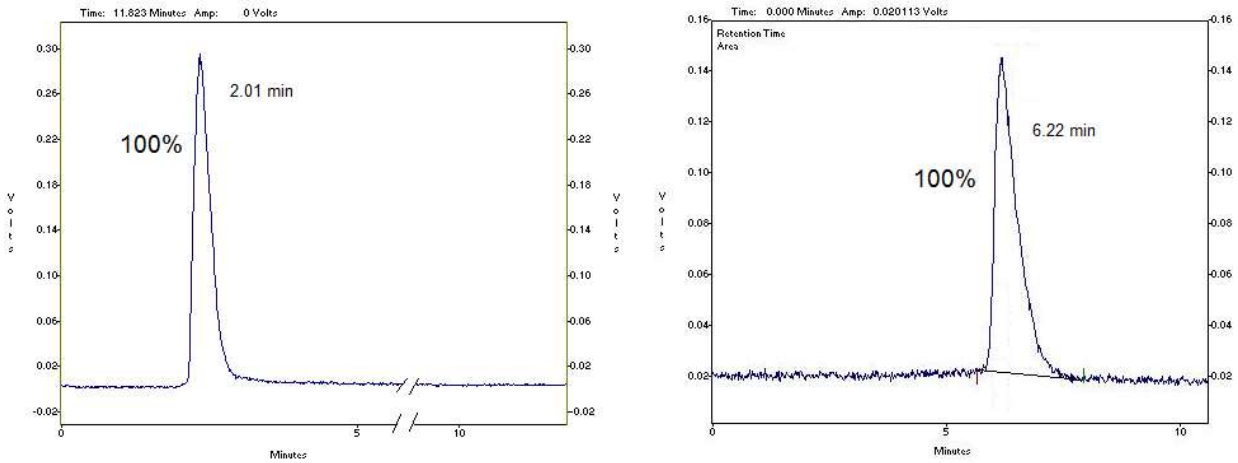

I.4. HPLC diagram for [^{61}Cu]Cu^{2+} (in acetate form, left) and [^{61}Cu]Cu-ATSM (right) using a reverse phase column with a mixture of H_2O:CH_3CN (1:1) as eluent (courtesy of A. Jalilian, IAEA, Austria).

I.2. BIODISTRIBUTION

For further studies in various tumour models, the distribution of [^{61}Cu]Cu-ATSM was determined in normal rats using tissue count studies within 2 h post injection, after intravenous injection of 37 MBq of the tracer into tail vein, see Fig. I.5.

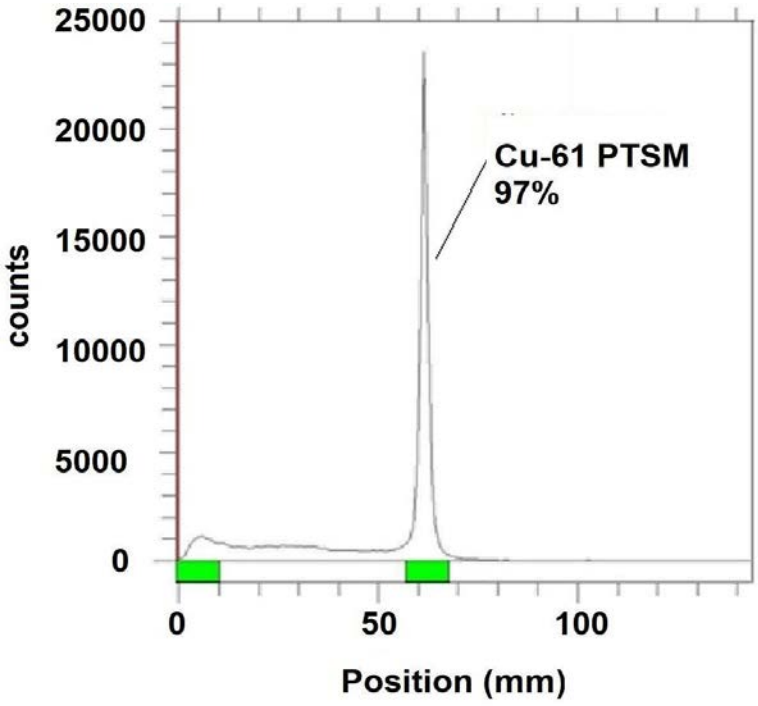

I.5. Radio-TLC scheme of the purified [^{61}Cu]Cu-PTSM assessed with ethyl acetate as mobile phase (courtesy of A. Jalilian, IAEA, Austria).

I.2.1. [^{61}Cu] Cu-PTSM

[^{61}Cu] Cu-PTSM was known as a possible perfusion agent for the study of blow flow in vital organs as well as tumours for the determination of perfusion. Various copper radionuclides were used for this purpose, the production and QC of [^{61}Cu]Cu-PTSM using solid target produced [^{61}Cu]$CuCl_2$.

I.2.2. Preparation of [^{61}Cu]Cu-PTSM

Synthesis of [^{61}Cu]Cu-PTSM was accomplished according to the former methods followed by detailed structural determination.

For the labelling process, which was similar to the former agent, i.e. ^{61}Cu-ATSM, [^{61}Cu]Cu-acetate (3700 MBq) was reacted with a mixture of H_2PTSM (1 mg, in 0.1 ml pure ethanol) followed by C_{18} solid phase extraction (Sep-Pak column). The product was eluted from the column by ethanol fractions (usually no. 4–6), the fractions with maximum activities were mixed. Based on required activity concentrations the fractions can be pooled and evaporated. The final formulation is prepared by the addition of NaCl 0.9% solution to keep a 5% ethanolic content followed by passing the solution through a 0.22 μm filter. The RP was assessed by radio-TLC, see Fig. I.5.

I.3. QC

I.3.1. RCP

The RCP of the [^{61}Cu]Cu-PTSM was measured using polymer backed silica gel to perform layer chromatography and dry ethyl acetate as the mobile phase, as well as high performance chromatography determination of the chemical content was also performed.

ABBREVIATIONS

ATSM	diacetyl-di(N^4-methylthiosemicarbazone)
CEX	cation exchanger
CT	computed Tomography
DGA	N,N,N′,N′-tetrakis-2-ethylhexyldiglycolamide
DOTA	1,4,7,10-tetraazacyclododecane-1,4,7,10-tetraacetic acid
DTPA	diethylenetriamine pentaacetate
EDTA	ethylenediaminetetraacetic acid
EOB	end of bombardment
GBCA	gadolinium based MRI contrast agents
GMP	good manufacturing practice
HER2	human epidermal growth factor receptor 2
HPGe	higher purity germanium
HPLC	high performance liquid chromatography
ICP-MS	inductively coupled plasma mass spectrometry
iTLC	instant thin layer chromatography
NOC	1-Nal3-octreotide
NODAGA	1,4,7-triazacyclononane,1-gluteric acid-4,7-acetic acid
NOTA	1,4,7-triazacyclononane-1,4,7-triacetic acid
PET	positron emission tomography
PSMA	prostate specific membrane antigen
PTSM	pyruvaldehyde-bis(N 4-methylthiosemicarbazone)
QC	quality control
RCP	radiochemical purity
SPECT	single photon emission computed tomography
SRIM	stopping and ranges of ions in matter
TATE	(Tyr^3)-octreotate
TLC	thin layer chromatography
TOC	D-Phe1-Tyr3-octreotide

CONTRIBUTORS TO DRAFTING AND REVIEW

Alves, F.	Institute for Nuclear Science Applied to Health, University of Coimbra, Portugal
DeGrado, T.	Department of Radiology, Mayo Clinic, Rochester, United States of America
Engle, J.	Department of Medical Physics, University of Wisconsin, United States of America
Gagnon, K.	Cyclotrons and TRACERcenter, GE Healthcare, Uppsala, Sweden
Hoehr, C.	Life Sciences Division, TRIUMF, Vancouver, Canada
Jalilian, A.	International Atomic Energy Agency, Vienna, Austria
Lapi, S.	Advanced Medical Imaging Research, University of Alabama at Birmingham, United States of America
Pandey, M.	Department of Radiology, Mayo Clinic, Rochester, United States of America
Radchenko, V.	Life Sciences Division, TRIUMF, Vancouver, Canada
Rösch, F.	Institut für Kernchemie, Johannes Gutenberg-Universität Mainz, Germany
Van der Meulen, N.	Laboratory of Radiochemistry, Paul Scherrer Institut, Villigen-PSI, Switzerland

During a consultancy meeting in April 2019 (ETV1805034) a recommendation was made to initiate a preparation of an IAEA publication on specific theranostic radiometals. Based on the recommendation in November 2019 from another consultancy meeting with the title of “Production of New Emerging Theranostic Radioisotopes (Sc-43/44, Cu-61, Y-86)” held with the participation of five experts, this publication was completed from their input and other selected scientists.

IAEA
International Atomic Energy Agency

No. 26

ORDERING LOCALLY

IAEA priced publications may be purchased from the sources listed below or from major local booksellers.

Orders for unpriced publications should be made directly to the IAEA. The contact details are given at the end of this list.

NORTH AMERICA

Bernan / Rowman & Littlefield

15250 NBN Way, Blue Ridge Summit, PA 17214, USA
Telephone: +1 800 462 6420 • Fax: +1 800 338 4550

Email: orders@rowman.com • Web site: www.rowman.com/bernan

REST OF WORLD

Please contact your preferred local supplier, or our lead distributor:

Eurospan Group

Gray's Inn House
127 Clerkenwell Road
London EC1R 5DB
United Kingdom

Trade orders and enquiries:

Telephone: +44 (0)176 760 4972 • Fax: +44 (0)176 760 1640
Email: eurospan@turpin-distribution.com

Individual orders:

www.eurospanbookstore.com/iaea

For further information:

Telephone: +44 (0)207 240 0856 • Fax: +44 (0)207 379 0609
Email: info@eurospangroup.com • Web site: www.eurospangroup.com

Orders for both priced and unpriced publications may be addressed directly to:

Marketing and Sales Unit
International Atomic Energy Agency
Vienna International Centre, PO Box 100, 1400 Vienna, Austria
Telephone: +43 1 2600 22529 or 22530 • Fax: +43 1 26007 22529
Email: sales.publications@iaea.org • Web site: www.iaea.org/publications

21-00696E

International Atomic Energy Agency
Vienna